Small-angle Scattering

Guinther Kellermann
Departamento de Física
Universidade Federal do Paraná
E-mail: keller@fisica.ufpr.br

NANOPARTICLES

Size-dependent melting temperature

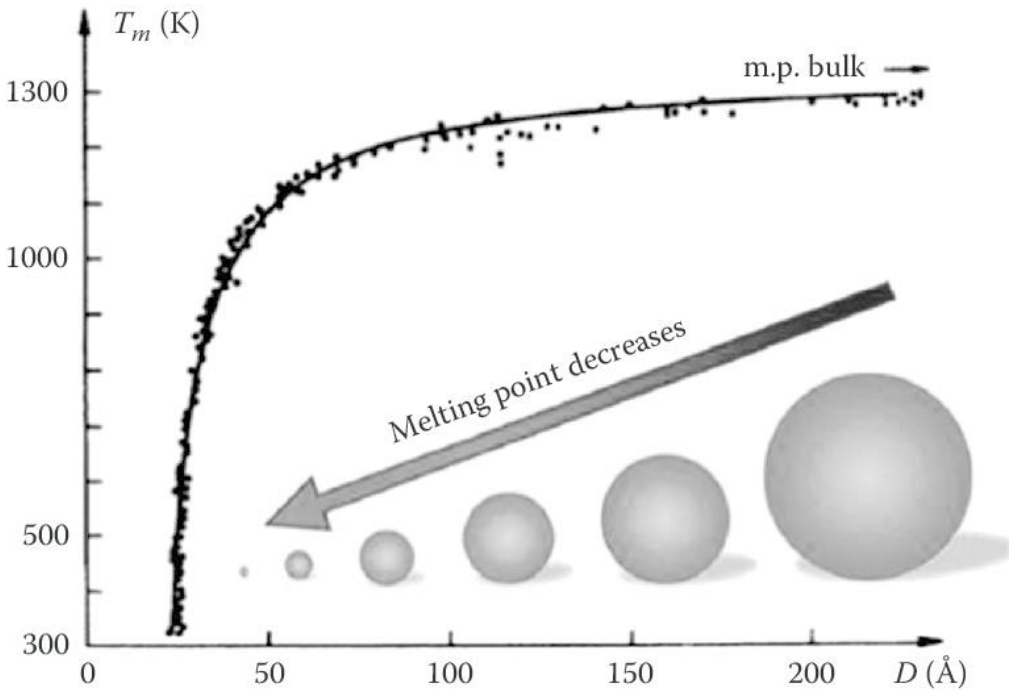

Relationship between melting temperature and particle diameter of gold nanoparticles. (From Yang, C. et al., J. Mater. Chem. C, 1(207890), 4052, 2013.

NANOPARTICLES

Size-dependent optical absorption and emission

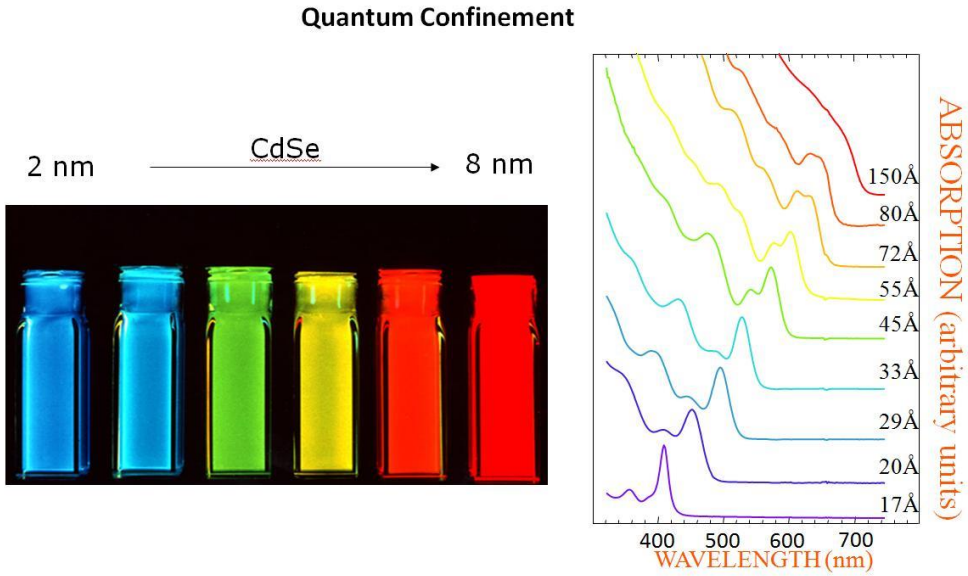

- Increase in the effective band gap of the material with decreasing crystallite size
- optical absorption and emission of quantum dots shift to the blue

https://serc.carleton.edu/msu_nanotech/nano_topics.html

Small-Angle Scattering (SAS)

Small-angle **X-ray**s scattering (SAXS)

Small-angle **neutrons** scattering (SANS)

Basic instrumentation

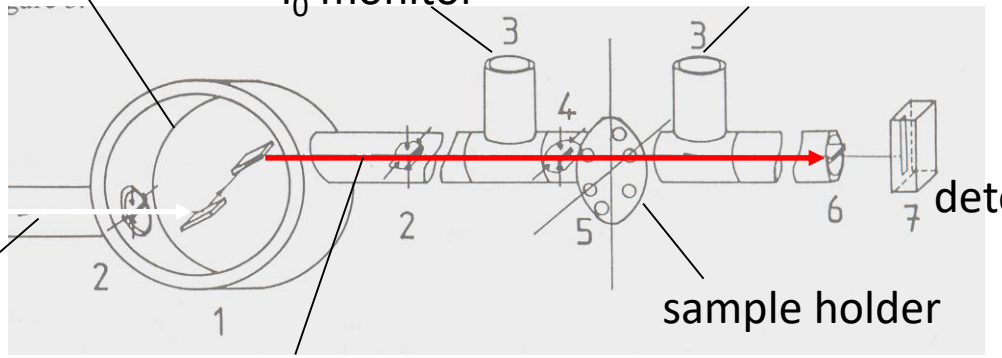

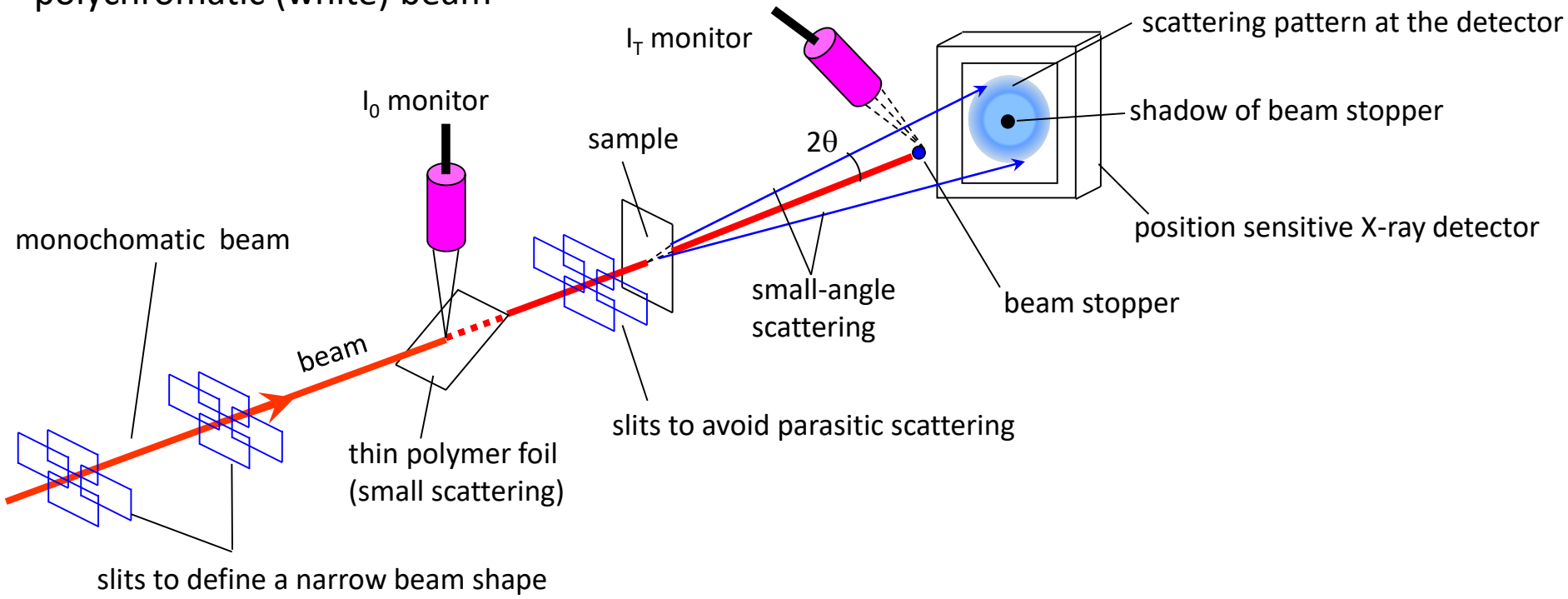

SAXS/SANS experiment:

•Determination of the scattering intensity as a function of scattering vector

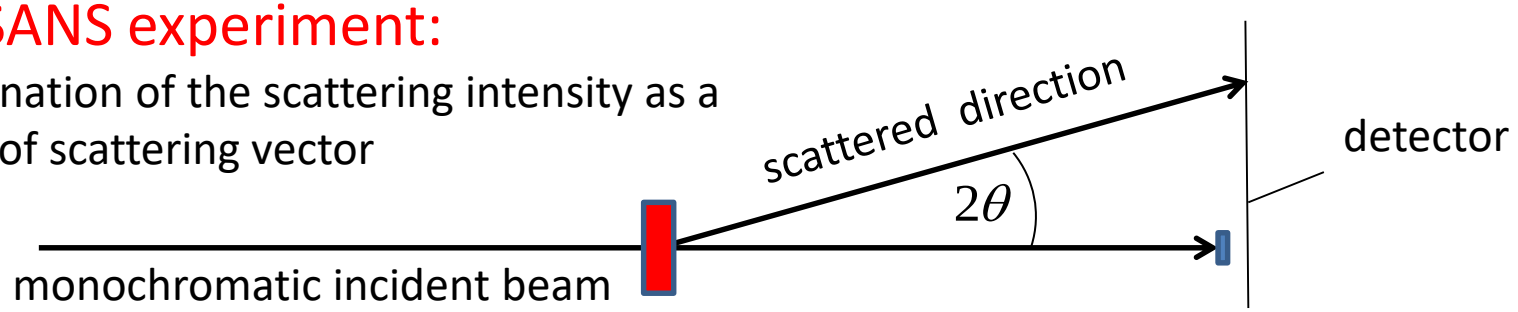

Wavevector of the incident particles



•same direction of the beam
•modulus: $2\pi/\lambda$

Wavevector of the scattered particles

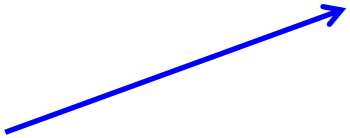

•same direction of the scattered beam
•modulus: $2\pi/\lambda$

Scattering vector:

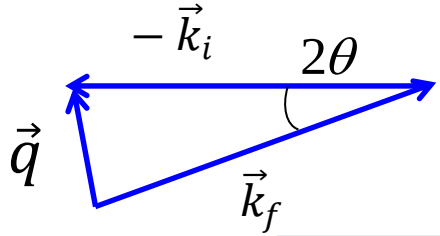

Elastic scattering energy of scattered particles (photons or neutrons) is the same as the energy of incident particles:

$$\vec{q} = \vec{k}_f - \vec{k}_i$$

$$k_f = k_i = \frac{2\pi}{\lambda}$$

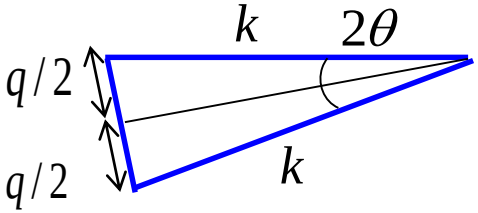

isosceles triangle

$$q = \frac{4\pi}{\lambda}\sin\theta$$

$$\sin\theta = \frac{q/2}{k}$$

Isotropic scattering

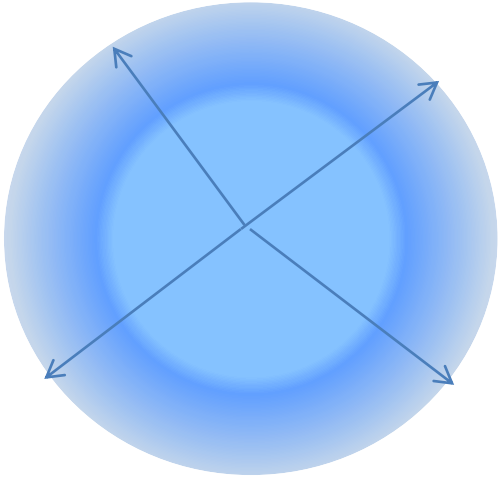

$I(q)$

Intensity depends of the modulus of scattering vector only

Anisotropic scattering

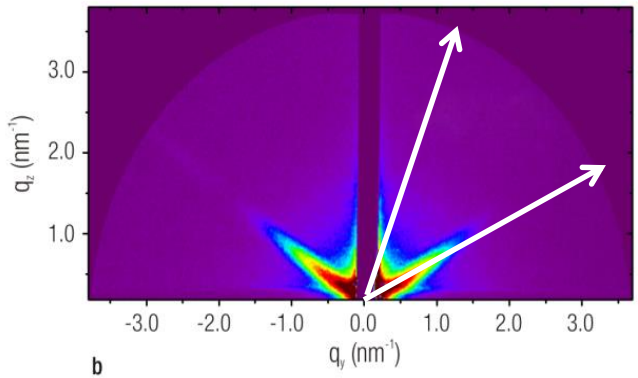

$I(\vec{q})$

Intensity depends of the modulus and direction of the scattering vector

Scattering by a single electron

$$I_e(\theta) = I_p {r_e}^2 \frac{1}{a^2} \underbrace{\frac{1+\cos^2 2\theta}{2}}$$

Polarization factor : ~ 1 in small angle region

I_p: intensity of the primary beam
a: sample-to-detector distance
2θ: scattering angle
r_e: classical electron radius (2.817×10^{-15} m)

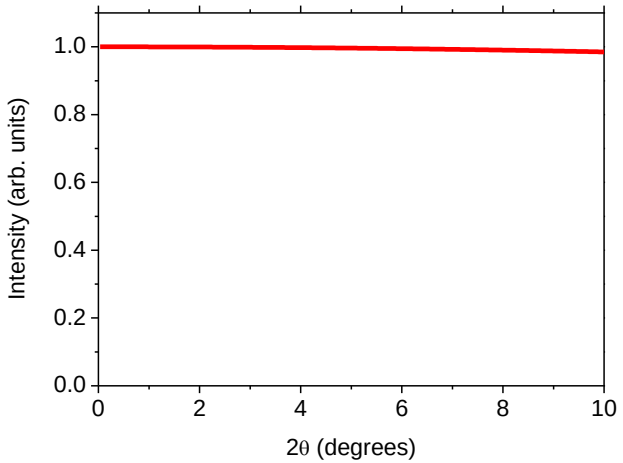

-1.5%

Atomic scattering factor (amplitude)

far from the absorption edges:

$$f_0(q) = \int_0^{\infty} \rho(r) \frac{\sin(qr)}{qr} dr \qquad q = \frac{4\pi}{\lambda} \cdot \sin(\theta)$$

$\rho(r)$: electron density

f_0: Fourier transform of electron density over the atomic volume

for q=0 f_0=Z (atomic number)

q= ∞ $f_0 \rightarrow 0$

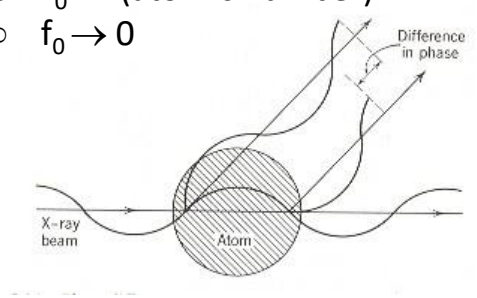

Scattering by a single atom. X-ray wavelength is of the order of the size of distribution of electrons around the atom

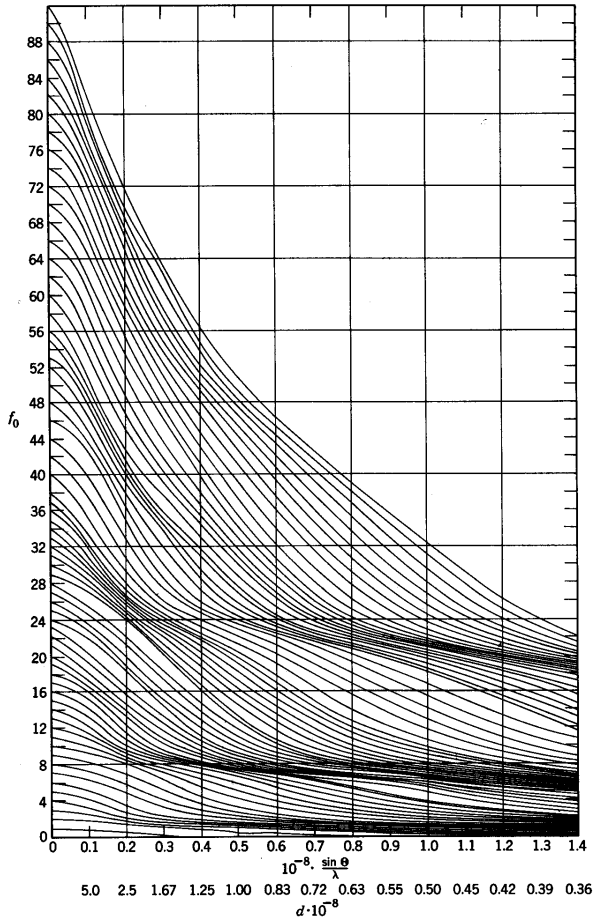

L. Pauling and J. Sherman, Z. Keystallogr.,81. 1(1932)

Coherent neutron scattering lengths [fm]

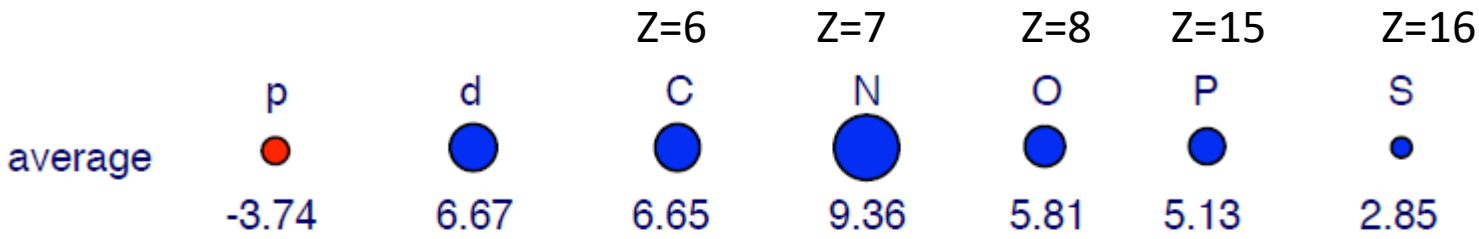



Spin-dependent scattering lengths

$$N_{b_{H_2O}} = \frac{2b_H + b_O}{V_{H_2O}} = \frac{(5.81 - 3.74 \cdot 2)\,fm}{30\,\text{Å}^3}$$

$$N_{b_{H_2O}} = -0.56 \cdot 10^{10}\,cm^{-2}$$

$$V_{H_2O} = \frac{M_{H_2O}\bar{v}_{H_2O}}{N_A}$$

Calculation of the scattering length density

neutrons deflected from hydrogen are 180° out of phase relative to those deflected by the other elements

Extracted from presentation “INTRODUCTION TO NEUTRON REFLECTOMETRY”, Giovanna Fragneto Institute Laue-Langevin

Setup for SAXS at XRD2 (LNLS)

Configuration using imaging plate film

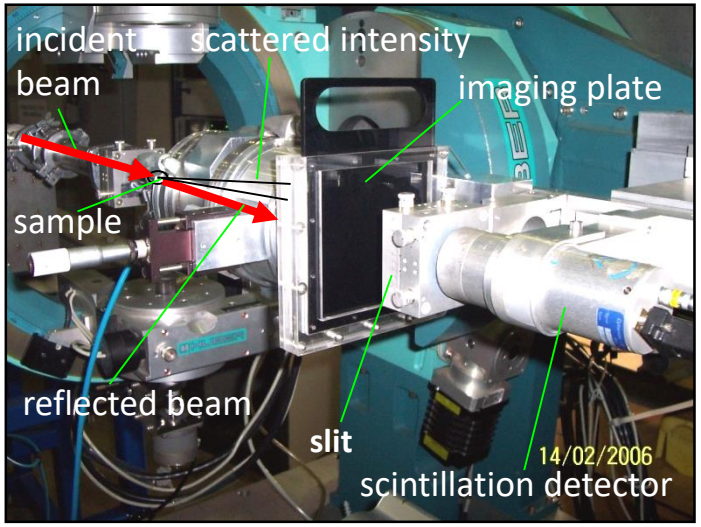

Configuration using a position-sensitive detector

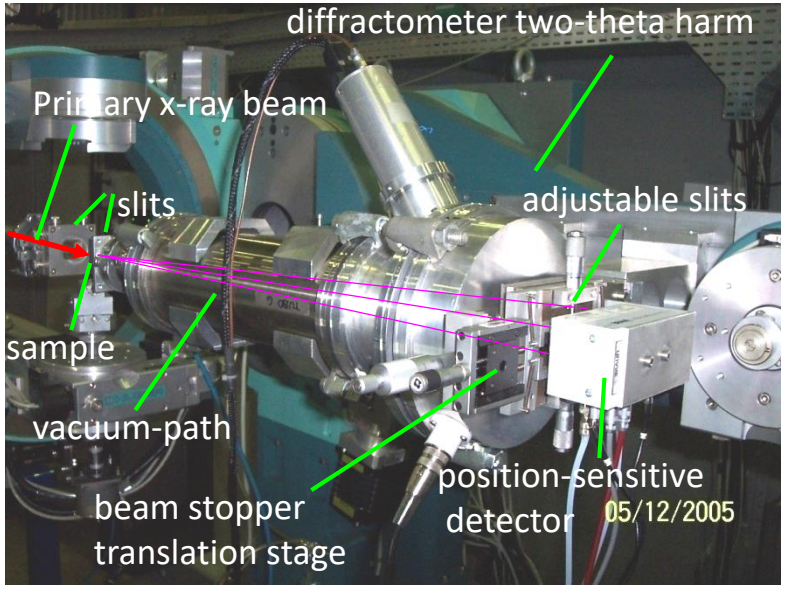

Detail of 2D window

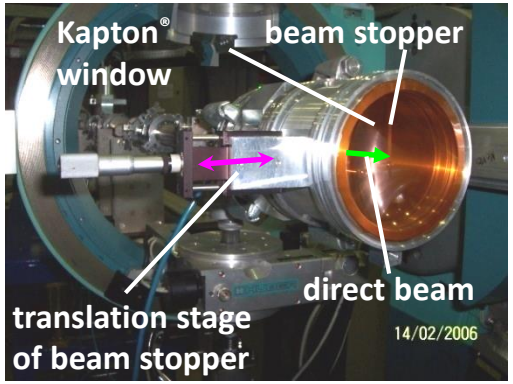

X-rays

CATERETÊ Experimental Capabilities

In vacuum detection tunnel

Sirius, Campinas, Brazil

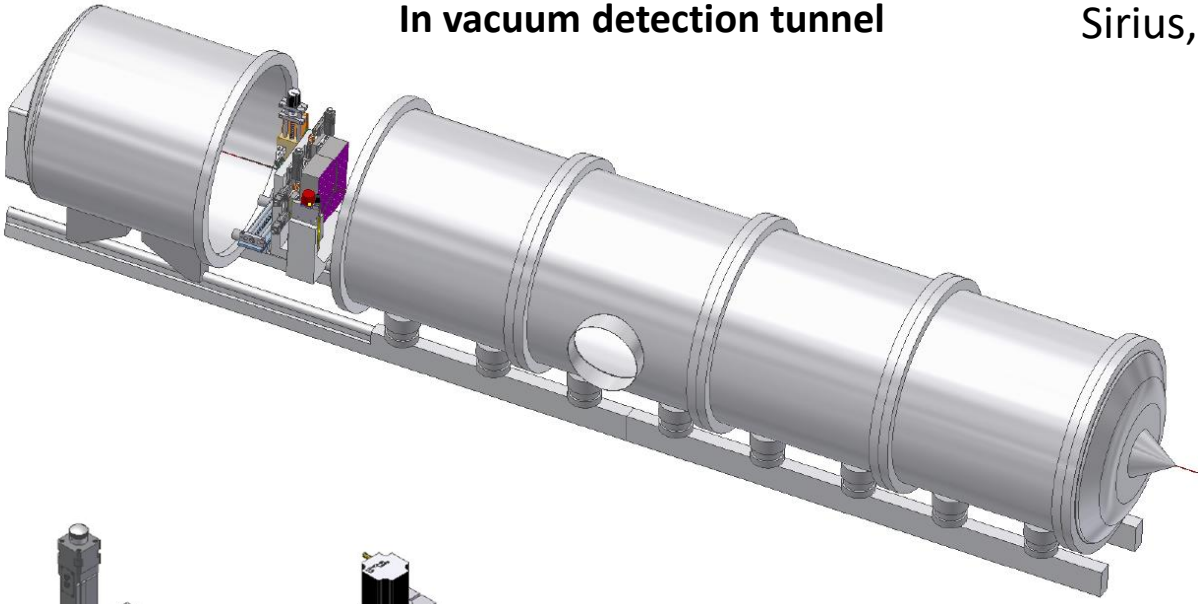

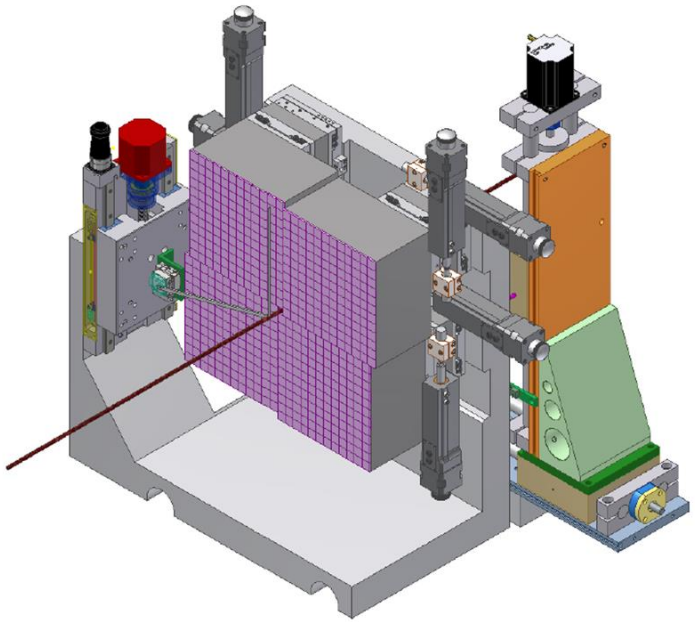

LNLS Medipix detector 6000 x 6000 pixels²

LNLS detector group

Medipix low energy possibilities, as function of the acquisition mode

	LNLS Medipix
Pixel size	55 x 55 µm²
Chip size	14.08 x 14.08 mm²
Number of pixels /chip	256 x 256
Active area / module	28.2 x 84.48 mm²
Number of thresholds / pixels	2
Number of counters /pixel	2 x 12bits
Min readout time / 12 bits images	0.3 ms
Max frame rate / 12 bits images	3200 images /s

Quokka – small-angle neutron scattering instrument

http://www.ansto.gov.au/ResearchHub/Bragg/Facilities/Instruments/Quokka

Similar D22 instrument at Institute Laue Langevin in Grenoble, France and the 30-metre instruments on NG3 and NG7 at the NIST in Gaithersburg in the USA

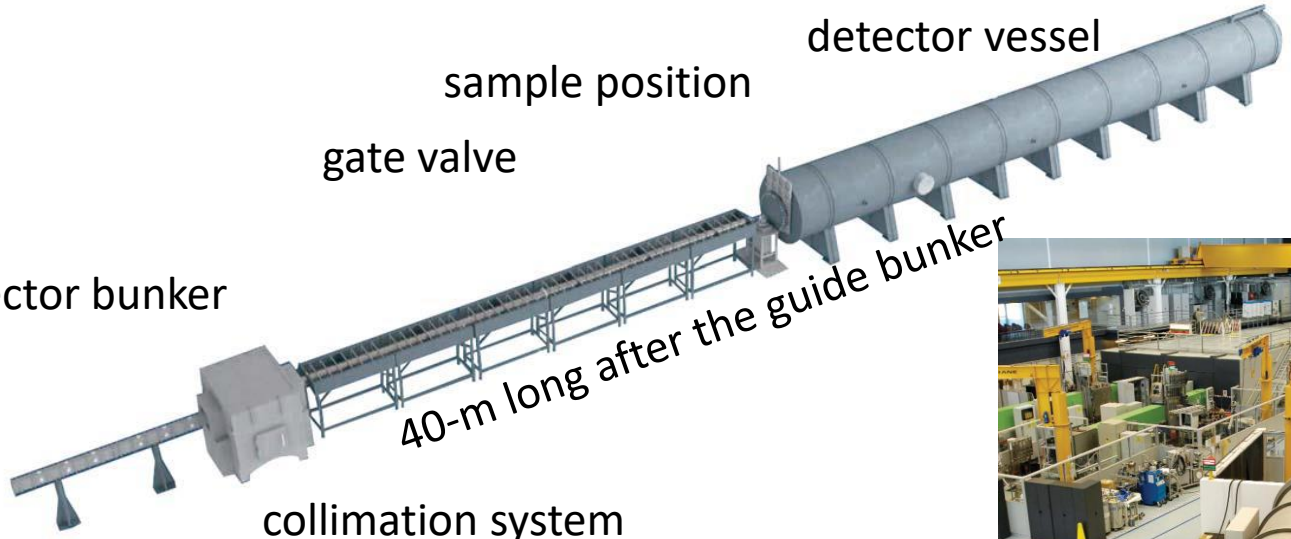



<u>The main features of Quokka are:</u>

- High brilliance of the cold source, CG1
- High performance selector (peak transmission 94%)
- Large (960 x 960 mm) detector of 5 x 5 mm pixels
- High dynamic q-range (in single configuration typical qmax/qmin of ca. 10 in central and 15 in offset position)

SAS (transmission)

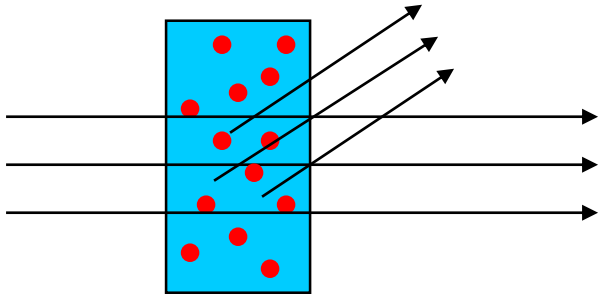

information is obtained over the entire irradiated volume

incidence normal to the sample surface

GISAXS (grazing-incidence)

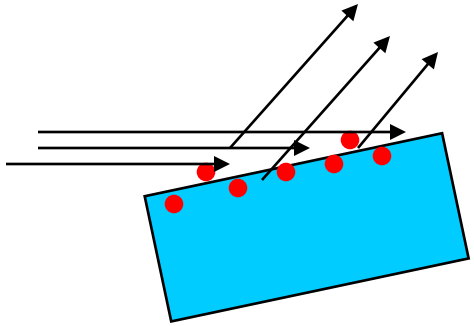

small information depth is obtained (5 to few hundred of nanometers from top surface)

incidence and/or exit angles of the radiation must be comparable to the critical angle α_c

SAS intensity from different objects



spheres R= 5 nm

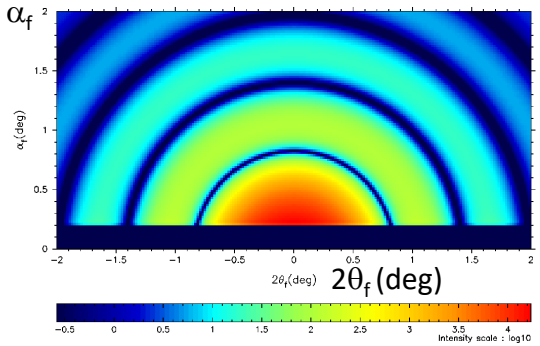

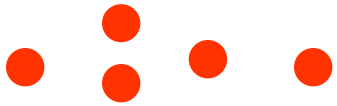

spheres R= 10 nm

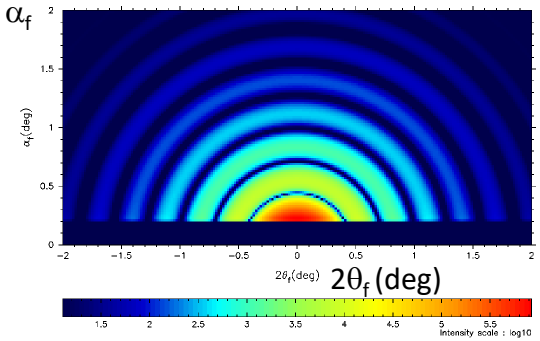



Prolate spheroid H/W=2

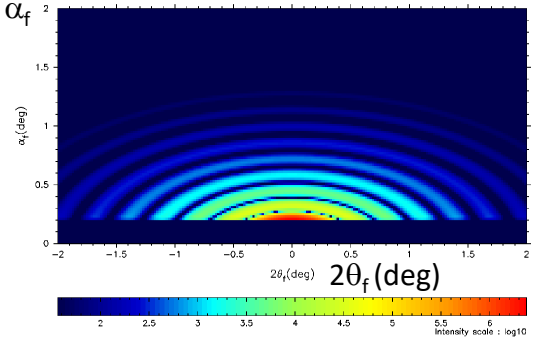



spheres $\langle R \rangle$= 5 nm

$\sigma/\langle R \rangle$=0.2

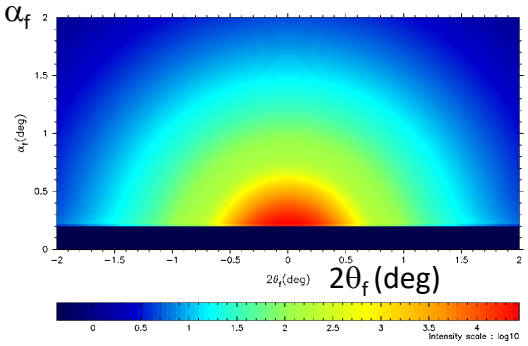



spheres $\langle R \rangle$= 10 nm

$\sigma/\langle R \rangle$=0.2

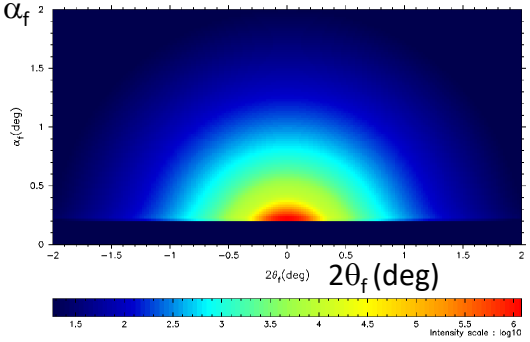

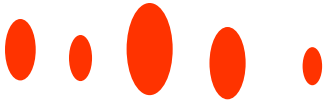

$\langle R \rangle = \langle W \rangle/2$=10 nm

$\sigma/\langle R \rangle$=0.2- H/W =2

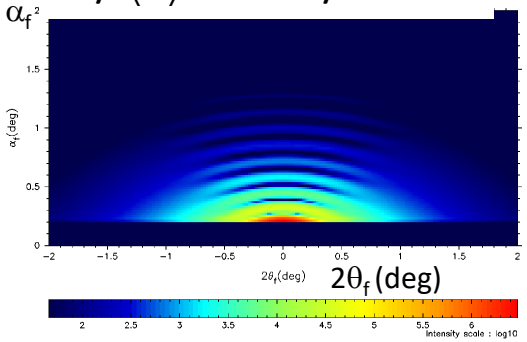

The analysis of SAS intensity allows determination of:

- **Shape,**
- **average size,**
- **size dispersion,**
- **spatial correlation,**
- **number density and**
- **orientation of nanoparticles**

Examples of application:

- Studies of nanocomposite thin films

- Studies of microdomain formation and ordering in thin films and surfaces of copolymer materials

- Studies of semiconductor and metallic nanostructures (quantum dots, wires, and wells). Nanometer-sized metallic particles embedded in glass matrix (candidates for applications in the fields of nonlinear integrated optics and photonics)

- macromolecules

Advantages:

- a non-destructive structural probe
- does not require a conducting surface or sample preparation (*this is not the case for TEM*)
- yields excellent sampling statistics (averages over macroscopic regions to provide information on nanometer scale)
- surface selectivity (GISAXS)
- in-situ characterization is possible

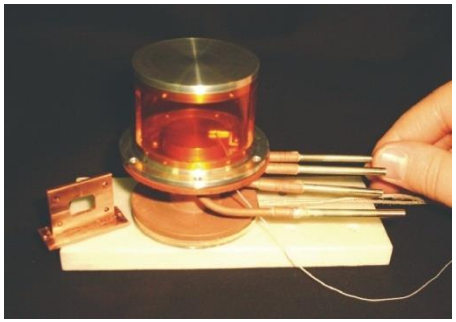

GISAXS furnace designed for He flowthrough and rapid thermal quenching of samples mounted in the horizontal plane (Queen's University)

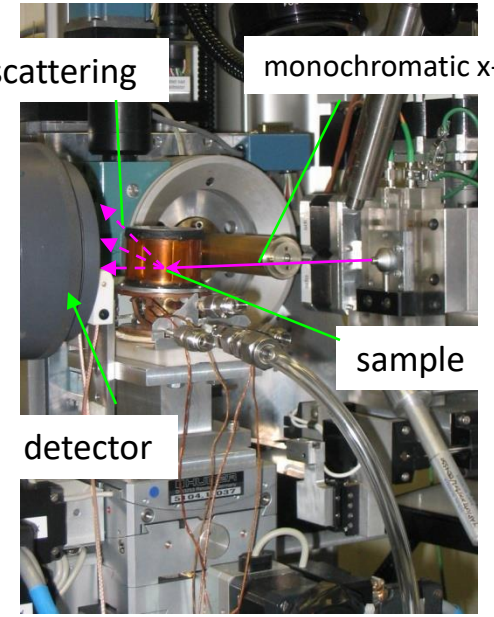

GISAXS experimental apparatus at NSLS Beamline X12B

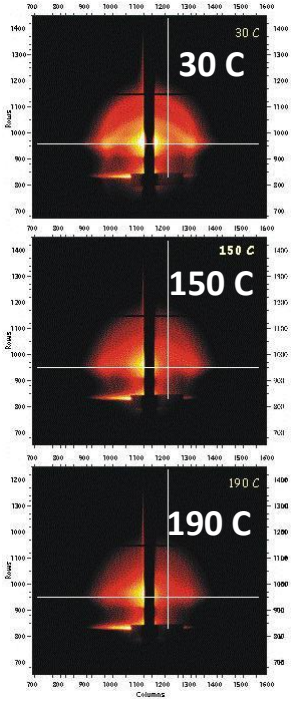

Symmetric diblock styrene-butadiene temperature dependence

The scattered intensity

Scattering **amplitude** of a single nanoparticle:

$$F(\vec{q}) = \int \rho(\vec{r})\mathrm{Exp}(\overrightarrow{q} \cdot \vec{r})\, d\vec{r}$$

(Fourier transform of object electron density)

Scattering **intensity** of a single nanoparticle:

$$I(\vec{q}) = F(\vec{q}) \cdot F^{*}(\vec{q})$$

Calculation of the form factor of a parallelepiped

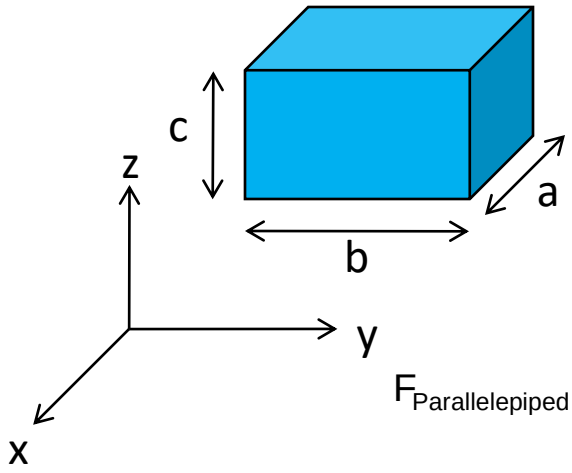

$$F(\vec{q}) = \int \rho(\vec{r})\,\mathrm{Exp}(\vec{q}\cdot\vec{r})\,d\vec{r}$$

$$F_{Parallelepiped}(q_x,q_y,q_z) = \rho \int_{x=-a/2}^{a/2}\int_{y=-b/2}^{b/2}\int_{z=-c/2}^{c/2} \exp[-i(q_x x + q_y y + q_z z)]dxdydz$$

$$F_{Parallelepiped}(q_x,q_y,q_z) = \rho \int_{x=-a/2}^{a/2}\int_{y=-b/2}^{b/2}\int_{z=-c/2}^{c/2} \exp[-iq_x x]dx\cdot\exp[-iq_y y]dy\cdot\exp[-iq_z z]dz$$

$$\int_{-a/2}^{a/2} \exp[-iq_x x]dx = \int_{-a/2}^{a/2} \cos(q_x x)dx - i\underbrace{\int_{-a/2}^{a/2} \sin(q_x x)dx}_{0}$$

$$\int_{-a/2}^{a/2} \exp[-iq_x x]dx = 2\int_{0}^{a/2} \cos(q_x x)dx = a\frac{\sin(q_x a/2)}{q_x a/2}$$

$$F_{Parallelepiped}(q_x,q_y,q_z) = \rho(abc)\frac{\sin(q_x a/2)}{q_x a/2}\cdot\frac{\sin(q_y b/2)}{q_y b/2}\cdot\frac{\sin(q_z c/2)}{q_z c/2}$$

$$I_{Parallelepiped}(q_x,q_y,q_z) = \rho^2 v^2\left(\frac{\sin(q_x a/2)}{q_x a/2}\cdot\frac{\sin(q_y b/2)}{q_y b/2}\cdot\frac{\sin(q_z c/2)}{q_z c/2}\right)^2 \qquad v = abc = \text{volume}$$

Calculation of the form factor of a sphere of radius R

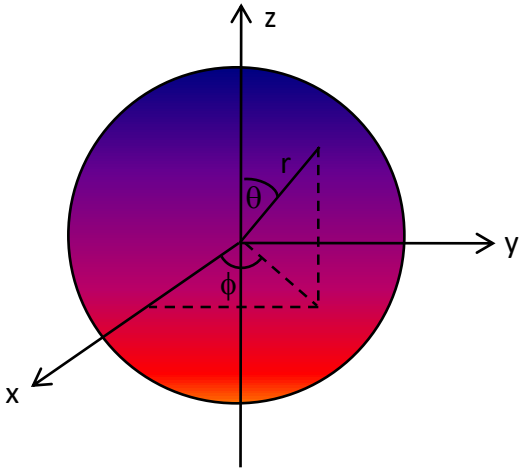

$$F(\vec{q}) = \int \rho(\vec{r})\mathrm{Exp}(\vec{q}\cdot\vec{r})\,d\vec{r}$$

$$F_{sphere}(q) = \rho \int_{r=0}^{R}\int_{\theta=0}^{\pi}\int_{\phi=0}^{2\pi} \exp(-iq_z r\cos\theta) r^2 \sin\theta\, d\theta\, d\phi\, dr$$

$$F_{sphere}(q) = 2\pi\rho \int_{r=0}^{R}\int_{\theta=0}^{\pi} \exp(-iq_z r\cos\theta) r^2 \sin\theta\, d\theta\, dr$$

$$u = -q_z\cos\theta \qquad du = q_z \sin\theta\, d\theta$$

$$F_{sphere}(q) = \frac{2\pi\rho}{q_z}\int_{r=0}^{R} r^2 \int_{u=-q_z}^{q_z} \exp(-iru)\,du\,dr$$

$$F_{sphere}(q) = \frac{2\pi\rho}{q_z}\int_{r=0}^{R} r^2 \left[\int_{u=-q_z}^{q_z} \cos(ur)\,du - i\int_{u=-q_z}^{q_z} \cancelto{0}{\sin(ur)\,du}\right] dr$$

$$F_{sphere}(q) = \frac{2\pi\rho}{q_z}\int_{r=0}^{R} r^2 \left[2\int_{u=0}^{q_z} \cos(ur)\,du\right] dr$$

$$\int_{u=0}^{q_z} \cos(ur)\,du = \frac{1}{r}\sin(ur)\Big|_0^{q_z} = \frac{1}{r}\sin(q_z r)$$

$$F_{sphere}(q) = \frac{4\pi\rho}{q_z}\int_{r=0}^{R} \sin(q_z r) r\,dr$$

$$F_{sphere}(q) = \frac{4\pi\rho}{q_z}\left[\frac{\sin(q_z r)}{q_z^2} - \frac{r\cos(q_z r)}{q_z}\right]_{r=0}^{R} = \frac{4\pi\rho}{q_z^3}[\sin(q_z r) - q_z r\cos(q_z r)]\Big|_{r=0}^{R}$$

$$F_{sphere}(q) = \frac{4\pi\rho}{q_z^3}[\sin(q_z R) - q_z R\cos(q_z R)]$$

$$I_{sphere}(q) = \left(\frac{4\pi\rho}{q_z^3}\right)^2 [\sin(q_z R) - q_z R\cos(q_z R)]^2$$

Scattering by spherical nanoparticles

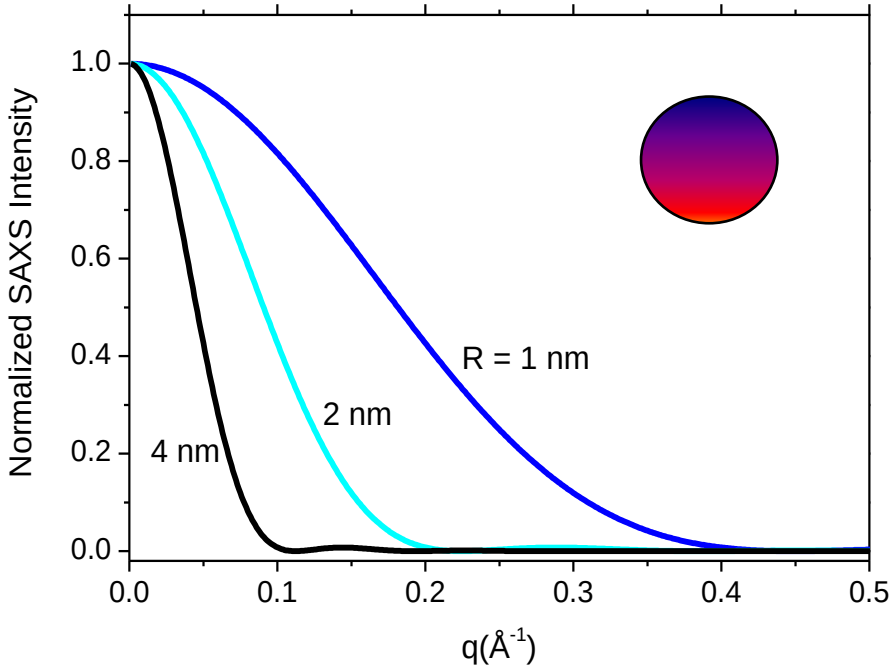

Tabulated Form Factors:

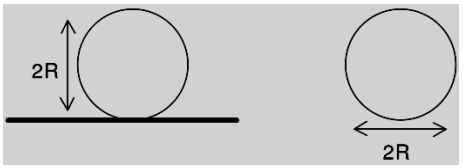

sphere

$$F_{fsp}(\mathbf{q}, R) = 4\pi R^3 \frac{\sin(qR) - qR\cos(qR)}{(qR)^3} \exp(-iq_z R)$$

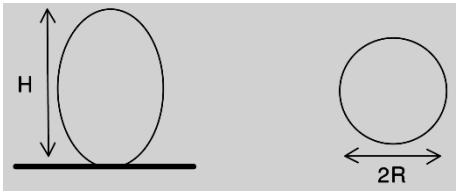

prolate spheroid

$$F_{fsph}(\mathbf{q}, R, H) = \exp(-iq_z H/2) \int_0^{H/2} 4\pi R_z^2 \frac{J_1(q_\parallel R_z)}{q_\parallel R_z} \cos(q_z z)\, dz$$

$$q_\parallel = \sqrt{q_x^2 + q_y^2},\ R_z = R\sqrt{1 - 4\frac{z^2}{H^2}}$$

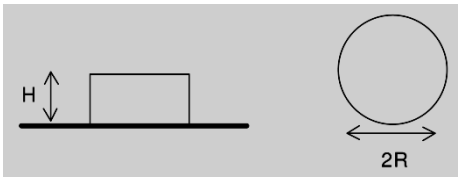

cylinder

$$F_{cy}(\mathbf{q}, R, H) = 2\pi R^2 H \frac{J_1(q_\parallel R)}{q_\parallel R} \mathrm{sinc}(q_z H/2) \exp(-iq_z H/2)$$

$$q_\parallel = \sqrt{q_x^2 + q_y^2}$$

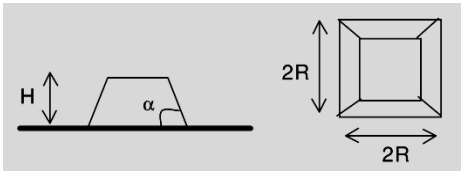

pyramid

$$F_{py}(\mathbf{q}, R, H, \alpha) = \int_0^H 4R_z^2 \mathrm{sinc}(q_x R_z)\mathrm{sinc}(q_y R_z) \exp(-iq_z z)\, dz$$

$$R_z = R - z/\tan(\alpha)$$

$$H/R < \tan(\alpha)$$

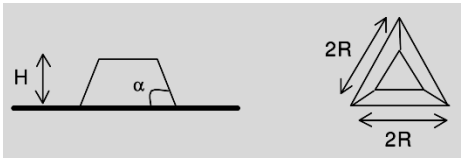

tetrahedron

$$F_{te}(\mathbf{q}, R, H, \alpha) =$$

$$\int_0^H \frac{2i\sqrt{3}}{q_x(q_x^2 - 3q_y^2)} \left[q_1 \sin(q_2 R_z/2) \exp(iq_x R_z/2) - q_2 \sin(q_1 R_z/2) \exp(-iq_x R_z/2)\right] \exp(-iq_z z) dz$$

$$q_1 = \sqrt{3}q_y - q_x,\ q_2 = \sqrt{3}q_y + q_x,\ R_z = R - 2z/\sqrt{3}\tan(\alpha)$$

$$H/R < \sqrt{3}/2\tan(\alpha)$$

Scattering intensity by a set of nanoparticles:

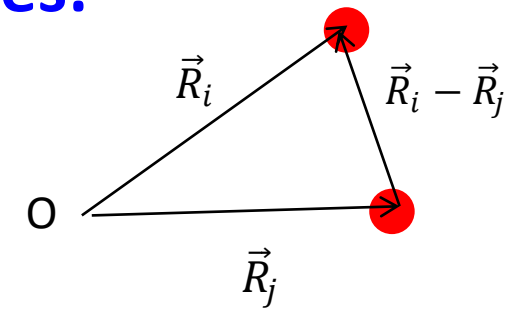

Amplitude $$F(\vec{q}) = \sum_i F_i(\vec{q}) \exp\left[-i\vec{q} \cdot \vec{R}_i\right]$$

Intensity $$F(\vec{q}) \cdot F(\vec{q})^* = \sum_i \sum_j F_j(\vec{q})^* F_i(\vec{q}) \exp\left[-i\vec{q} \cdot \left(\vec{R}_i - \vec{R}_j\right)\right]$$

By isolating the i = j terms, one has:

$$I(\vec{q}) = F(\vec{q}) \cdot F(\vec{q})^* = \underbrace{\sum_i F_i(\vec{q}) F_i(\vec{q})^*}_{\text{Sum of the intensity of all particles}} + \underbrace{\sum_i \sum_{j \neq i} F_j(\vec{q})^* F_i(\vec{q}) \exp\left[-i\vec{q} \cdot \left(\vec{R}_i - \vec{R}_j\right)\right]}_{\text{term accounting for interparticle interference (structure factor)}}$$

In absence of correlation in particles distances (diluted systems)

If particles are randomly displaced:

$$I(\vec{q}) = F(\vec{q}) \cdot F(\vec{q})^* = \sum_i F_i(\vec{q}) F_i(\vec{q})^* + \sum_i \sum_{j \neq i} F_j(\vec{q})^* F_i(\vec{q}) \exp[-i\vec{q} \cdot (\vec{R}_i - \vec{R}_j)]$$

0

$$I(\vec{q}) = \sum_i F_i(\vec{q}) F_i(\vec{q})^* = \sum_i I_i(\vec{q})$$

Monodisperse

(particles are identical)

$$I(\vec{q}) = N I_1(\vec{q})$$

number of particles

If randomly oriented

$$I(q) = N \langle I_1(\vec{q}) \rangle$$

< > : orientation average

Polydisperse

(in general case: different sizes and shapes)

For particles with same shape having a size dispersion given by $N(R)$:

$$I(\vec{q}) = F(\vec{q}) \cdot F(\vec{q})^* = \sum_i I_i(\vec{q}) = \int N(R) \, |F(\vec{q}, R)|^2 v^2(R) dR$$

$N(R)\mathrm{d}R$: number of particles with radius between R and $R+\mathrm{d}R$

Monodisperse interacting particles

$$I(q) = \sum \langle |F^i(\vec{q})|^2 \rangle + \langle \sum_{i,j \neq i} F^i(\vec{q}) F^j(\vec{q}) \exp[-i\vec{q} \cdot (\vec{R}^i - \vec{R}^j)] \rangle$$ (general equation)

For randomly oriented nanoparticles

$$F^i(\vec{q}) = F^j(\vec{q}) \quad \Rightarrow \quad I(q) = N\langle |F^1(\vec{q})|^2 \rangle + N\langle |F^1(\vec{q})|^2 \rangle [S(q) - 1]$$

or

$$I(q) = N\langle |F^1(\vec{q})|^2 \rangle S(q)$$

where

$$S(q) = 1 + \rho \int g(R^{ij}) \exp[-iq \cdot R^{ij}] dR^{ij}$$

Debye hard-core model:

$$g(R^{ij}) = 1 \quad \text{if} \quad R^{ij} > 2R$$

$$g(R^{ij}) = 0 \quad \text{if} \quad R^{ij} \leq 2R$$

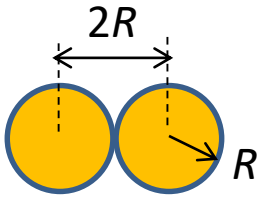

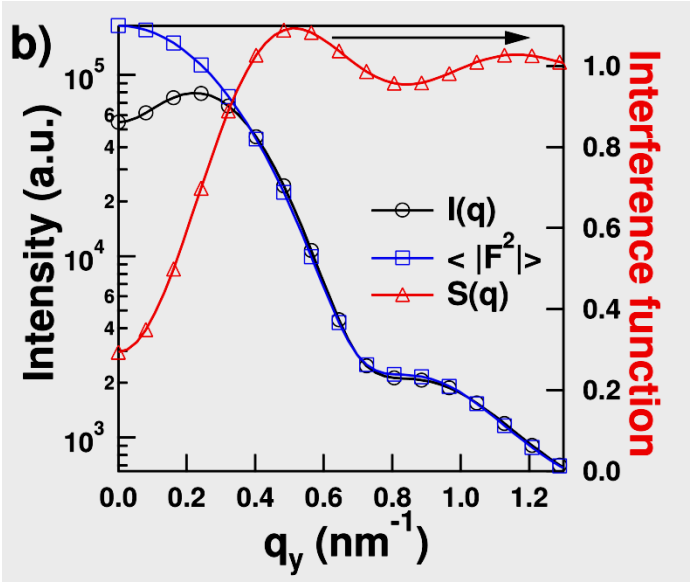

Small-angle scattering

Some examples of applications

Application in Biology

Beatriz Tremarin[1], Fabiano Yokaichiya[1], Guinther Kellermann[1], Margareth K.K.D. Franco[2], Christian Schmidt[3], Joachim Storsberg[3]

Anticorpo: proteína gerada pela resposta imune que ataca vírus e bactéria

IgG é o anticorpo mais abundante no soro humano (forma de Y)

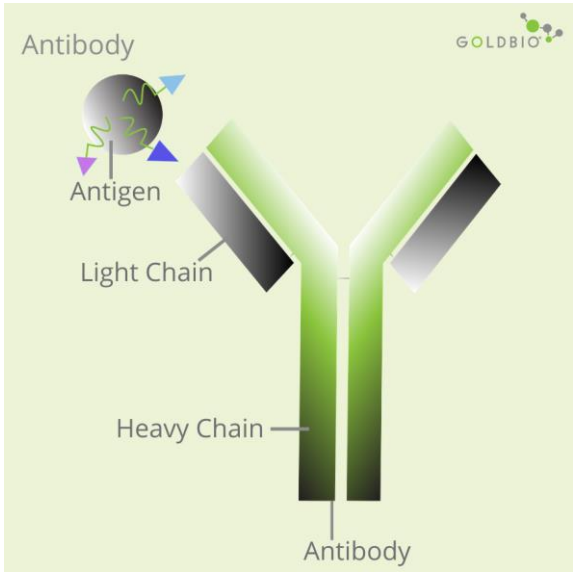

https://www.goldbio.com/articles/article/an-introduction-to-primary-antibodies-and-secondary-antibodies

Imunoglobulina linfoma anti-canino

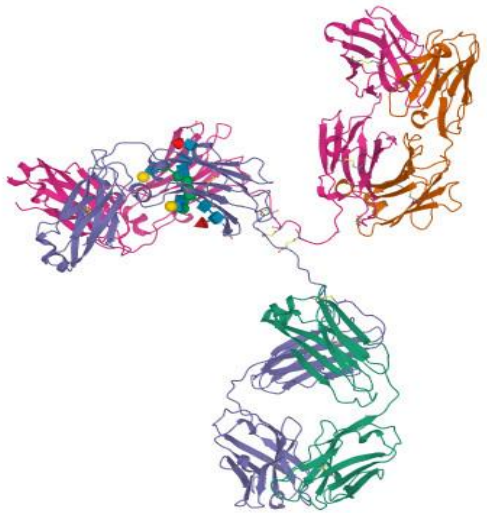

Massa molecular: 150 kDa

Estrutura tridimensional do anticorpo monoclonal linfoma anti-canino determinada pela técnica de cristalografia de proteínas (PDB - 1IGT)

Curva de intensidade de SAXS

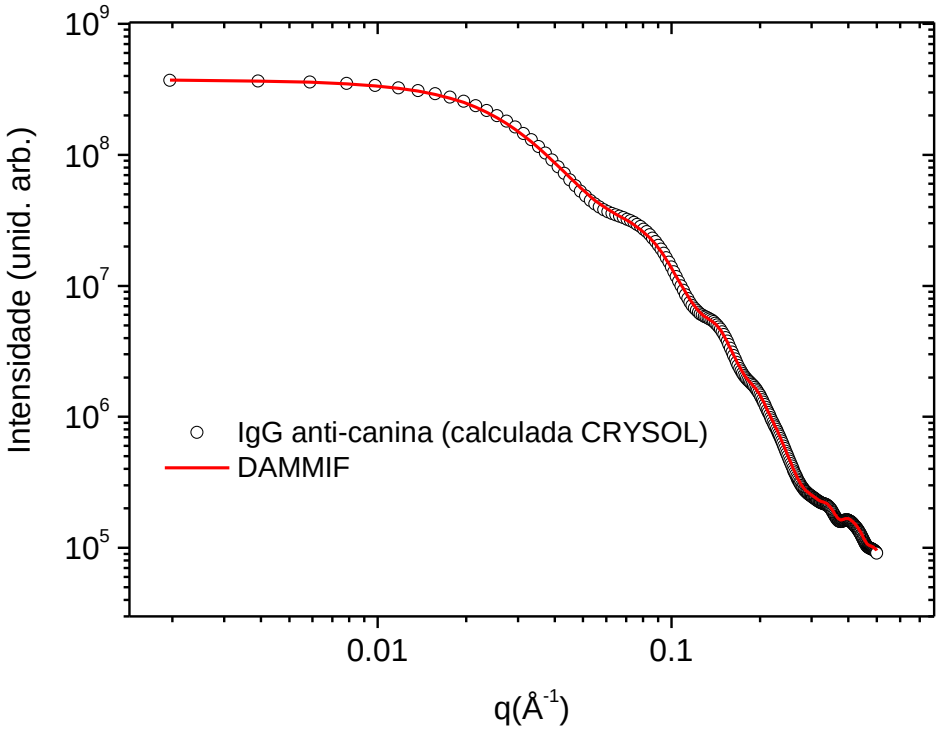

Estrutura 3D da imunoglobulina monoclonal linfoma anti-canina.

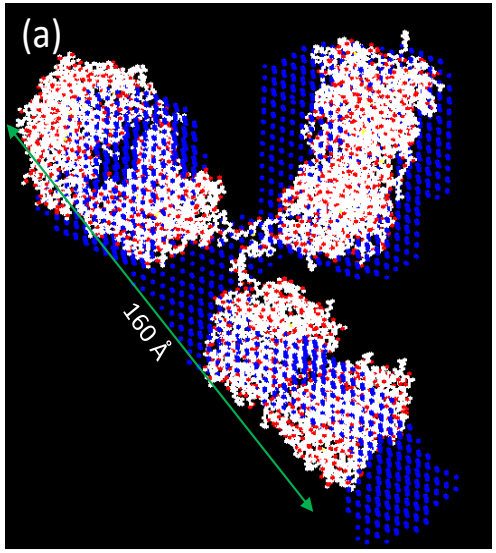

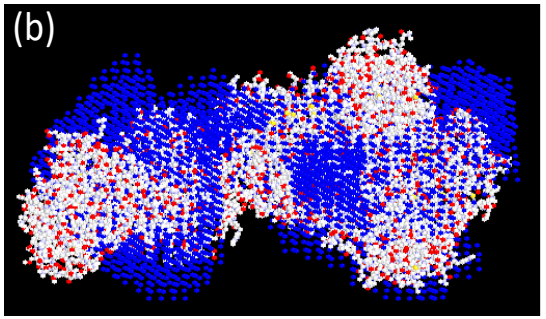

- Esferas brancas e vermelhas: estrutura tridimensional determinada por cristalografia de raios X.

- Esferas azuis: estrutura tridimensional da mesma imunoglobulina determinada da curva de intensidade de SANS calculada usando o programas GNOM e DAMMIF

RESULTS: Transmission Electron Microscopy

LME / LNLS, Campinas, SP

- Nearly spherical Bi nanocrystals

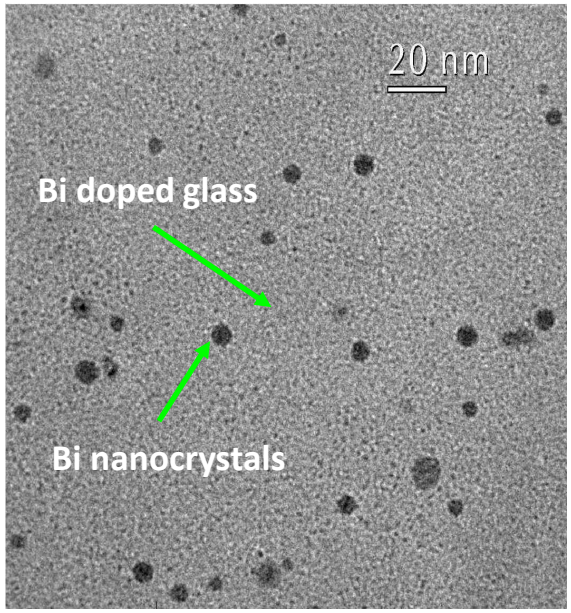

Bright Field TEM image of Bi nanocrystals in a $28Na_2O$-$72B_2O_3$ glass. Nanocrystals were obtained after thermal annealing of the doped Bi glass at 843 K during 2 hours.

- Single-mode size distribution function

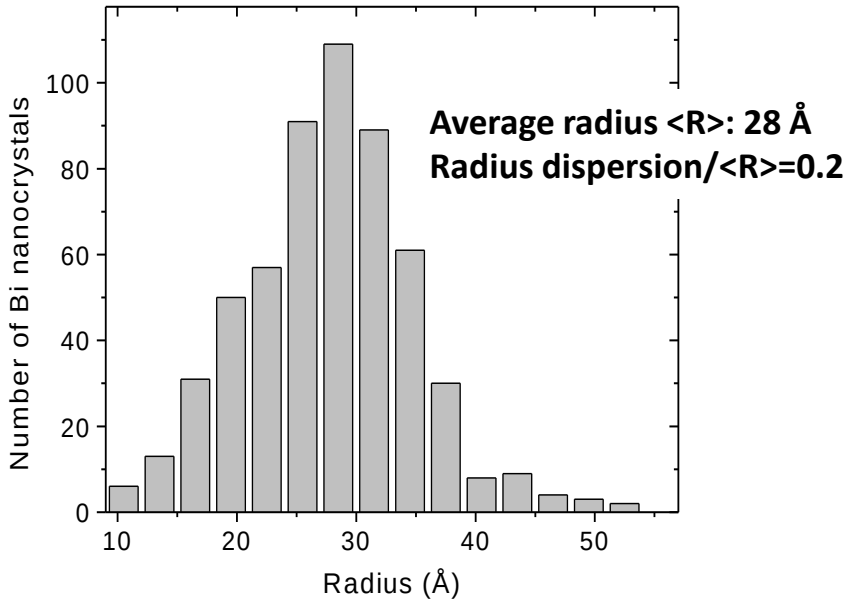

Histogram of the particle radius dispersion.

Small-Angle X-ray Scattering - SAXS

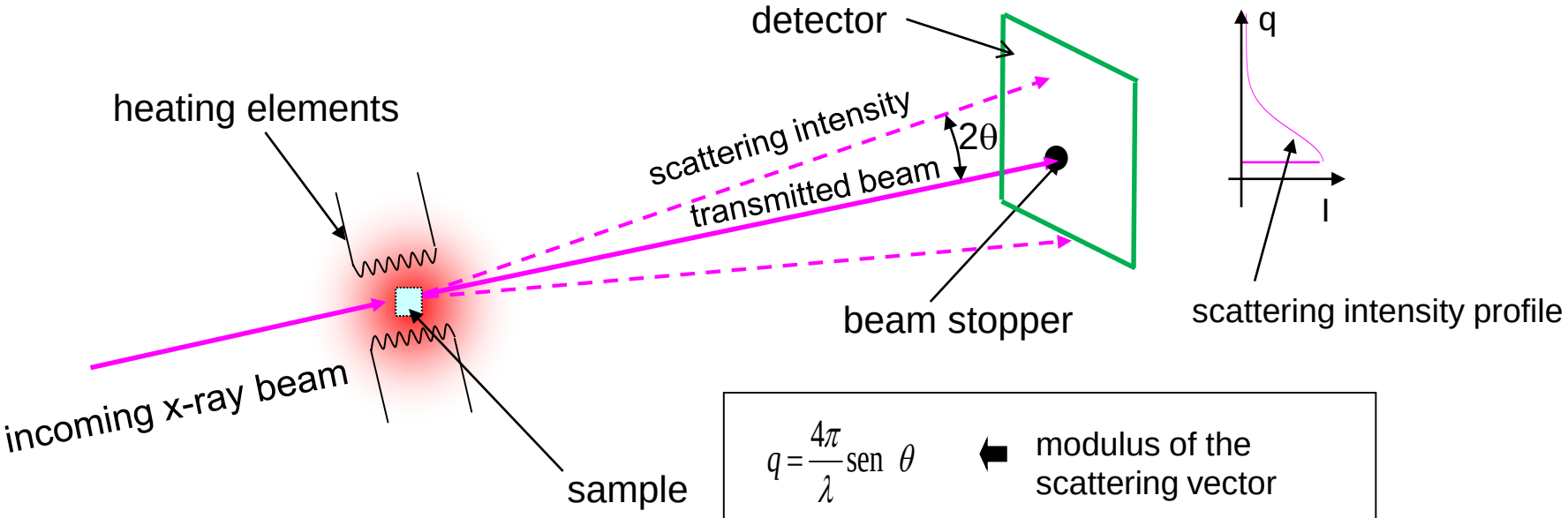

$$q = \frac{4\pi}{\lambda} \operatorname{sen}\ \theta$$

modulus of the scattering vector

λ: x-ray wavelength

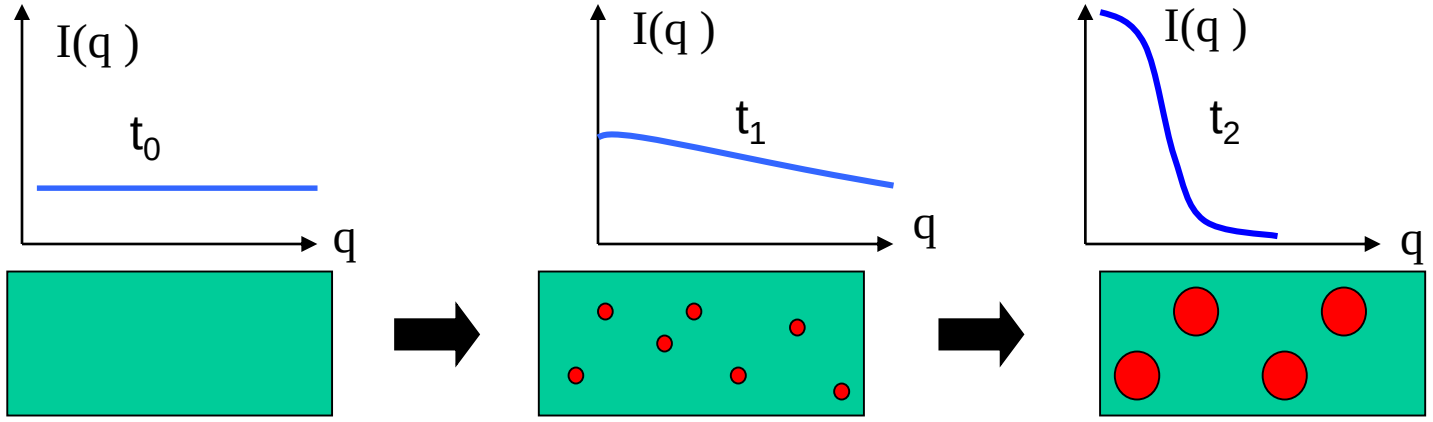

Isothermal transformation

SAXS intensity for diluted polydisperse system:

$$I(q) = I_0(\rho - \langle p \rangle)^2 \int N(R)\,|F(q,R)|^2 v^2(R) dR$$

ρ_p: particle electron density.
$\langle\rho\rangle$: matrix electron density.
N(R)dR : number of particle per unity volume between *R* and *R+dR*.
q : modulus of the scattering vector.
F(q,R) : particle form factor
I_0: scattering intensity by a single electron

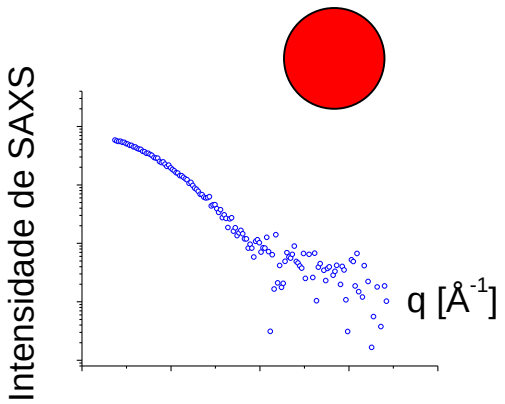

Numeric methods

$$P(q,R) = \left[3\frac{\text{sen}(qR) - qR\cos(qR)}{(qR)^3} \right]^2$$

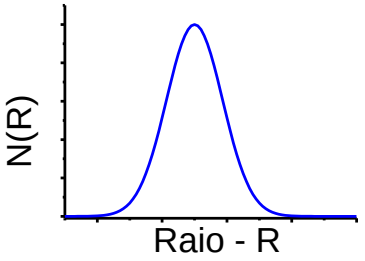

Fraction of total volume occupied by the nanoparticles

Integrated SAXS intensity

$$Q = 4\pi \int_{q=0}^{\infty} I(q) \cdot q^2 dq$$

Volume fraction

$$\varphi(t) = \frac{1}{2} - \left(\frac{1}{4} - \frac{Q(t)}{4\pi^3 r_0^2 \Delta\rho^2} \right)^{1/2}$$

Radius distribution function: N(R)

Average radius

$$< R >= \frac{\int R \cdot N(R) \cdot dR}{n}$$

Number density

$$n = \int N(R) dR$$

Relative size dispersion

$$\sigma_R / \langle R \rangle = \frac{\sqrt{\frac{\int (R - \langle R \rangle)^2 \cdot N(R) \cdot dR}{n}}}{\langle R \rangle}$$

Volume fraction

$$\varphi = \frac{4\pi}{3} \int N(R) R^3 dR$$

LNLS SAXS beam line

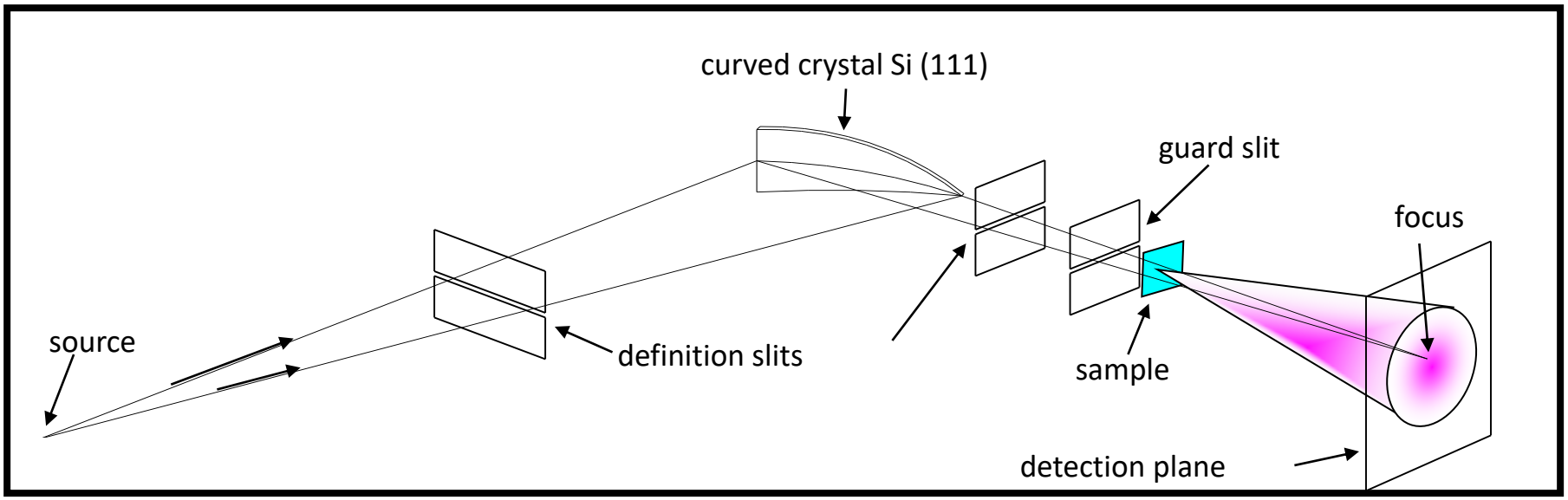

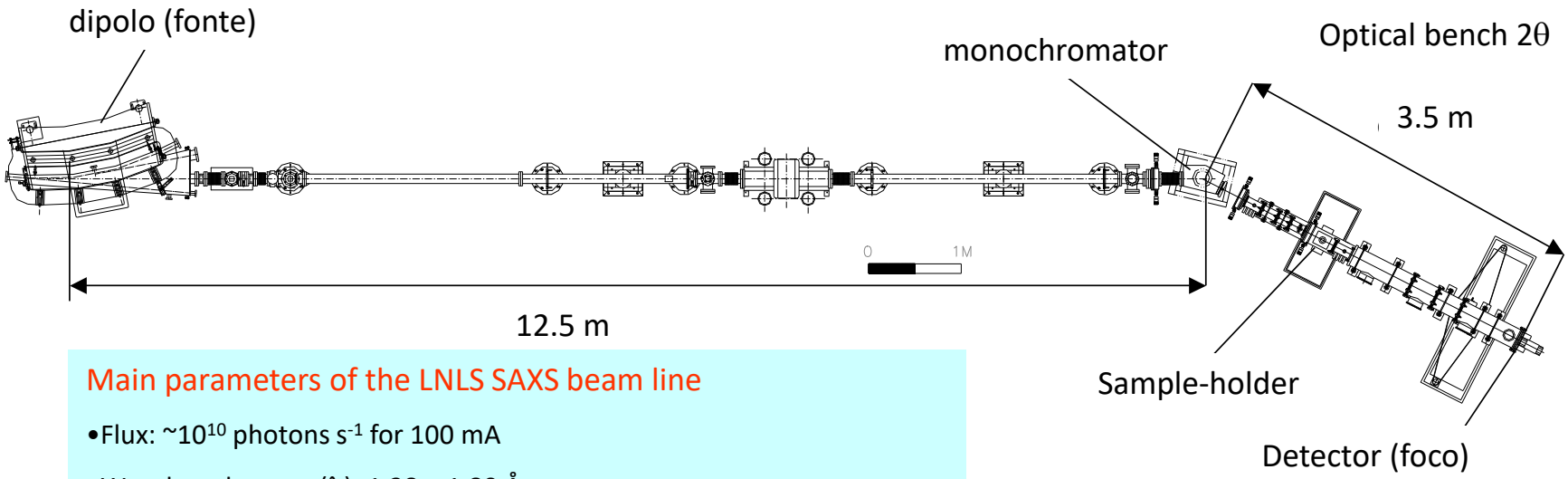

Main parameters of the LNLS SAXS beam line

- Flux: ~10^{10} photons s^{-1} for 100 mA
- Wavelength range (λ): 1.38 – 1.80 Å.
- Scattering vector (for λ=1.61 Å):
  0.01 – 1 $Å^{-1}$ (sample to detector distance: 30 cm) ,
  0.005 – 0.2 $Å^{-1}$ (sample to detector distance : 160 cm).
- Energy resolution ($\Delta E/E$): 5×10^{-3} @ 7.7 KeV.

G. Kellermann, F. Vicentin, E. Tamura, M. Rocha, H. Tolentino, A. Barbosa, A. F. Craievich and I. L. C. Torriani,
J. Appl. Cryst. (1997). 30, 880-883

Experimental setup for *in situ* de WAXS/SAXS at high temperatures

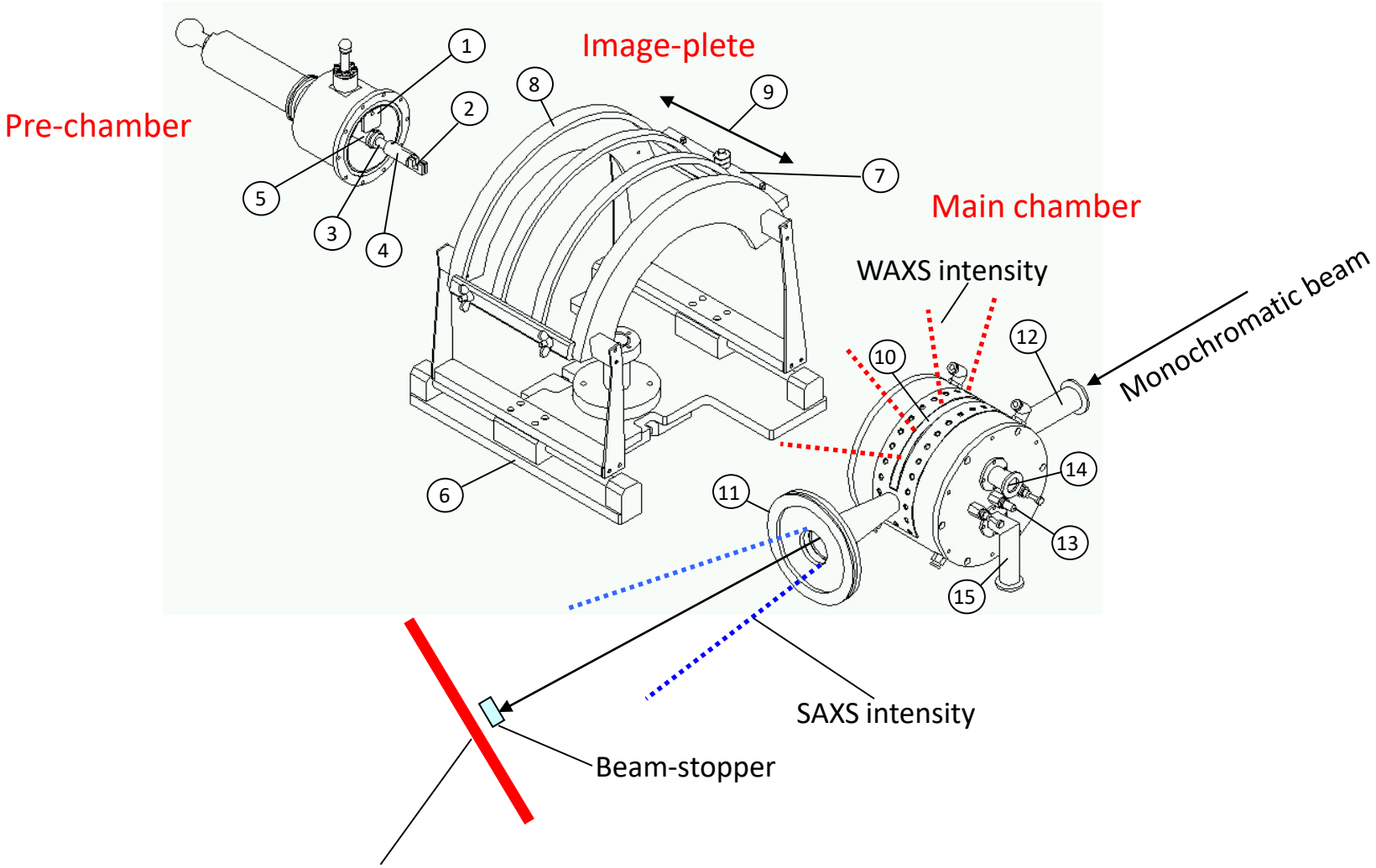

G. Kellermann, A. F. Craievich, R. Neuenschwander and T. S. Plivelic, *Nuclear Instruments and Methods in Physics Research B* 199 (2003), 112-116.

Nucleation and growth of Bi nanoclusters in sodium borate glass

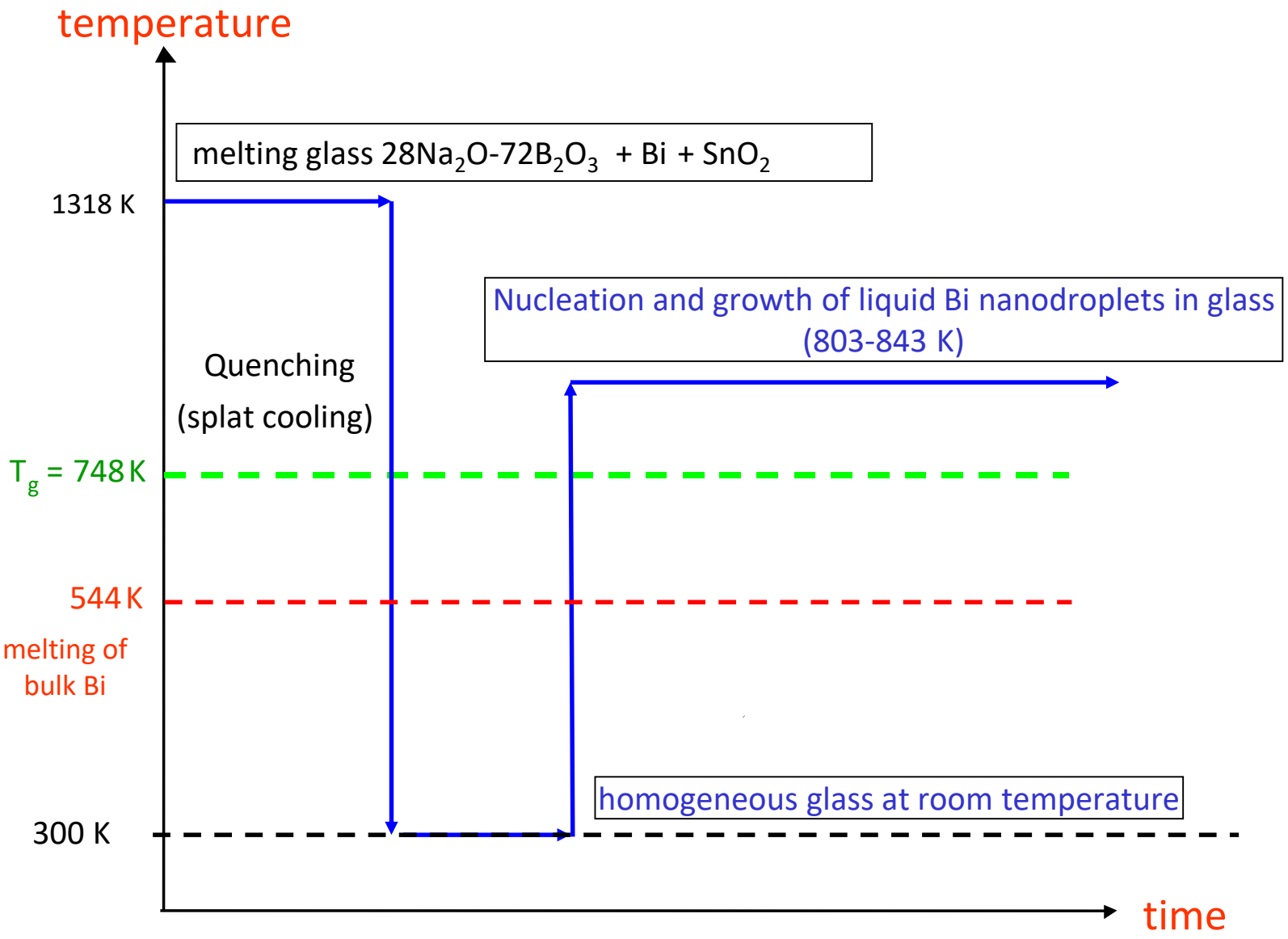

SAXS RESULTS

Modelled intensity

$$I(q) = r_0^{\,2} \cdot \left(\rho_p - \langle\rho\rangle\right)^2 \cdot \left(\frac{4\pi}{3}\right)^2 \cdot \int_0^{\infty} N(R) \cdot \left[3\frac{\mathrm{sen}(qR) - qR\cdot\cos(qR)}{(qR)^3}\right]^2 \cdot R^6 \cdot dR$$

LOGNORMAL: $$N(R) = \frac{n}{\sqrt{2\pi\exp(w^2)}\cdot wr} e^{-(\ln(R/r)/w)^2/2}$$

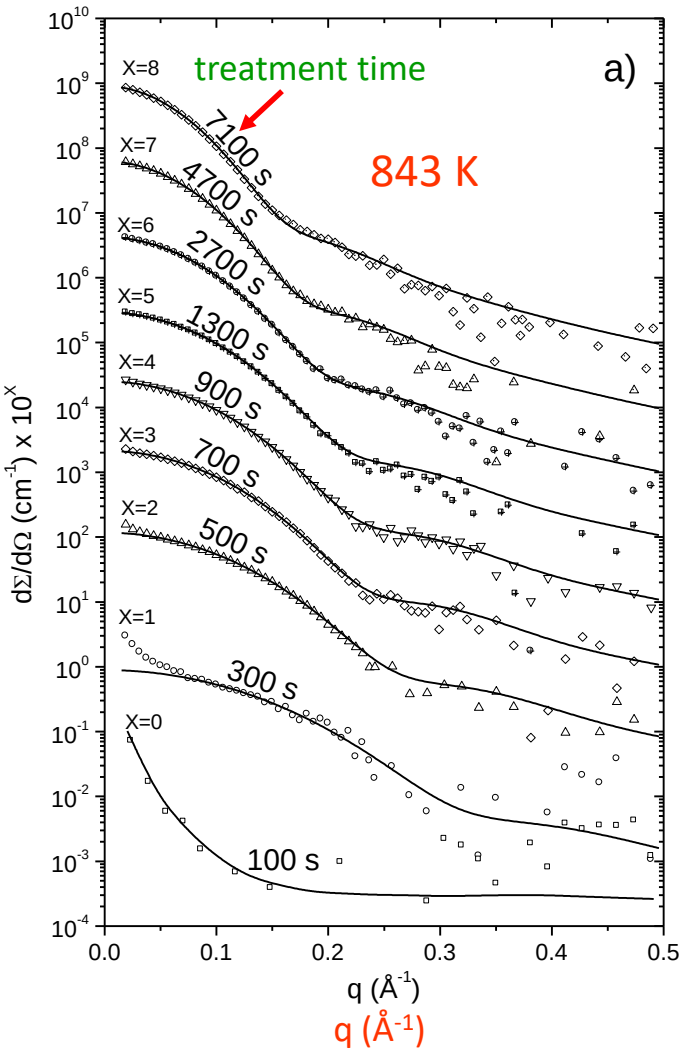

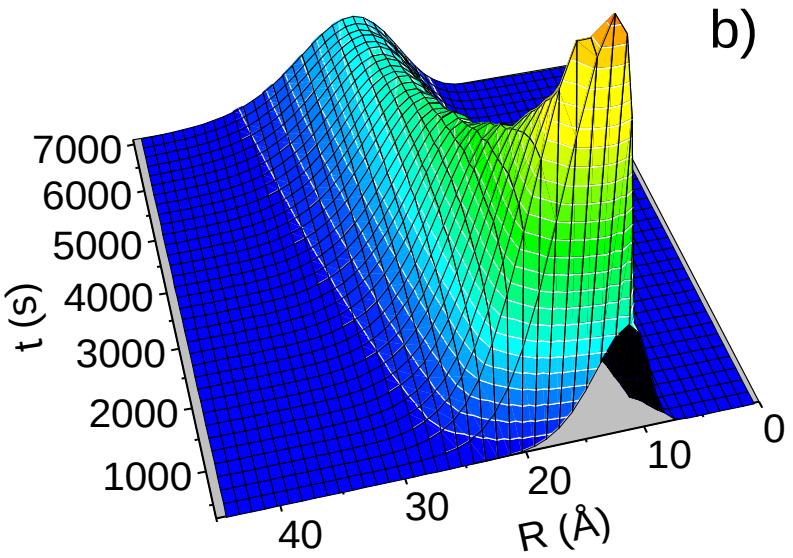

Time dependence of structural parameters

Temperature range: 803-843 K

Average radius: $\langle R(t) \rangle$

Nanodroplets number per unity volume: n(t)

Relative radius dispersion: $\sigma_R / \langle R(t) \rangle$

Volume fraction: $\varphi(t)$

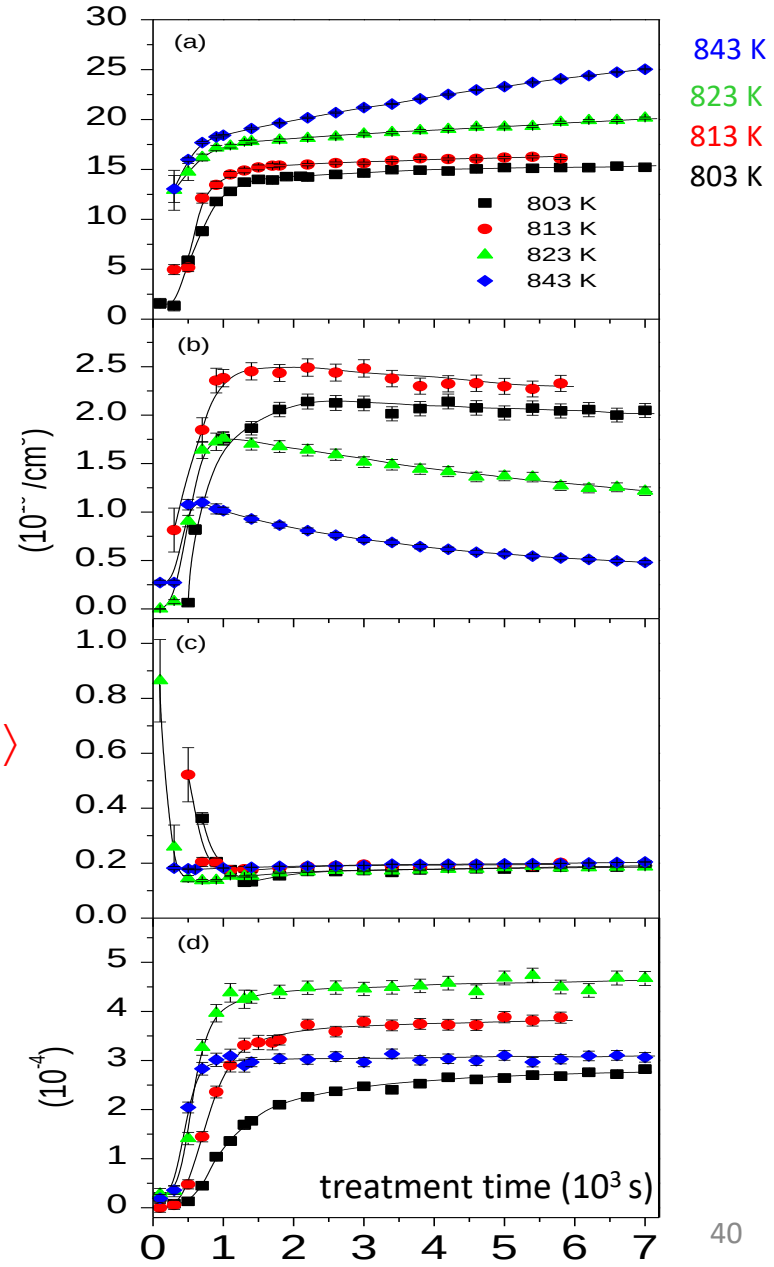

Advanced stages of thermal treatment

According to the theoretical model proposed by Lifshits-Slyosov (1961) e Wagner (1961) – LSW model:

<R>: nanodroplets average radius

$$< R >^3 (t) =< R_0 >^3 + \kappa (t - t_0)$$

n: number density of nanodroplets

$$n^{-1}(t) = n_0^{-1} + \beta (t - t_0)$$

ϕ: volume fraction of the total volume

$$\varphi(t) = \varphi_e - [\chi'(t - t_0)]^{-1/3}$$

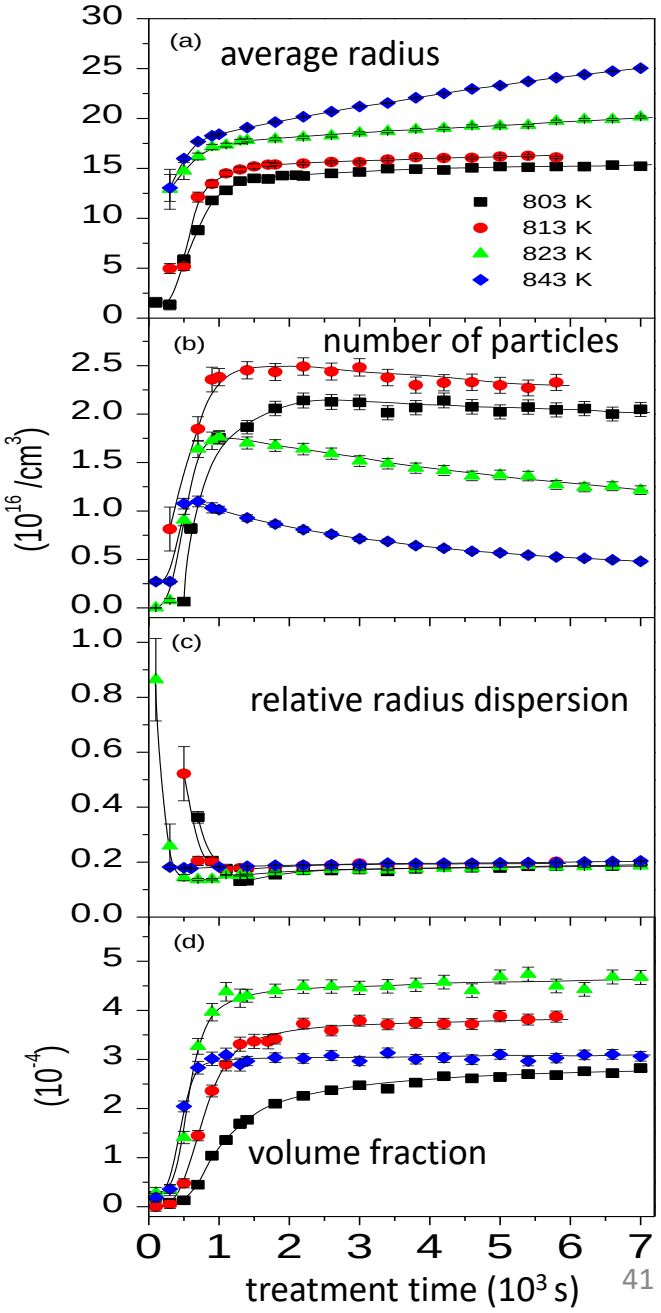

Advanced stages of thermal treatment

According to the theoretical model proposed by Lifshits-Slyosov (1961) e Wagner (1961) – LSW model:

<R>: nanodroplets average radius

$$[< R >^3 (t)] =< R_0 >^3 + \kappa(t - t_0)$$

n: number density of nanodroplets

$$n^{-1}(t) = n_0^{-1} + \beta(t - t_0)$$

ϕ: volume fraction of the total volume

$$\varphi(t) = \varphi_e - [\chi'(t - t_0)]^{-1/3}$$

$<R>^3$ versus t

n^{-1} versus t

φ versus $(t\text{-}t_0)^{-1/3}$

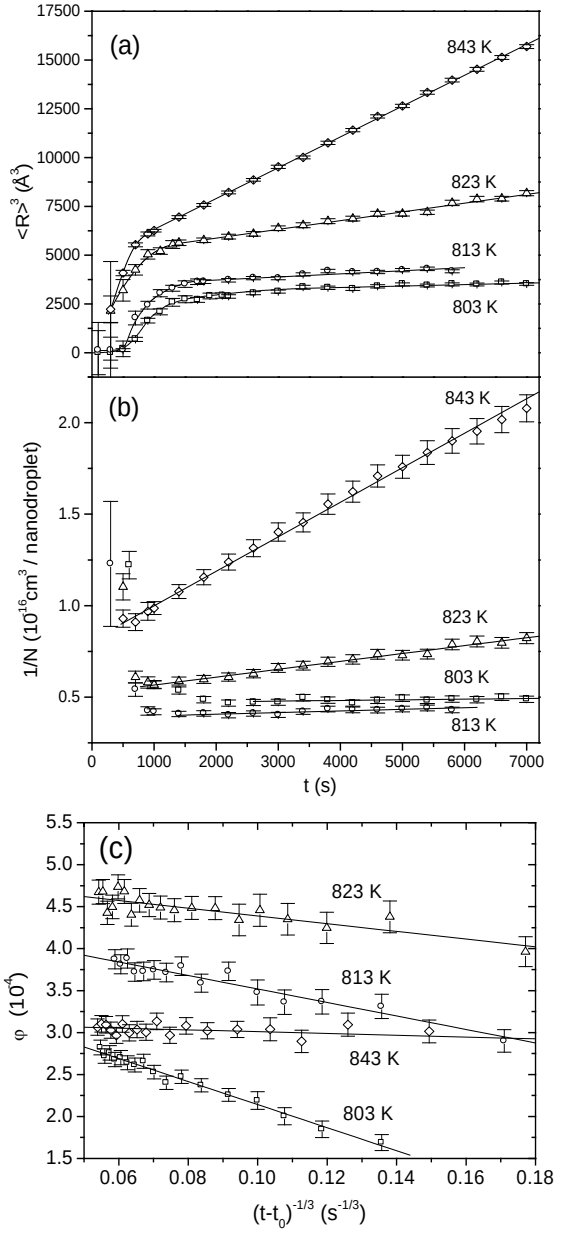

Determination of the diffusion coeficients from SAXS results

The κ, β e χ' are related with the atomic diffusion coefficients D by:

$$\kappa = \frac{8\sigma v^2 c_e D}{9kT} \qquad \beta = \frac{4\sigma c_e v D}{(c_0 - c_e)kT} \qquad \chi' = \left(\frac{1/v - c_e}{1-\varphi_e}\right)^3 \chi$$

σ: free energy per unity área of the nanodroplet-glass interface,
v: solute atomic volume; c_e: equilibrium concentration of solute.

Since the parameters σ and c_e are in most of cases not known, the above equations cannot be directly used to determine the diffusion coefficient

Assuming $[1/v\text{-}c_e] \approx [1/v]$, we have

$$D = \frac{9}{4}(\kappa^2 \chi')^{1/3}$$

Cubic average radius

$$[< R >^3 (t)] =< R_0 >^3 + \kappa(t - t_0)$$

Nanodroplets average radius

$$\varphi(t) = \varphi_e - [\chi'(t - t_0)]^{-1/3}$$

Activation energy

Temperature dependence of Bi self-diffusion coefficient in sodium borate glass

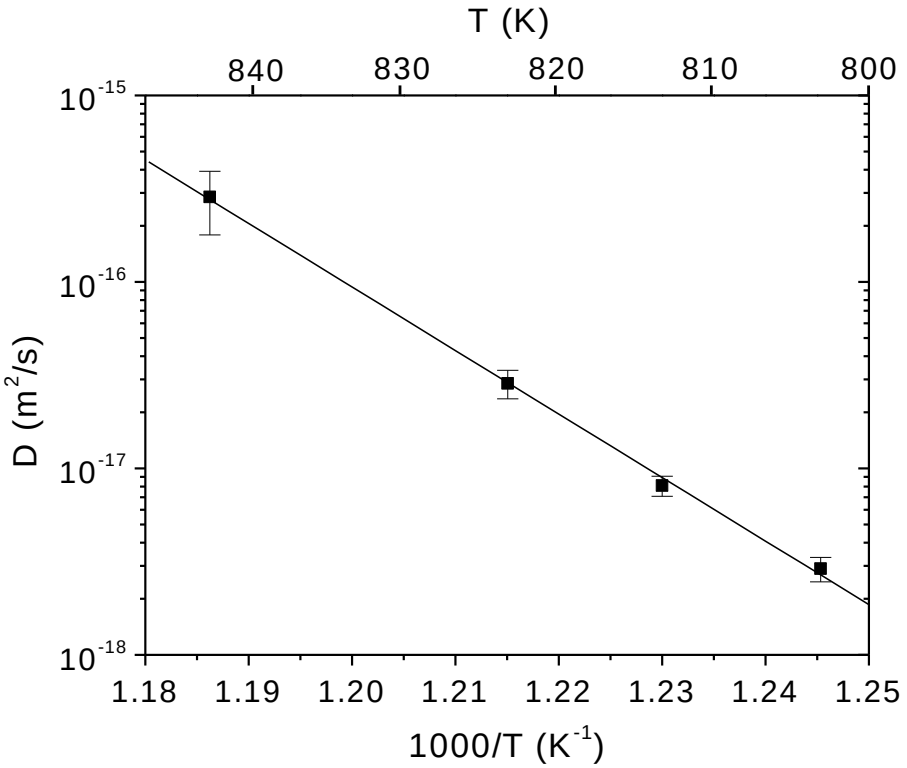

Arrhenius law

$D(T) \propto e^{-E/\Re T}$

slope: $E = (64 \pm 3) \times 10^4$ J/mol

Study by GISAXS of PbTe(SiO_2)/SiO_2 multilayer deposited on Si (111)

G. Kellermann[1], E. Rodriguez[2], C. L. Cesar[2], L. C. Barbosa[2] and A. F. Craievich[3]
[1] *Laboratório Nacional de Luz Síncrotron, Campinas SP,Brazil.*
[2] *DEQ, Instituto de Física Gleb Wataghin, UNICAMP,Campinas SP, Brazil*
[3] *Instituto de Física, Universidade de São Paulo, São Paulo SP, Brazil*

$PbTe/SiO_2$ multilayer on Si (111)

G. Kellermann[1], E. Rodriguez[2], C. L. Cesar[2], L. C. Barbosa[2] and A. F. Craievich[3]
[1] *Laboratório Nacional de Luz Síncrotron, Campinas SP,Brazil.*
[2] *DEQ, Instituto de Física Gleb Wataghin, UNICAMP,Campinas SP, Brazil*
[3] *Instituto de Física, Universidade de São Paulo, São Paulo SP, Brazil*

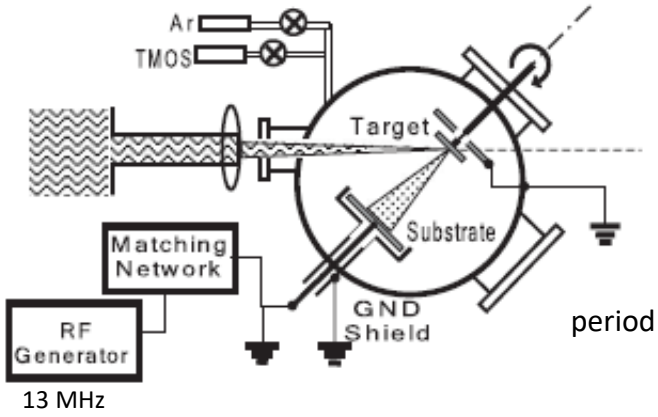

Glassy SiO_2 layers were deposited by plasma enhanced chemical vapor deposition (PCVD) using tetrametilorthosilicate (TMOS) as a precursor material.

PbTe layer deposition is produced by pulsed laser deposition technique (PLD)

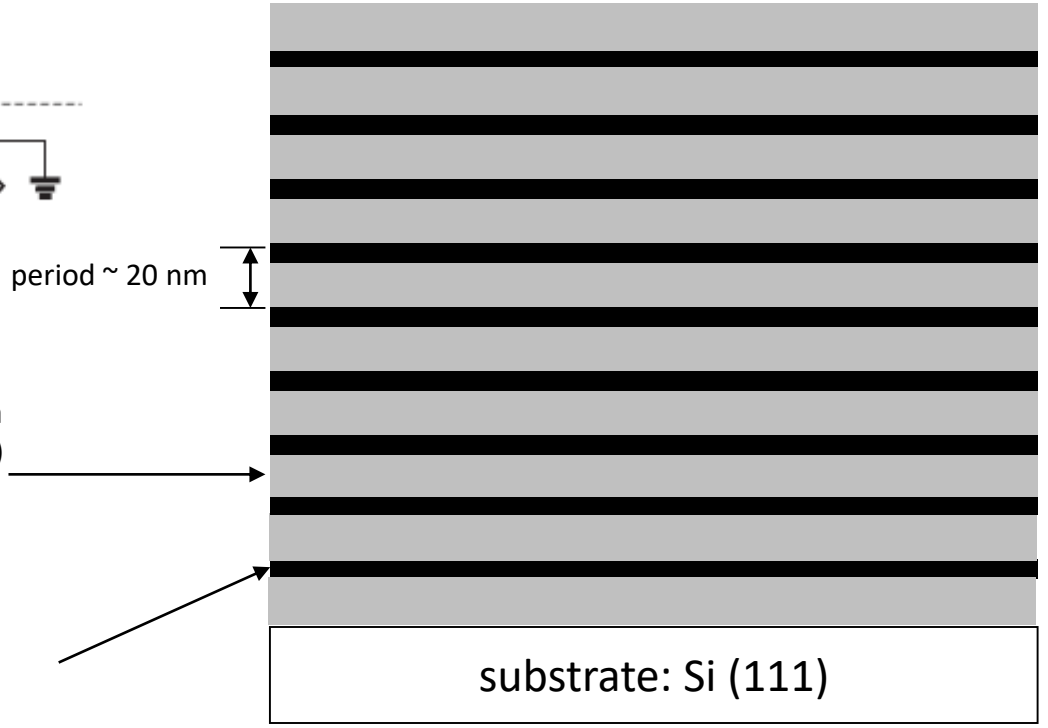

Samples prepared by Eugenio Rodriguez, Carlos Lens Cesar and Luiz Carlos Barbosa
Department of Quantum Electronics – IFGW – UNICAMP, Campinas SP

TEM results:

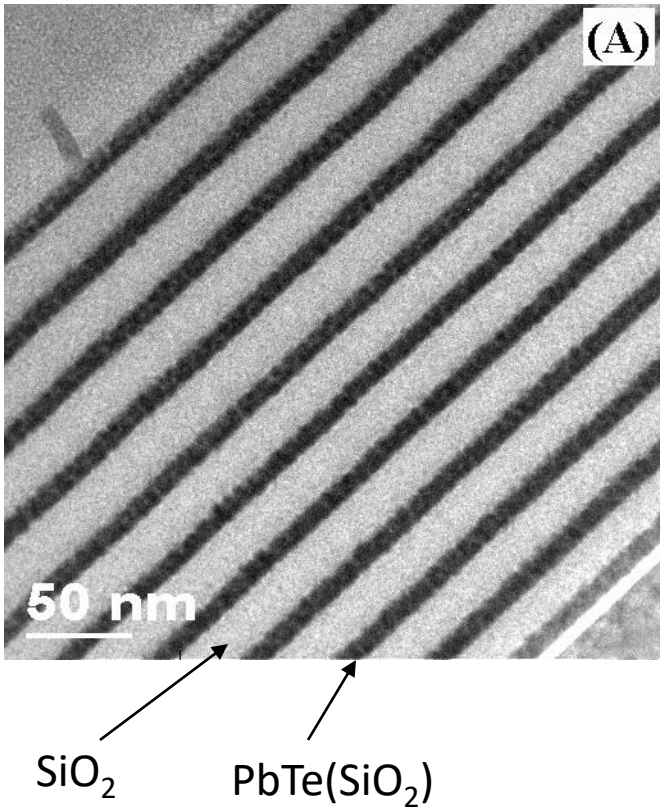

Low resolution image of $PbTe/SiO_2$ multilayer

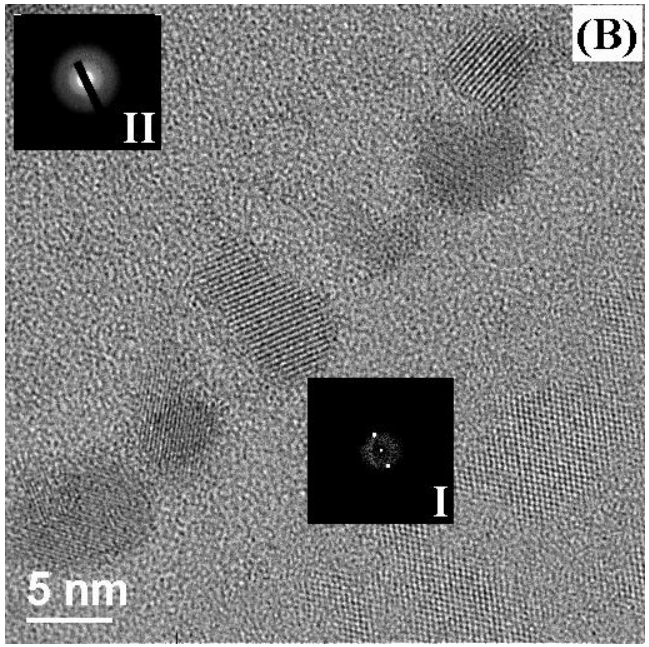

HRTEM showing the substrate and the native oxide, first nanoparticles row and the first SiO_2 layer.

by E. Rodriguez, DEQ – IFGW – UNICAMP

GISAXS results:

50 laser pulses

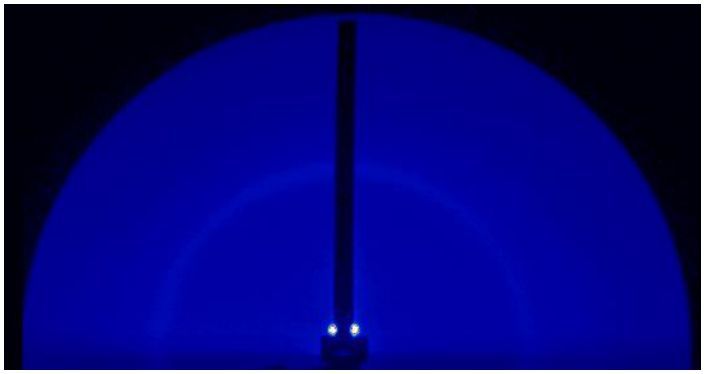

100 laser pulses

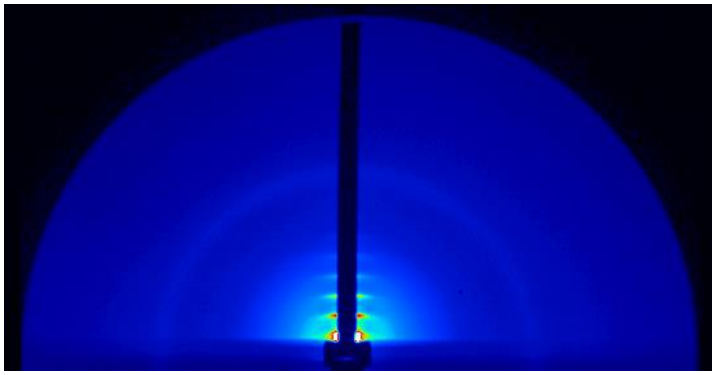

150 laser pulses

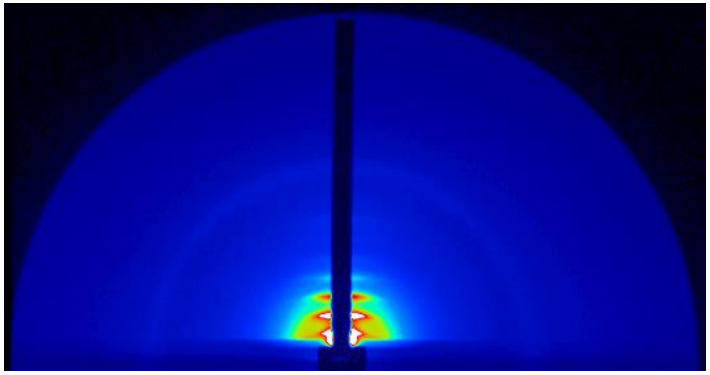

200 laser pulses

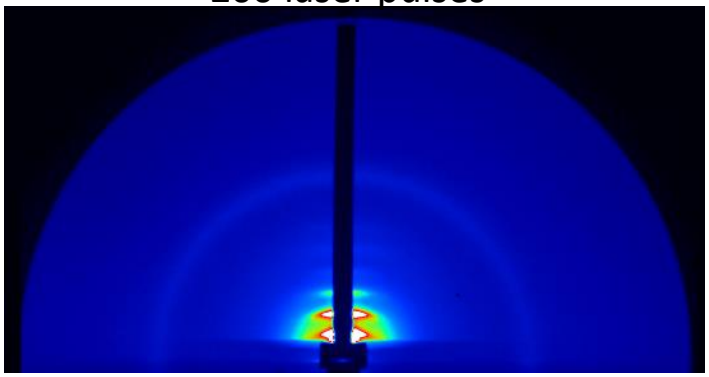

Nearly isotropic intensity related do average form factor of PbTe nanocrystals

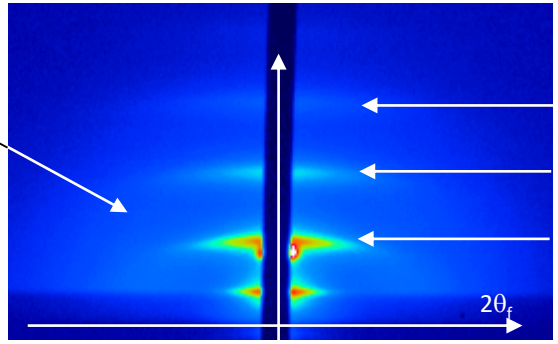

Horizontally elongated maximums due the correlation between nanocrystals in different layers

2D GISAXS patterns:

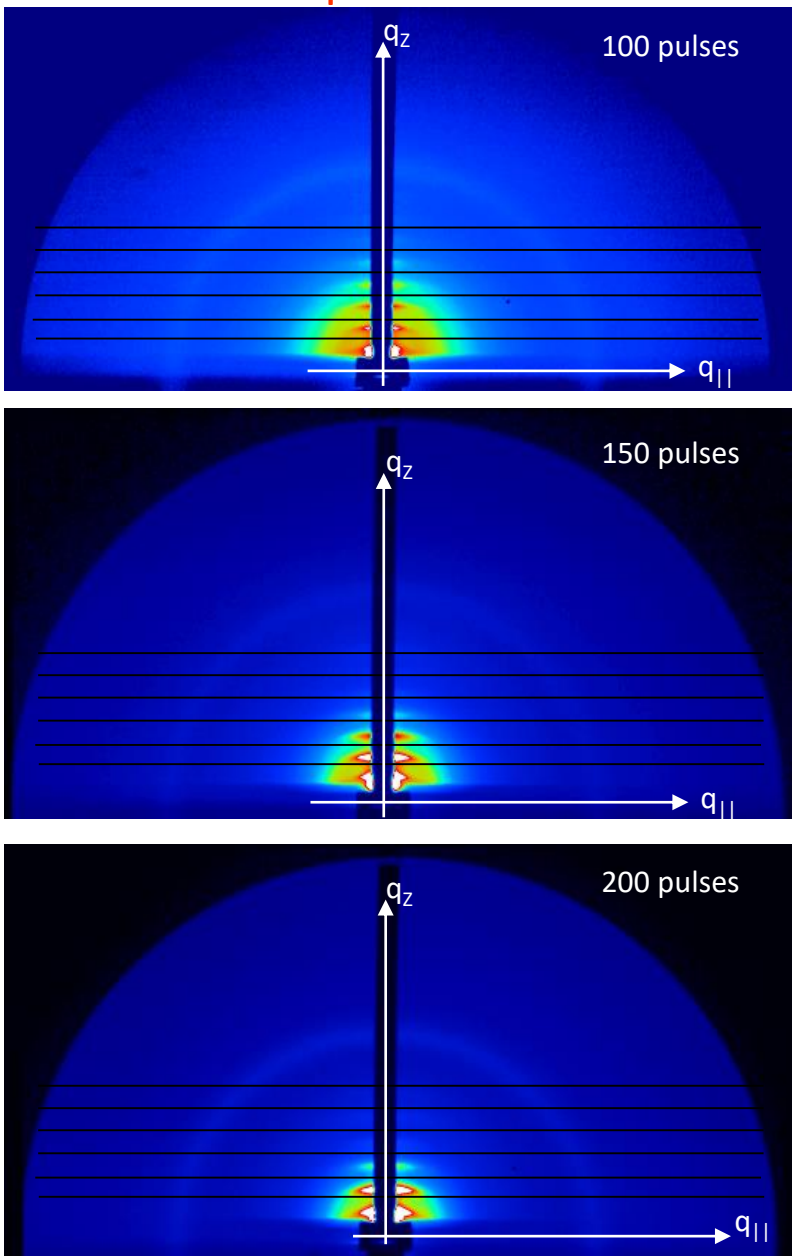

In-plane GISAXS profiles:

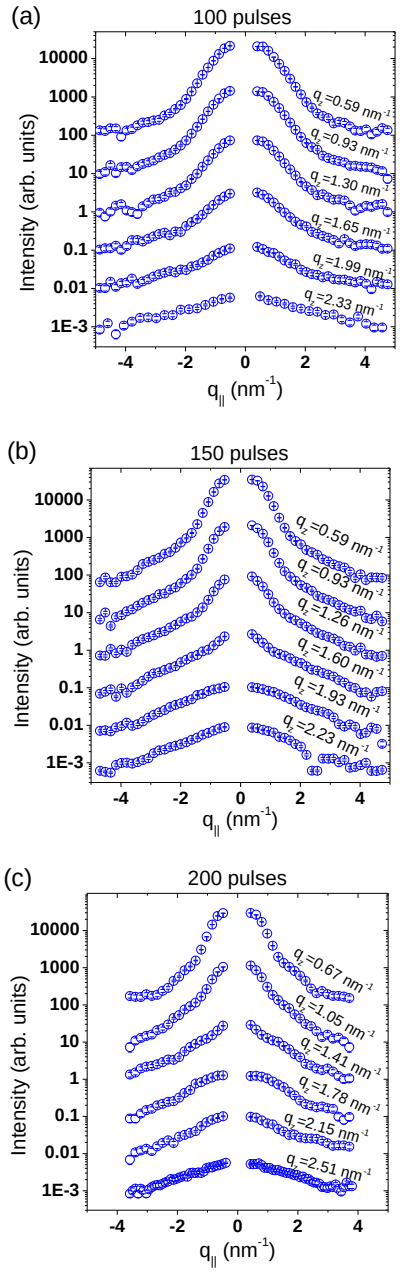

Modeling for GISAXS intensity at large q values:

For $|q_{||}| > 0.7\ nm^{-1} \rightarrow S_{tot}(q_{||}, q_z) \sim 1$

$$I_{||}(q_{||}, q_z, \alpha_i, \alpha_f) \propto (\rho_p - \rho_m)^2 |T(\alpha_i)|^2 |T(\alpha_{fi})|^2 \left\langle |F(q,R)|^2 \right\rangle$$

F(q,R): Form factor nanoparticles:



$$F(q,R) = \left[3 \frac{\sin(qR) - qR\cos(qR)}{(qR)^3} \right]^2$$ (*sphere with radius R*)

N(R): Radius distribution function:

$$N_G(R) = (1/\sqrt{2\pi\sigma_R}) \exp[-(R - \langle R \rangle)^2 / (2\sigma_R^2)]$$ (*gaussian function*)

<R>: average radius

σ_R : radius dispersion

Intensity profiles

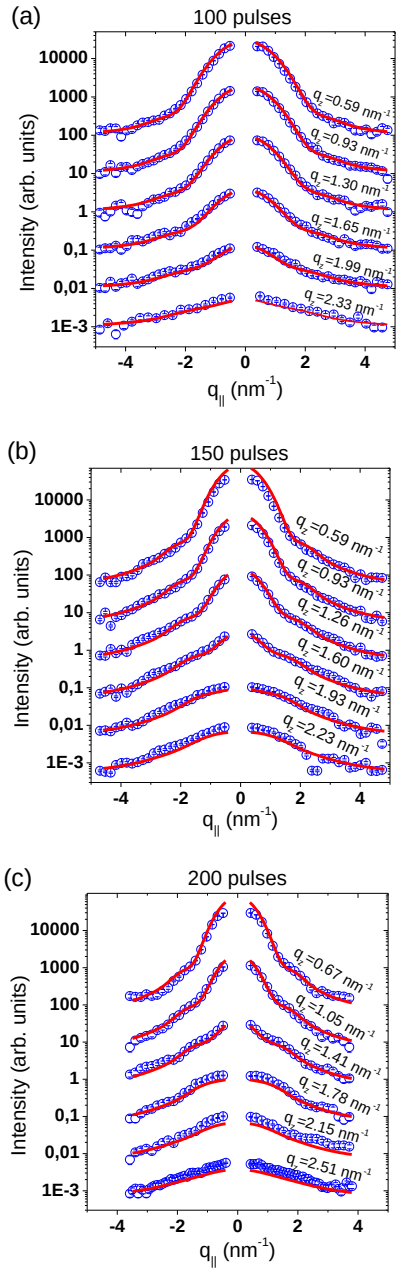

Results from the best fitting procedure

Normalized radius distribution function

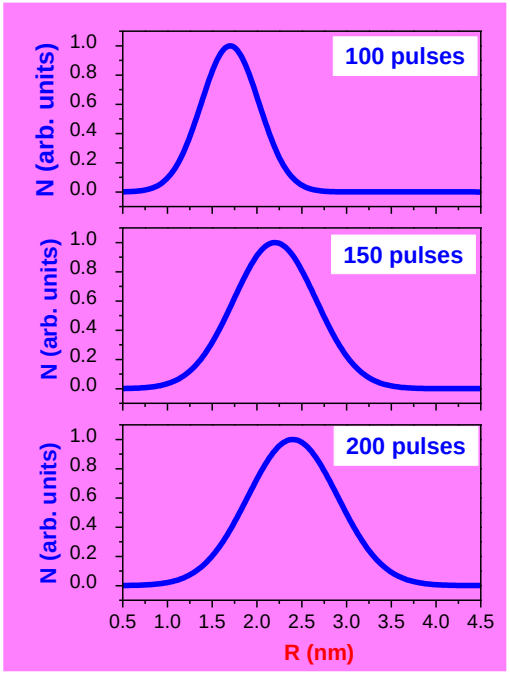

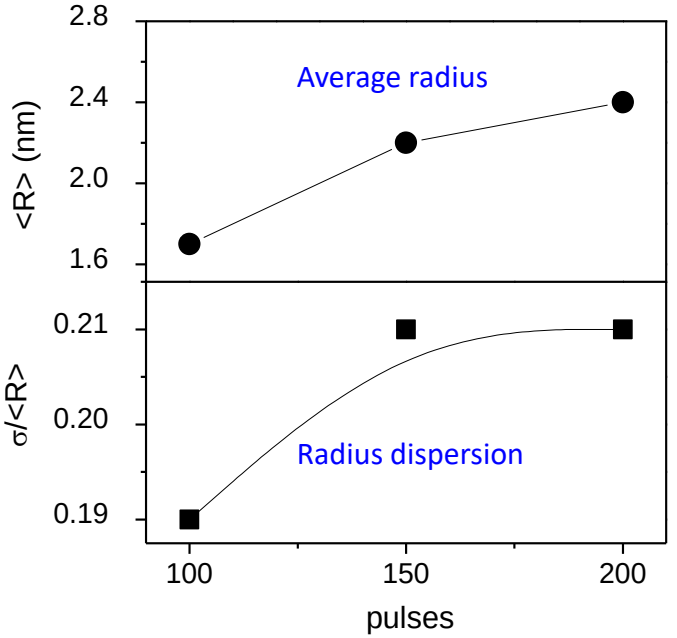

Radius distribution function determined from the best fitting procedure. Results show a continuous growth of the average radius and a progressive increase in the size dispersion (standard deviation of the $N(R)$ curves) of nanocrystals for increasing amount of deposited PbTe.

increasing the number of laser pulses from 100 to 200, the volume of the average nanocrystal increases by a rather higher factor (~ 2.8)

Fitting of the out-of-plane profiles

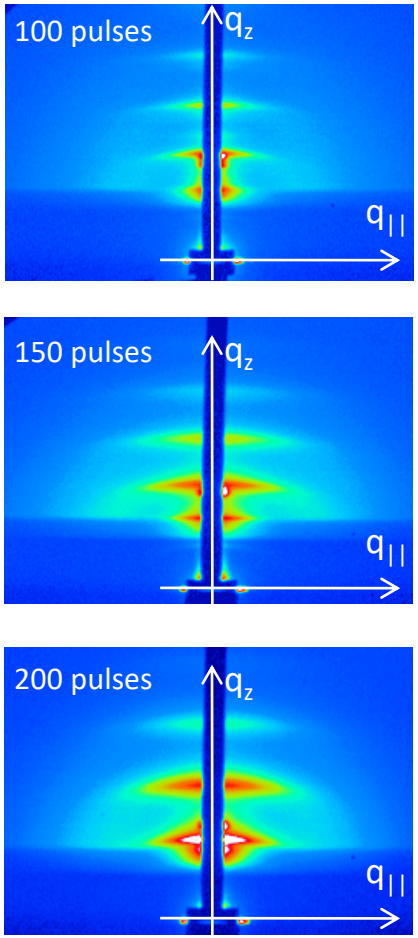

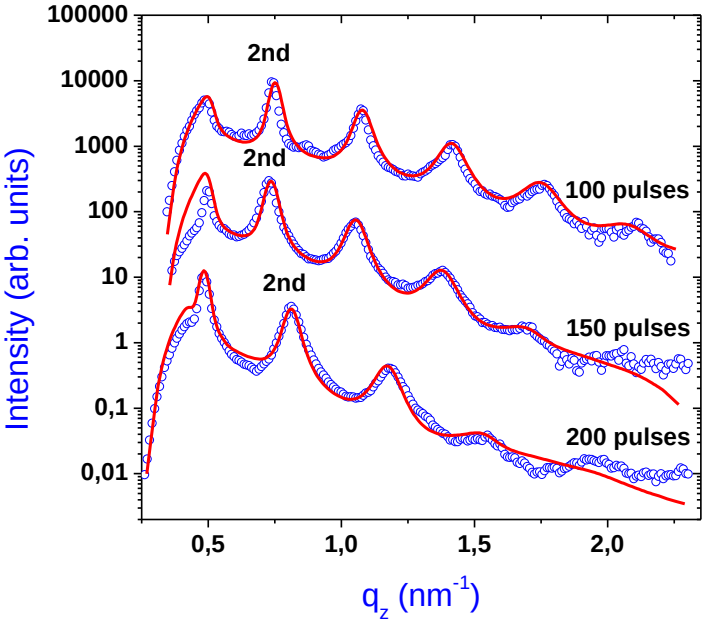

Parameters from the best fit

n_{LP}	D (nm)	ω_z (nm)	ω_z /D (%)
100	18.3±0.1	0.95±0.05	5.2
150	18.8±0.1	1.07±0.05	5.7
200	16.8±0.2	1.02±0.05	6.1

$$I_{\perp}(q_{||}=0, q_z, \alpha_i, \alpha_f) \propto (\rho_p - \langle\rho\rangle)^2 \, |T(\alpha_i)|^2 \, |T(\alpha_f)|^2 \, [\langle |F(q,R)|^2\rangle - |\langle F(q,R)\rangle|^2 + |\langle F(q,R)\rangle|^2 S_{\perp}(q_z)] * V(q_z)$$

Paracrystal interference function (by *Hosemann,* 1951):

$$S_{\perp}(\tilde{q}_z) = \mathrm{Re}\left[\frac{1+P(\tilde{q}_z)}{1-P(\tilde{q}_z)}\right] \qquad P(q_{\parallel},\tilde{q}_z) = \exp[-\tilde{q}_z^2\omega_z^2/2]\exp[i\tilde{q}_z D]$$

Function accounting for the finite multilayer Thickness *L*

$$V(\tilde{q}_z) = \frac{\sin^2(\tilde{q}_z L/2)}{(\tilde{q}_z L/2)^2}.$$

D: multilayer period, ω_z: dispersion in *D*

Formation of thin $CoSi_2$ nanohexagon arrays buried in single crystalline Si substrates.

Grazing-incidence small-angle x-ray scattering (GISAXS)

Global characterization of the nano-object over a large sample volume (footprint of x-ray on the sample: 3 x 20 mm)

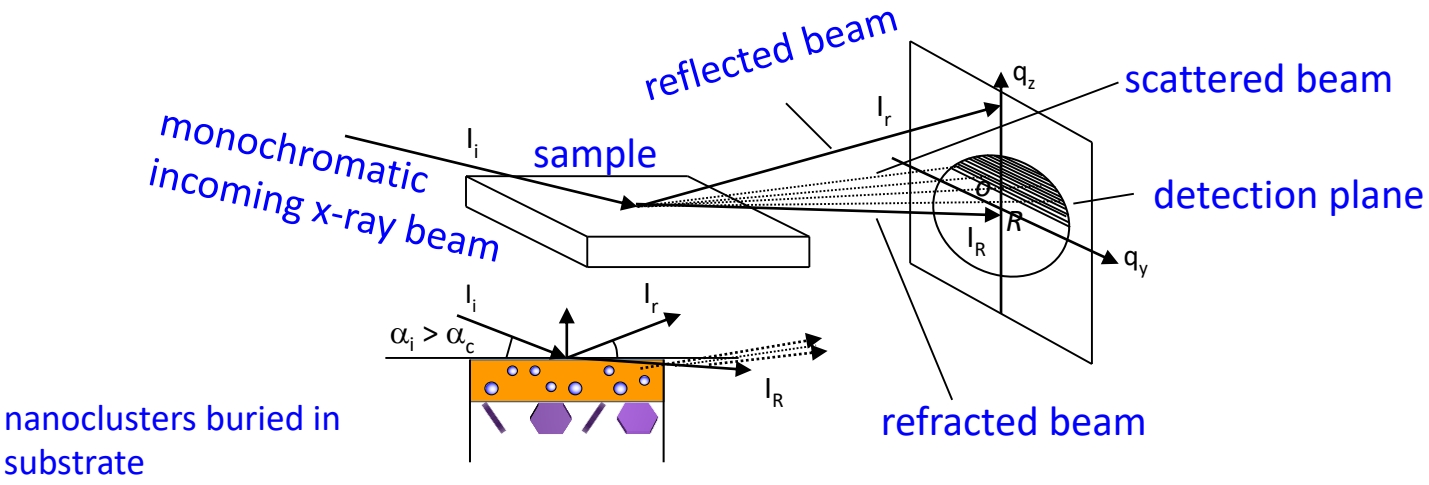

Formation of coherent $CoSi_2$ thin nanohexagon array buried in silicon single crystal

Guinther Kellermann[1], Luciano A. Montoro[2], Lisandro J. Giovanetti[3,4], Paula C. dos Santos Claro[3,4], Liang Zhang[5], Antonio J. Ramirez[2]; Félix G. Requejo[3,4] and Aldo F. Craievich[6].

[1]*Departamento de Física, Universidade Federal do Paraná, Curitiba, PR*

[2]*Brazilian Synchrotron Light Laboratory (LNLS), Campinas, SP*

[3]*Instituto de Investigaciones Fisicoquímicas Teóricas y Aplicadas*
[4]*Departamento de Química, Facultad de Ciencias Exactas, Universidad Nacional de La Plata, Argentina*
[5]*Energy and Environment Directorate, Pacific Northwest National Laboratory, Richland, WA 99352, USA*
[6]*Instituto de Física, Universidade de São Paulo, São Paulo, SP*

Guinther Kellermann
Departamento Física
Universidade Federal do Paraná (UFPR)

Objective:

Investigate the nanostructures formed after thermal treatment of Cobalt-doped SiO_2 thin film onto a Si(100) flat substrate

Sample preparation

The basic idea is to build up a Co-doped buffer layer and then to promote de diffusion of Co atoms into the Si wafer by a controlled thermal treatment

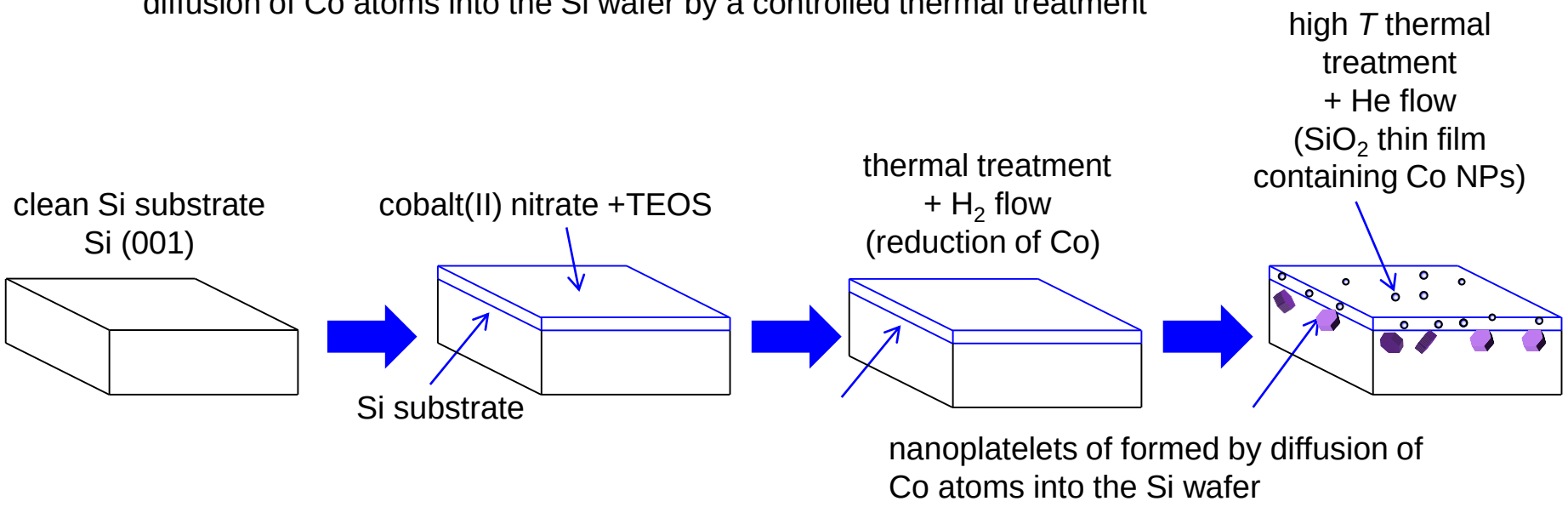

Objective: Investigate the nanostructures formed after thermal treatment of Cobalt-doped SiO_2 thin film onto a Si single crystals for several surfaces having different crystallographic orientations

Motivation: $CoSi_2$ has low resistivity (20 $\mu\Omega$/cm) and high thermal stability (attractive properties for potential applications in high-speed microelectronic devices)

Previous investigation
TEM analysis for Si(001) surface

Co nanoparticles

$CoSi_2$ nanoplatelet

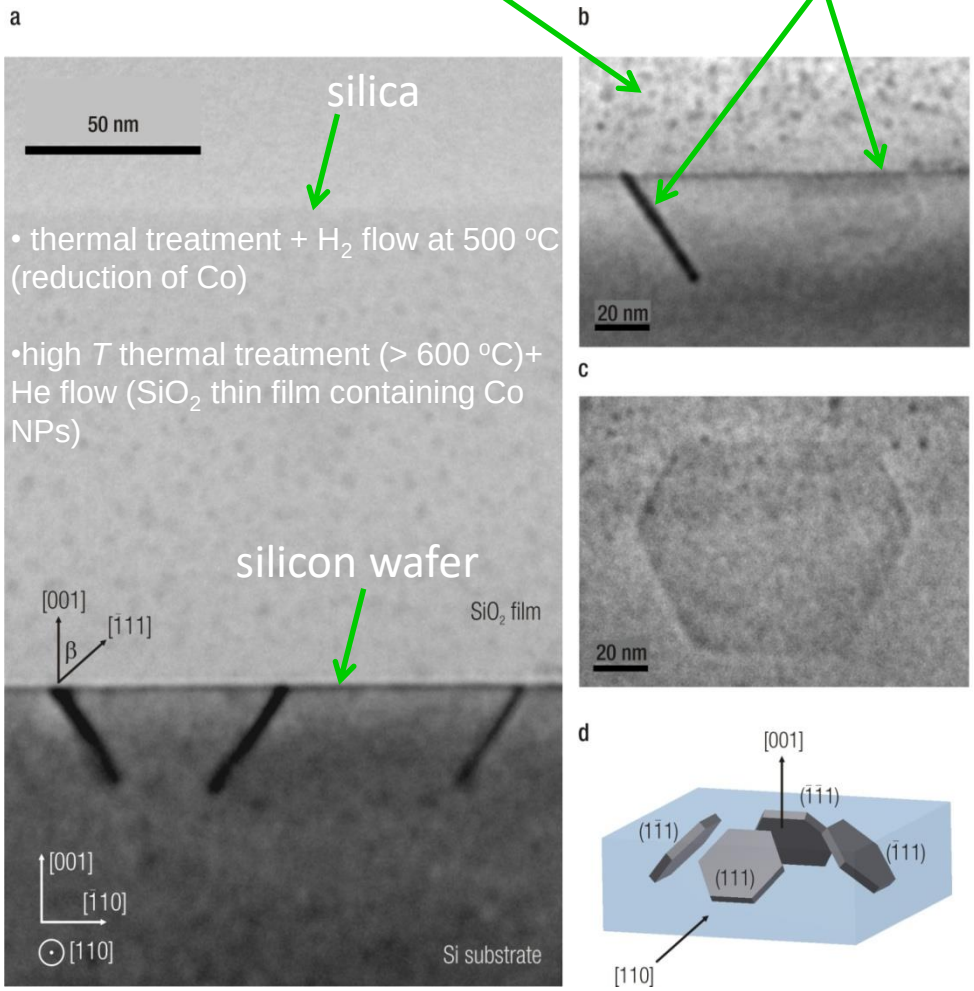

Appl. Phys. Lett. 100, 063116 (2012)

HRTEM

$CoSi_2$ phase
Cubic lattice
CaF_2 (fluorite)-like structure

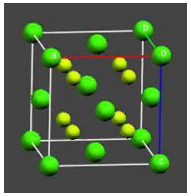

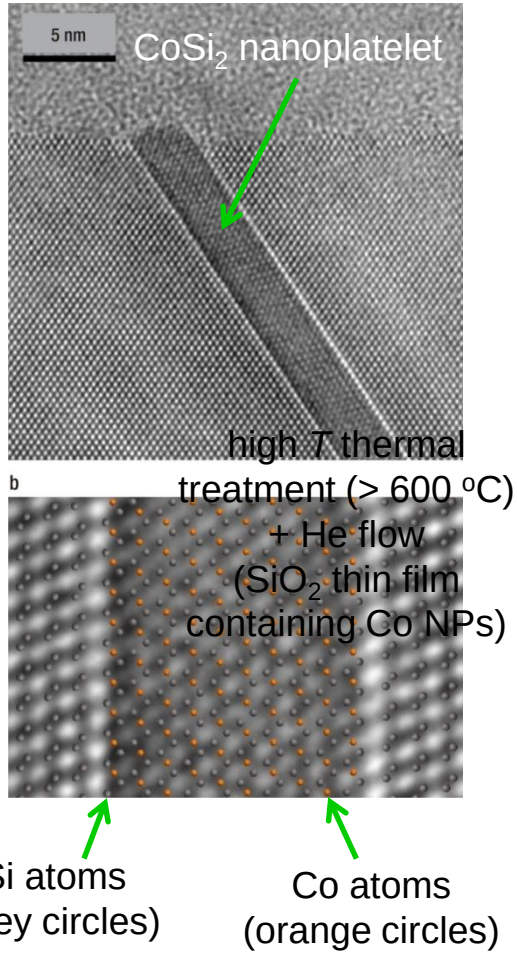

TEM RESULTS

•TEM experiments show that nearly spherical Co nanoparticles are embedded in the silica thin film covering the Si substrate and small nano-objects buried into the Si(001) single crystal

•each nanoplate has its two faces parallel to one of the four planes of the {111} crystallographic form of the host Si matrix

•nanoplates are hexagonal with two sides parallel to the external surface of the Si wafer

•TEM with X-Ray Energy Dispersive Spectroscopy (XEDS) analyses (3 nm electron probe) indicated that the composition and the structure of the buried nanoplatelets correspond to those of the stoichiometric $CoSi_2$ phase

•$CoSi_2$ nanoplates have a homogeneous thickness t = (3.17 ± 0.23) nm and an average length of hexagon sides d = (24 ± 3) nm

Model for GISAXS intensity

Scattering amplitude: $F(\vec{q}) = \int \rho(\vec{r})\mathrm{Exp}(\vec{q}\cdot\vec{r})\,d\vec{r}$ **Scattering intensity:** $I(\vec{q}) = F(\vec{q})\cdot F^{*}(\vec{q})$

Sphere of radius R:

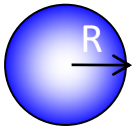

$$A_{\mathrm{sph}}(q,R) = 4\pi(\rho_{sph} - \rho_{SiO_2})\left[\frac{\sin(qR) - qR\cos(qR)}{q^3}\right]$$

Intensity from an uncorrelated set of homogeneous spheres: $I_{\mathrm{sphere}}(q) = \int_{R=0}^{R_{max}} N_{sph}(R)\left|A_{sph}(q,R)\right|^2 dR$

$N_{sph}(R)\mathrm{d}R$ being the number of spheres having radius between R and $R+\mathrm{d}R$.

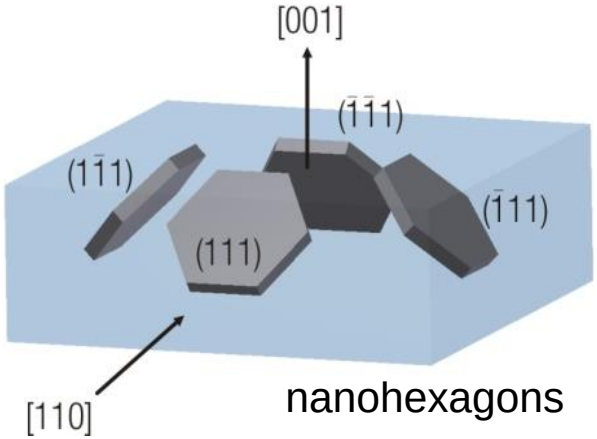

nanohexagons

$$I_{\mathrm{hex}}(\vec{q}) = \left|A_{hex(111)}\right|^2 + \left|A_{hex(1\bar{1}1)}\right|^2 + \left|A_{hex(\bar{1}\bar{1}1)}\right|^2 + \left|A_{hex(\bar{1}11)}\right|^2$$

$A_{hex(111)}$, $A_{hex(1\bar{1}1)}$, $A_{hex(\bar{1}\bar{1}1)}$ and $A_{hex(\bar{1}11)}$ are the scattering amplitudes of nanohexagons

Scattering amplitude of the nanohexagons

In the case of Si(001) interface:

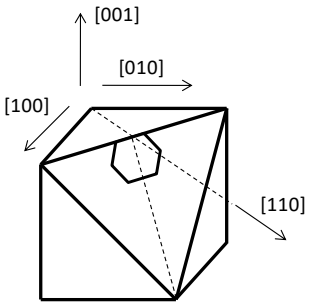

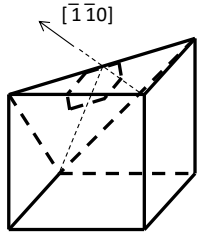

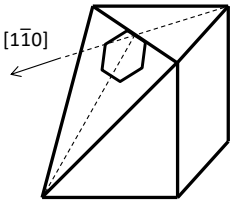

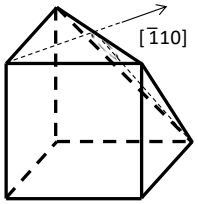

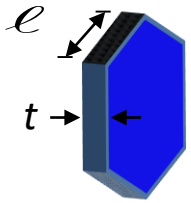

$$A_{hex(111)} = \frac{(\rho_{hex} - \rho_{Si})}{q'_y q'_x (q'^2_y - 3q'^2_z)} \{i \exp[-i(2\ell q'_y + \sqrt{3}\ell q'_z + q'_x t)/2](-1 + \exp[i q'_x t])[-2\sqrt{3}\exp[i\sqrt{3}\ell q'_z/2]q'_y$$
$$- 2\sqrt{3}\exp[i\ell(4q'_y + \sqrt{3}q'_z)/2]q'_y + \exp[3i\ell q'_y/2](\sqrt{3}q'_y - 3q'_z) + \exp[i\ell(q'_y + 2\sqrt{3}q'_z)/2](\sqrt{3}q'_y - 3q'_z)$$
$$+ \mathrm{Exp}[i\ell q'_y/2](\sqrt{3}q'_y + 3q'_z) + \exp[i\ell(3q'_y + 2\sqrt{3}q'_z)/2](\sqrt{3}q'_y + 3q'_z)]\}$$

where:
$$\begin{pmatrix} q'_x \\ q'_y \\ q'_z \end{pmatrix} = \begin{pmatrix} q_x \cos\gamma - q_z \sin\gamma \\ q_y \\ q_x \sin\gamma + q_z \cos\gamma \end{pmatrix}, \qquad (q'_x \neq 0,\ q'_y \neq 0)$$

γ= 35.3°: angle between the Si[111] and Si[110] directions

ρ_{hex} : electron density of nanohexagons

ρ_{Si} : electron density of Si

$A_{hex(1\bar{1}1)}$,$A_{hex(\bar{1}\bar{1}1)}$ and $A_{hex(\bar{1}11)}$ are obtained by applying the mathematical transformations associated to a rotation around the q_z axis

$$\begin{pmatrix} q'_x \\ q'_y \\ q'_z \end{pmatrix} = \begin{pmatrix} \cos\varphi & -\sin\varphi & 0 \\ \sin\varphi & \cos\varphi & 0 \\ 0 & 0 & 1 \end{pmatrix} \begin{pmatrix} q_x \\ q_y \\ q_z \end{pmatrix}$$

φ = 90°, 180° and 270°, respectively.

Transformation to account for incidence and azimuthal angles

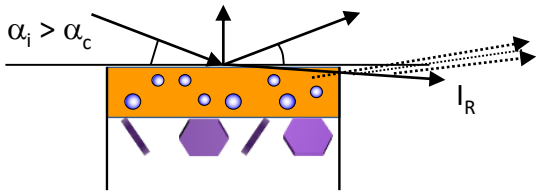

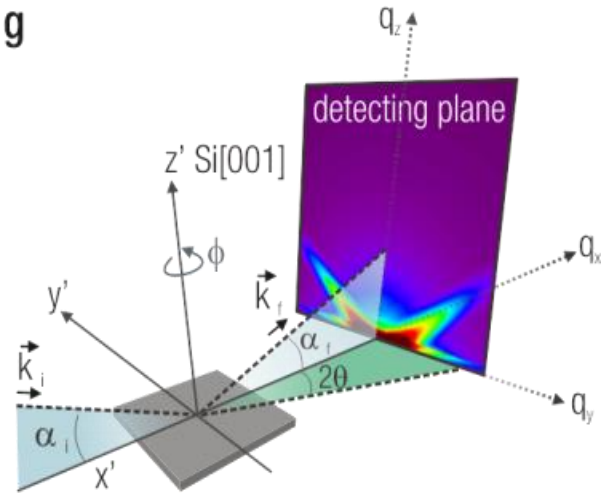

$$\begin{pmatrix} q'_x \\ q'_y \\ q'_z \end{pmatrix} = \begin{pmatrix} cu_z + 2(1-c)u_x^2 u_z & s(u_x^2 - u_z^2) & cu_x + 2(1-c)u_x u_z^2 \\ su_z & c & -su_x \\ -cu_x + (1-c)(u_x u_z^2 - u_x^3) & 0 & cu_z - (1-c)(u_x^2 u_z - u_z^3) \end{pmatrix} \begin{pmatrix} q_x \\ q_y \\ q_z \end{pmatrix}$$

where

$c = \cos\phi$

$s = \sin\phi$

$u_x = -\sin\alpha$

$u_z = \cos\alpha$

α : angle between the Si[100] direction and the $\vec{k}_i$ vector

ϕ : the angle between the Si[110] direction and the component of $\vec{k}_i$ along the Si(001) plane (azimuthal angle)

Total GISAXS intensity for our nanostructure model :

$$I \propto |T(\alpha_i)|^2 |T(\alpha_f)|^2 \left(c \sum_{kkl} \left| A_{hex(hkl)}(\alpha, \phi, q_x, q_y, \tilde{q}_z, \ell, t) \right|^2 + \int \left| A_{sph}(q_x, q_y, q'_z, R) \right|^2 N_{sph}(R) dR \right)$$

$|T(\alpha_i)|$, $|T(\alpha_f)|$: effective Fresnel transmission coefficients for incidence and exit angles

GISAXS intensity

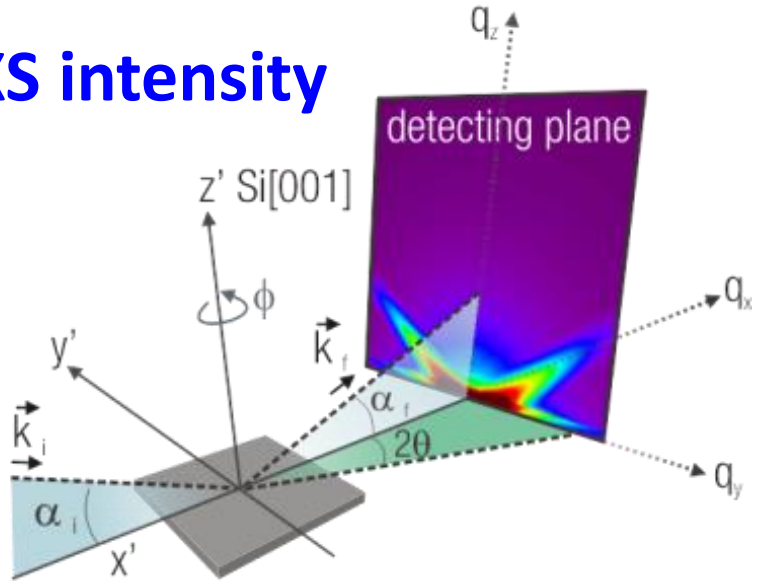

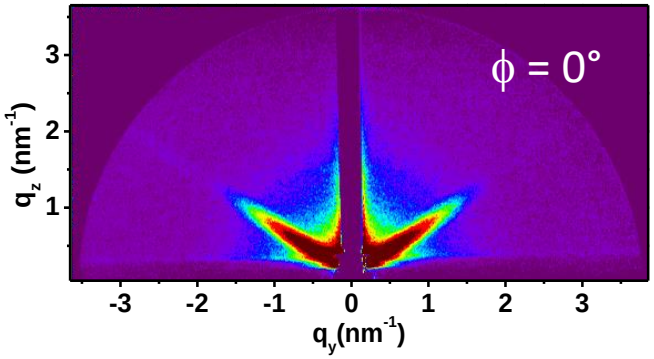

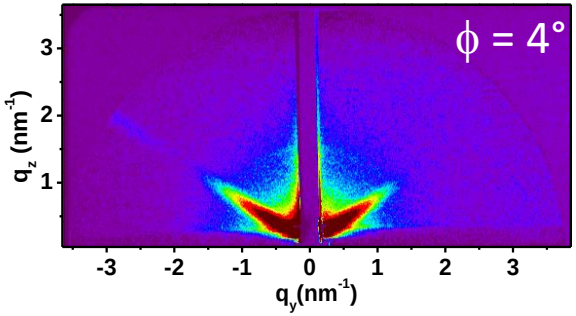

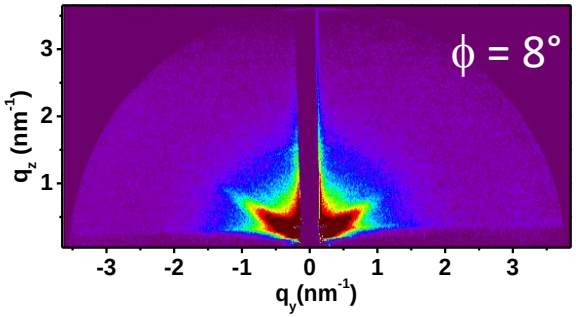

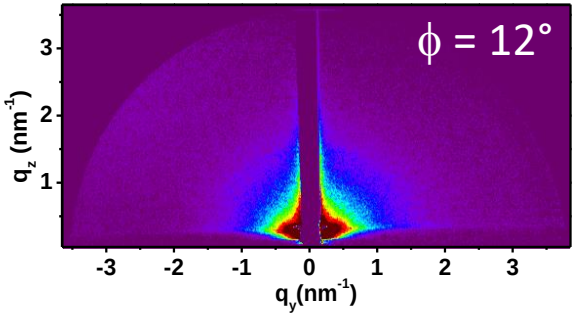

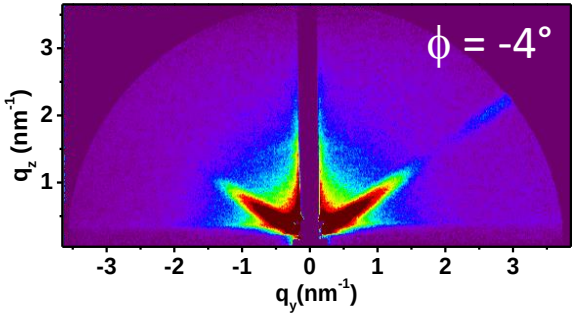

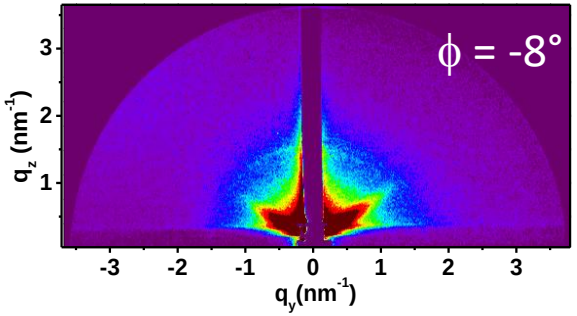

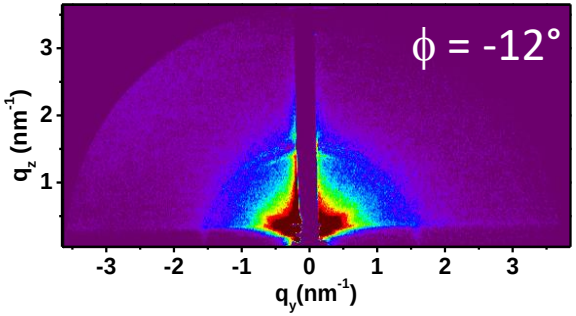

Best fit of GISAXS intensity curves

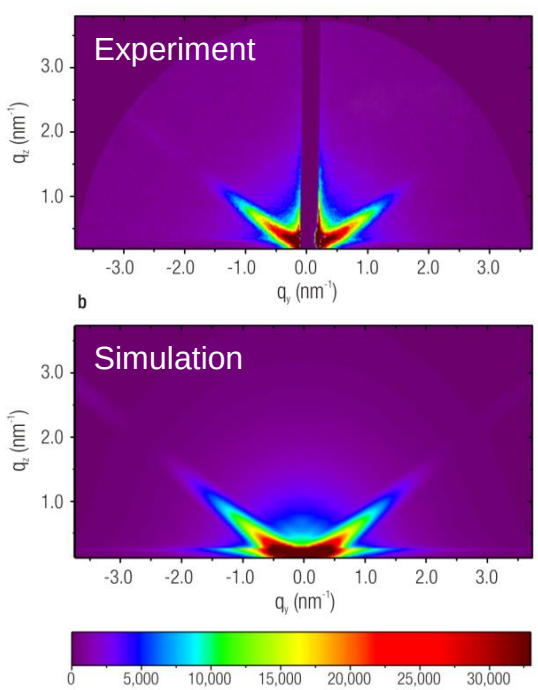

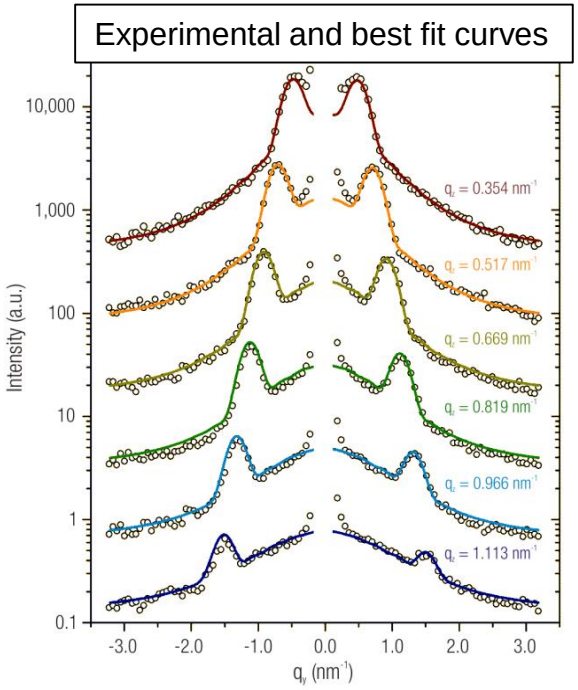

GISAXS results:

The best fit procedure yielded a thickness and a lateral side of the $CoSi_2$ nanoplatelets buried into the Si wafer t = (2.5 ± 0.3) nm and d = (19.5 ± 0.5) nm, respectively

The average radius of the spherical nanoparticles embedded in the silica thin film was established to be $\langle R \rangle$= (0.43 ± 0.03) nm, and its relative standard deviation $\sigma_R / \langle R \rangle$, being equal to 0.58 ± 0.06

The non-perfect symmetry at the curves (right figure) is only due to the non-centered position of the sample at the azhimutal angle, which was fitted in 1.5°.

Formation of thin $CoSi_2$ nanohexagon arrays buried in single crystalline Si substrates. Effects of the orientation of the external surface of the Si host

Guinther Kellermann
University Federal of Parana, Curitiba, Brazil

Aldo Felix Craievich
Physics Institute, University of São Paulo, São Paulo, Brazil

Felix G. Requejo, Lisandro .J. Giovanetti, Paula Cecilia dos Santos Claro
Instituto de Investigaciones Fisico-Químicas Teóricas y Aplicadas (INIFTA),
FCE, UNLP – CONICET, La Plata, Argentina

Luciano A. Montoro, Antonio J. Ramirez
Brazilian Nanotechnology National Laboratory (LME-LNNano), Campinas, Brazil

Melting and crystallization of Bi nanoclusters embedded in B_2O_3-Na_2O glass

Some differences between nonosized and bulk materials:

- crystalline lattice contraction
- melting and crystallization temperature (M. Takagi, 1954)

Dependence of melting temperature with the nanocrystal radius

Theoretical models using simple thermodynamic principles relate the melting temperature T_m with the radius R of small spherical crystals embedded in matrixes:

Couchman - Jesser (1977) and Allen *et al.*, (1980)

$$T_m = T_b\left[1-\frac{3}{RL}\left(\frac{\sigma_{vc}}{\rho_c}-\frac{\sigma_{vl}}{\rho_l}\right)+K_E\right]$$

T_b: bulk melting temperature
L: latent heat of melting
ρ_c and ρ_l : specific mass of nanocrystals and nanodroplets
σ_c, σ_l : Interface energy between glass-nanocrystals and glass-nanodroplets
K_E: term related to the difference in the strain energy due to volume changes

Nanocrystals with different radius embedded in glass

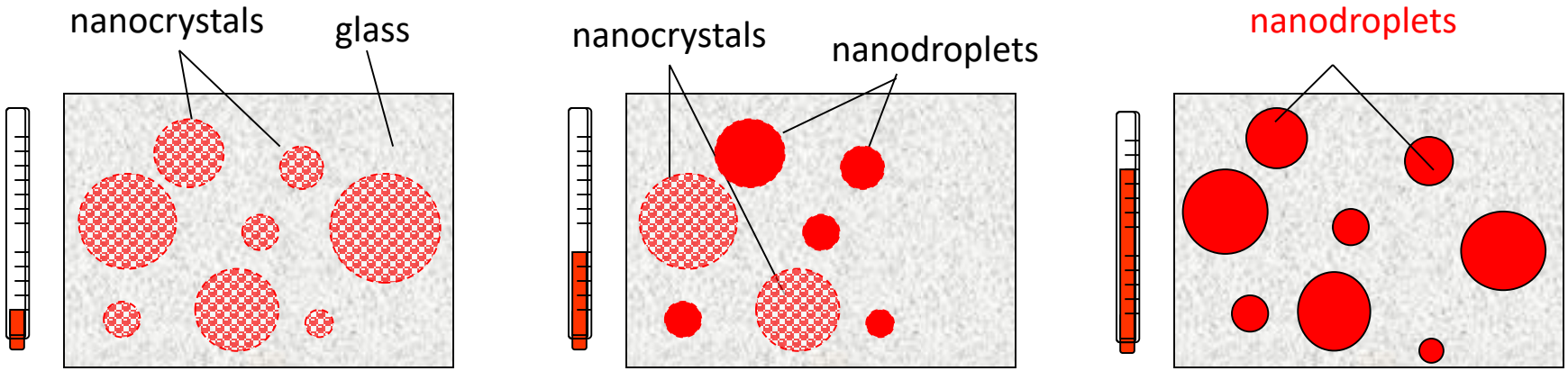

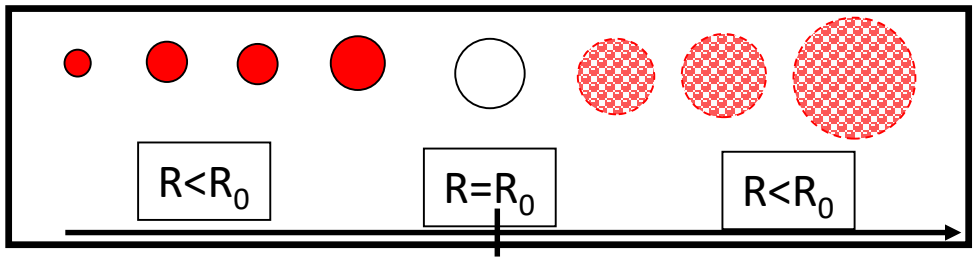

Methods used to determine de size dependence on the melting temperature:

- transmission electron microscopy — Changes in the nanocrystals shape
- optic techniques (measure the optical reflectivity)
- calorimetric techniques (melting enthalpy)
- x-ray diffraction (parameters of the crystalline structure)

Probes a large number of particles having, in general, a very large dispersion in size

EXPERIMENTAL SETUP

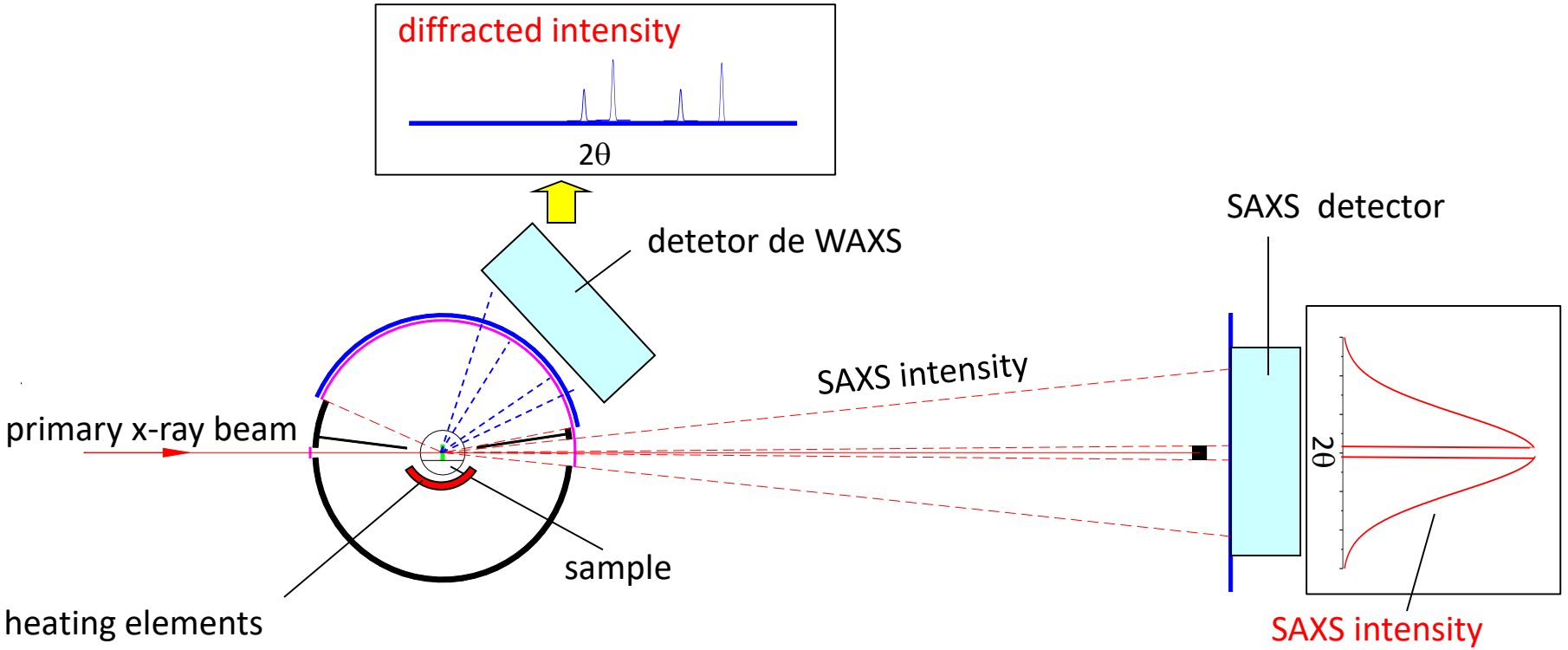

structure x temperature

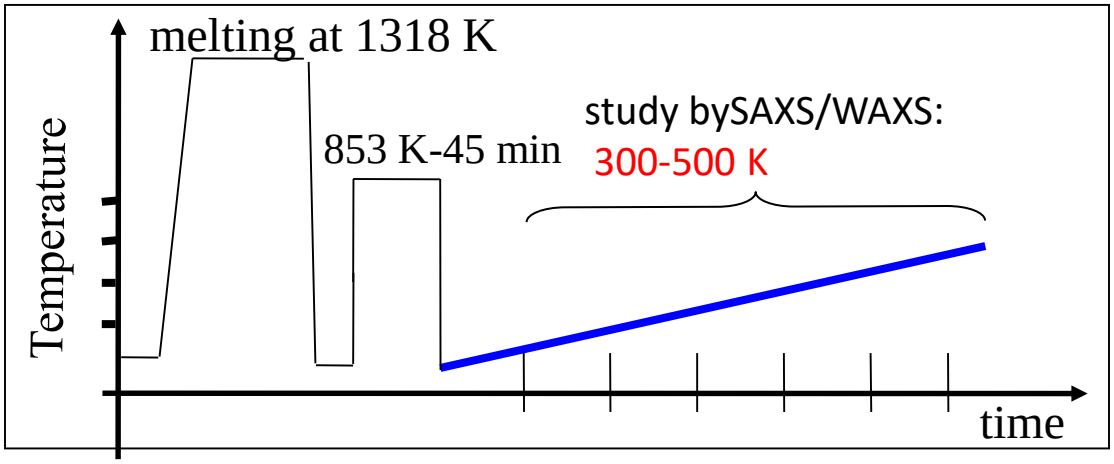

SAXS RESULTS

SAXS intensity

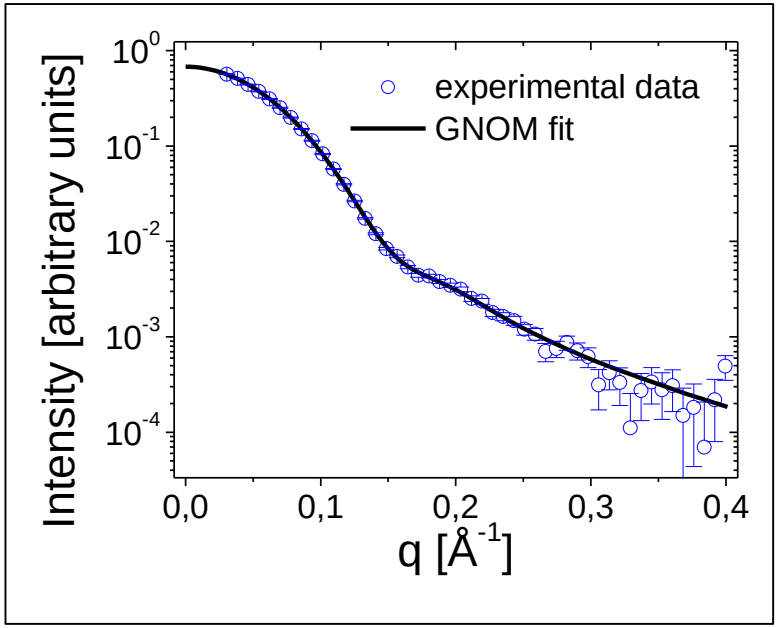

Volume distribution function

$$V(R) = \frac{4\pi}{3} R^3 N(R)$$

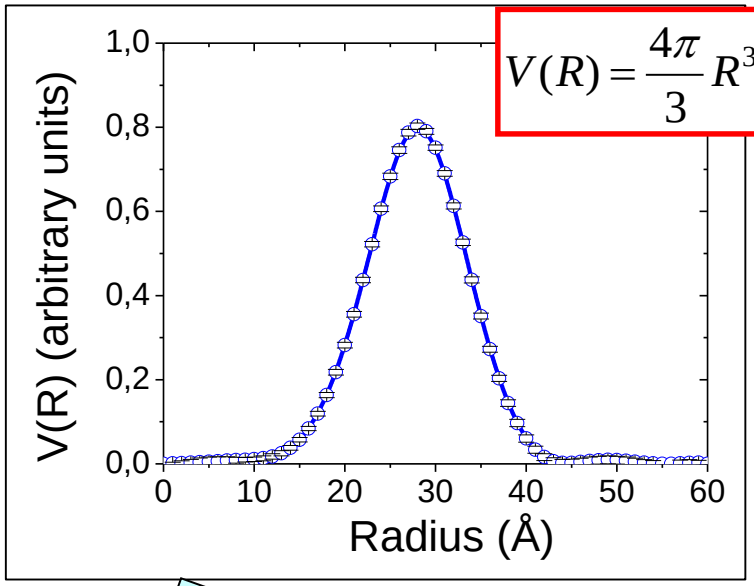

Average radius = 24,1 ± 0,2 Å,

Relative size dispersion: $\sigma_R / \langle R \rangle$ = 0,236 ± 0,004

WAXS RESULTS

WAXS intensity

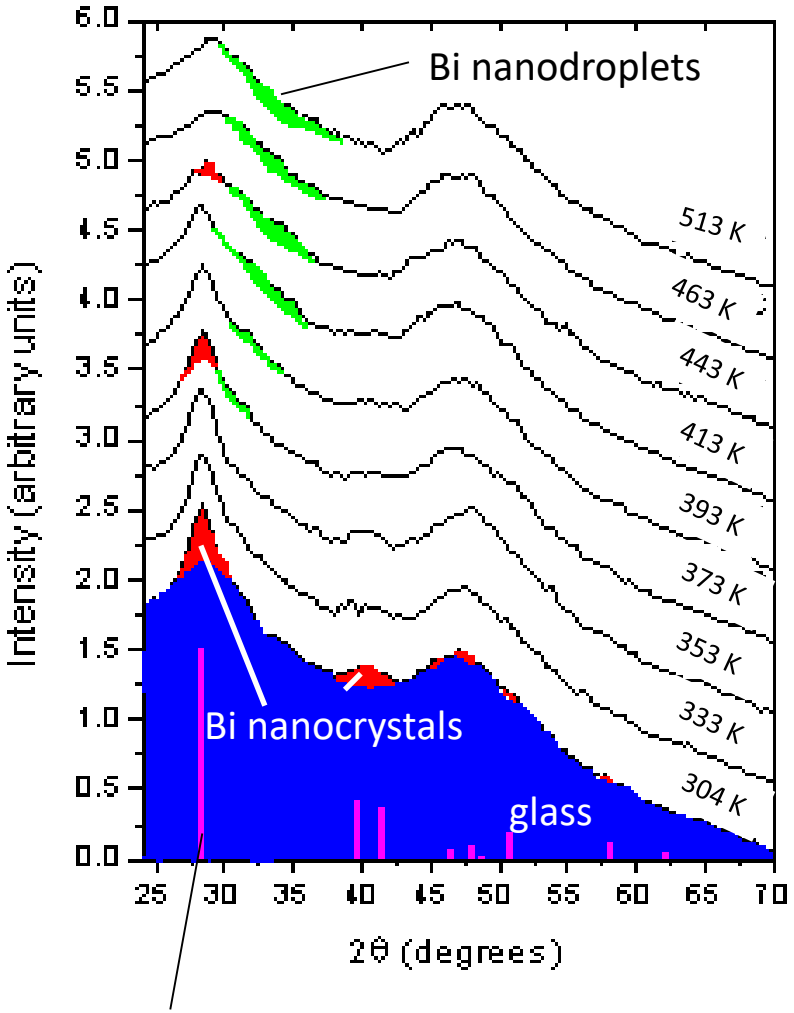

Bulk Bi diffraction lines(rombohedral)

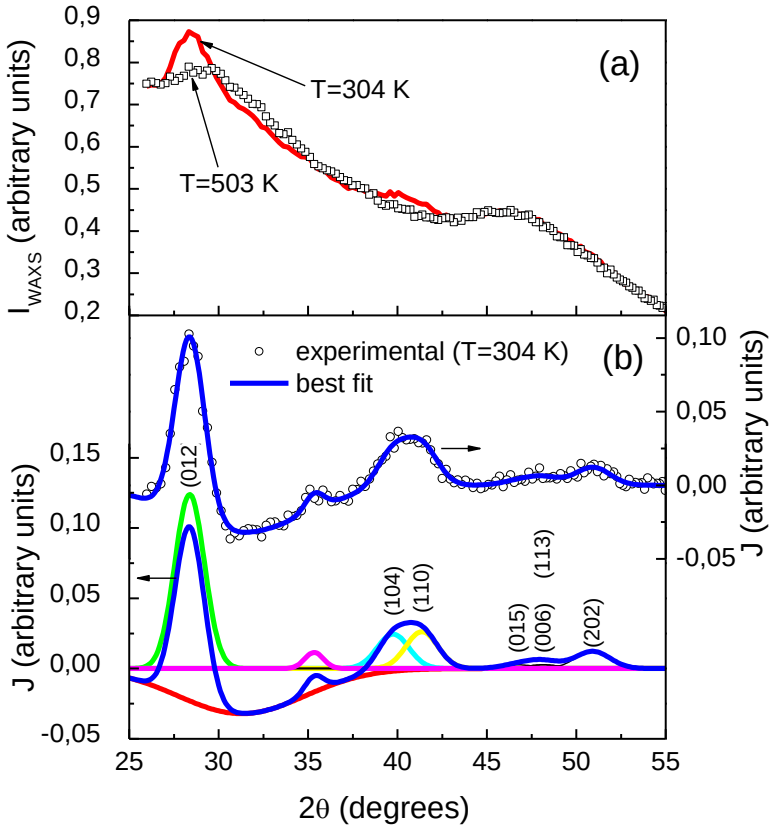

Fitting parameters

- a and c parameters of the hexagonal unitary cell
- integrated area of the (012) peak
- Integral width of the $\Delta(2\theta)_{012}$ Bragg peak.

WAXS RESULTS

Contribution of Bi nanocrystals

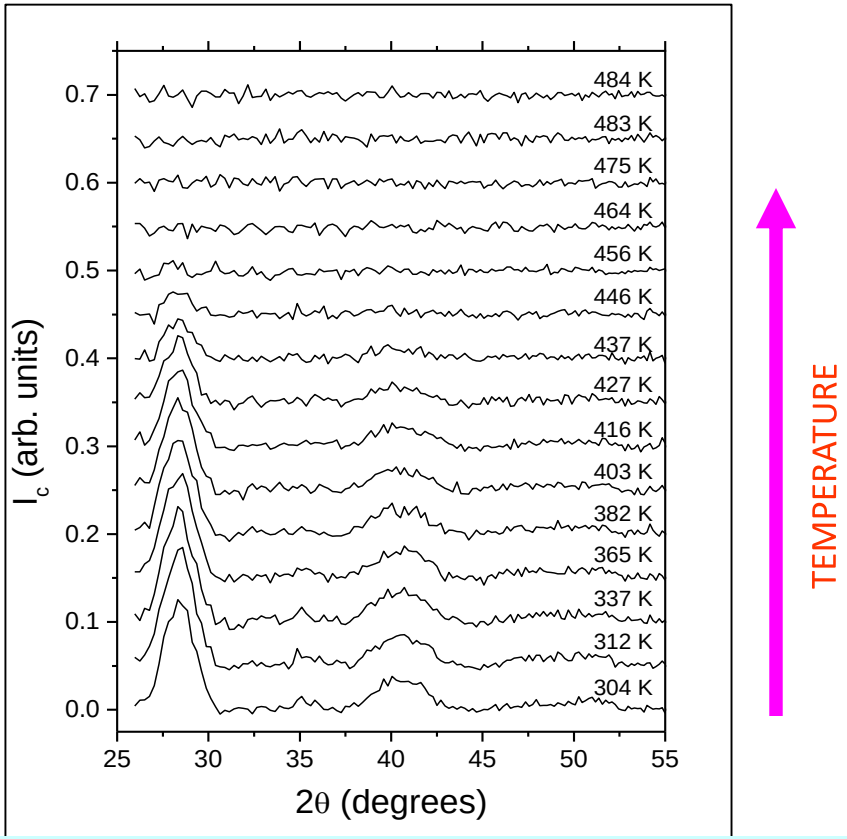

The area under the Bragg peaks decreases continuously in the 365-464 K range. Above 464 K the peaks disappear indicating the Bi nanoclusters are completely melted.

Average nanocrystal size in direction perpendicular to 012 planes

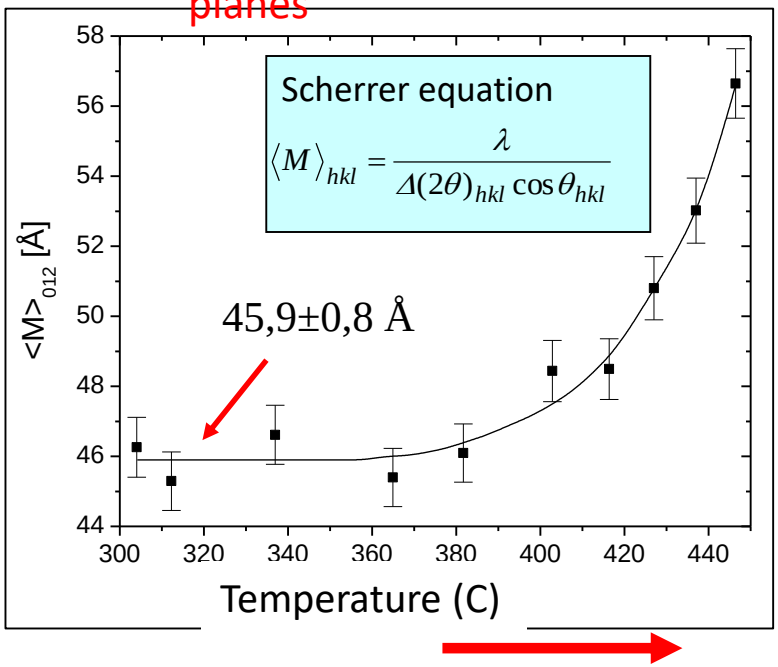

Average size of Bi nanocrystals as a function of the temperature. Above 373 K a progressive increase in the average size for incresing temperatures can be observed.

From the SAXS measurements

$$\langle M \rangle_{sph} = \frac{3}{2} \frac{\int_0^\infty V(R) \cdot R \cdot dR}{\int_0^\infty V(R) \cdot dR} = 41{,}9 \pm 0{,}4 \text{ Å}$$

Lattice contraction

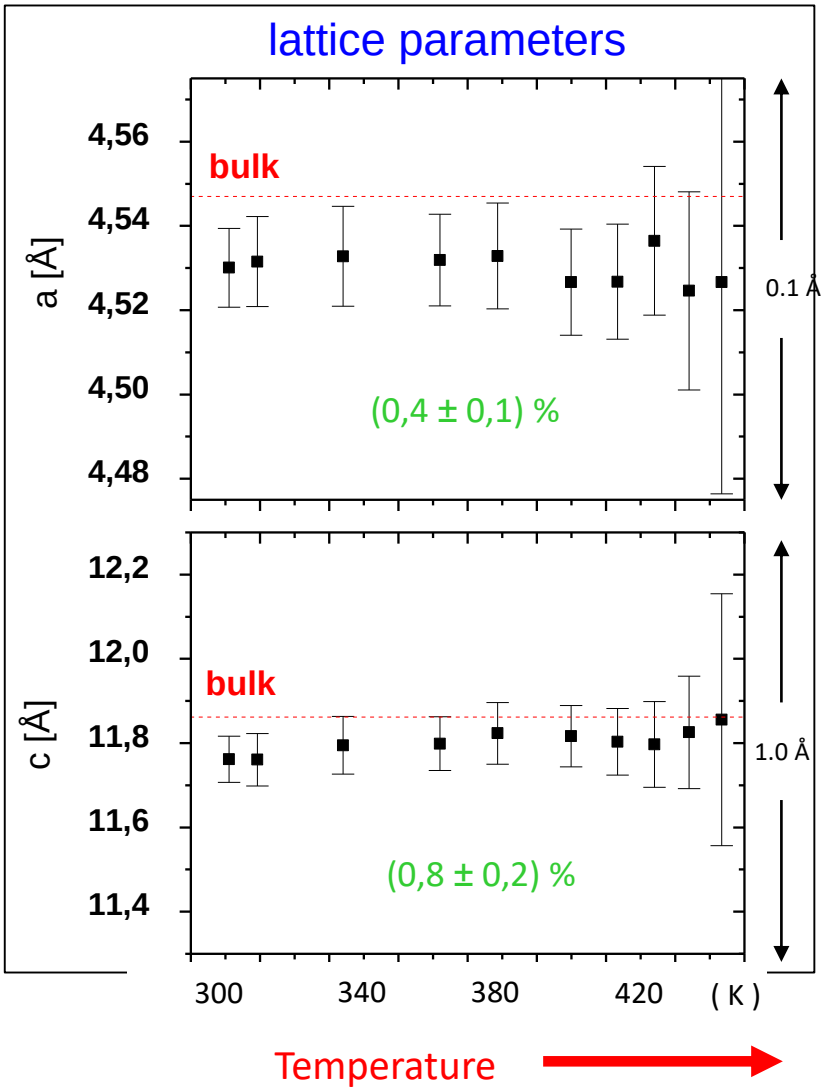

How to determine the relation:

Melting temperature x nanocrystal radius

from WAXS and SAXS measurements?

FROM SAXS RESULTS:

All clusters crystalline

melted

crystalline

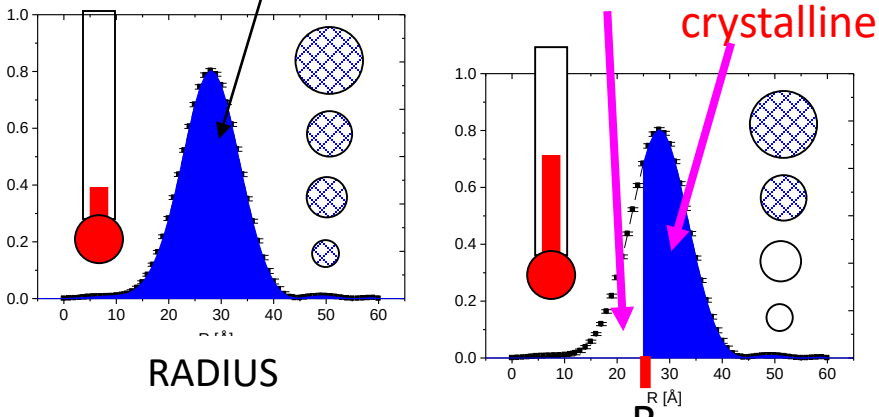

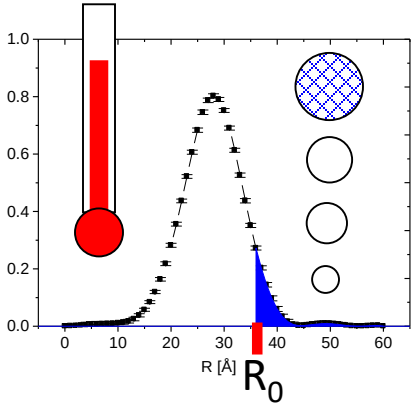

All clusters melted

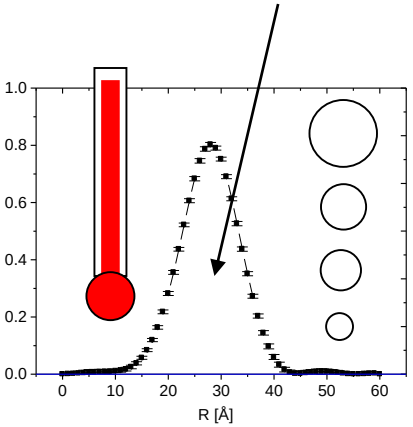

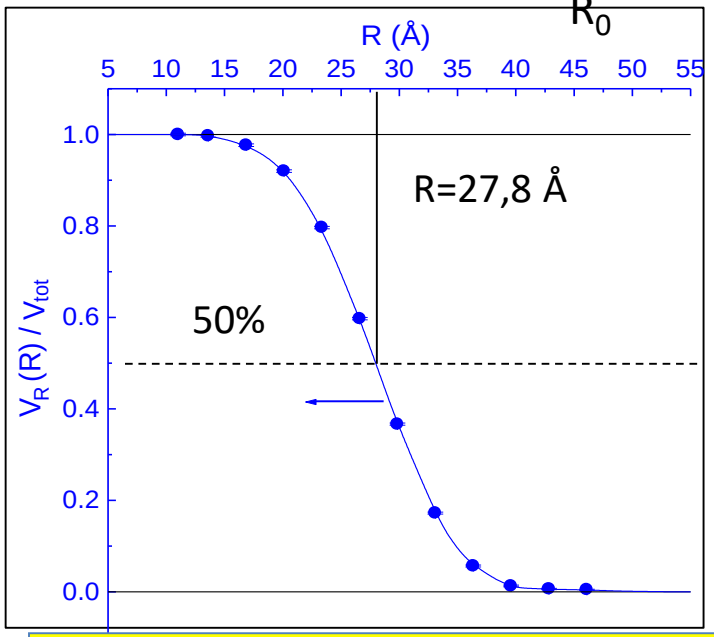

VOLUME FRACTION occupied by the nanocrystals having radius larger than R_0

$$\frac{V_R(R_0)}{V_{tot}} = \frac{\int_{R_0}^{\infty} V(R')\cdot dR'}{\int_{0}^{\infty} V(R')\cdot dR'} = \frac{\text{Bi clusters with } R > R_0}{\text{Total Bi volume}}$$

$V_R(R)/ V_{tot}$ depends of the shape of the V(R) function

DIFFRACTED INTENSITY X TEMPERATURE

Diffracted intensity by Bi nanocrystals

TEMPERATURE

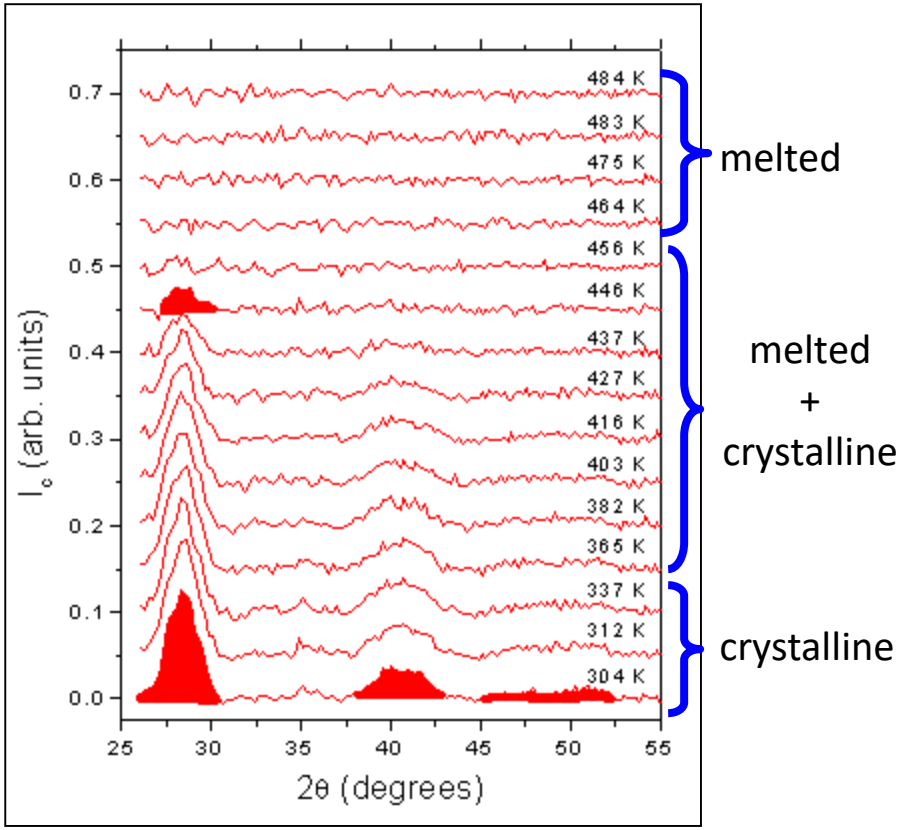

Volume fraction of crystalline Bi

$$\frac{I_c(T)}{I_c(304\ K)}$$

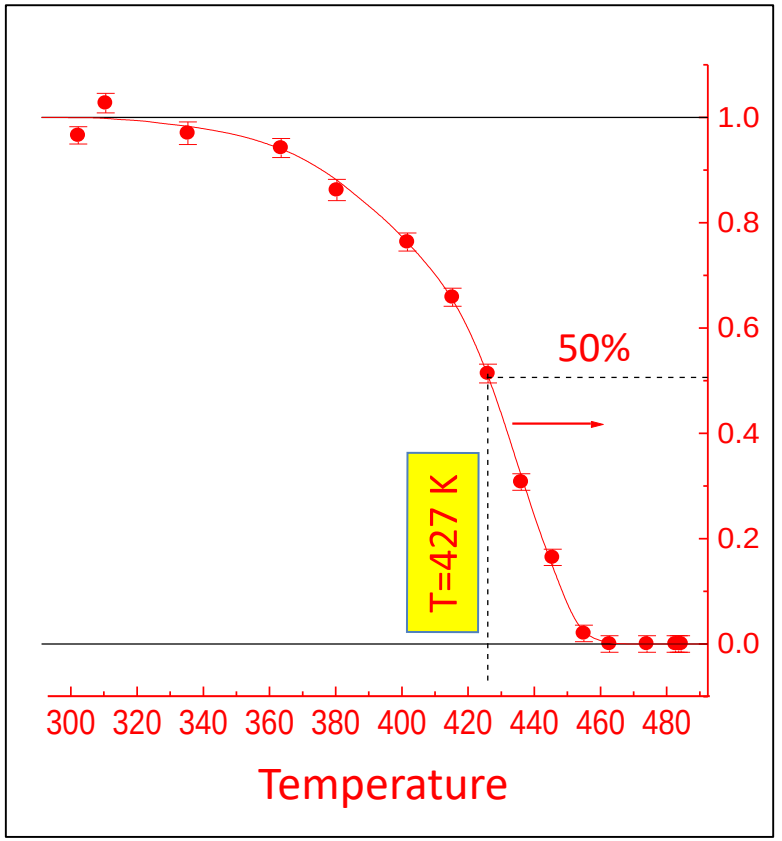

Crystalline fraction

Volume fraction as a function of R

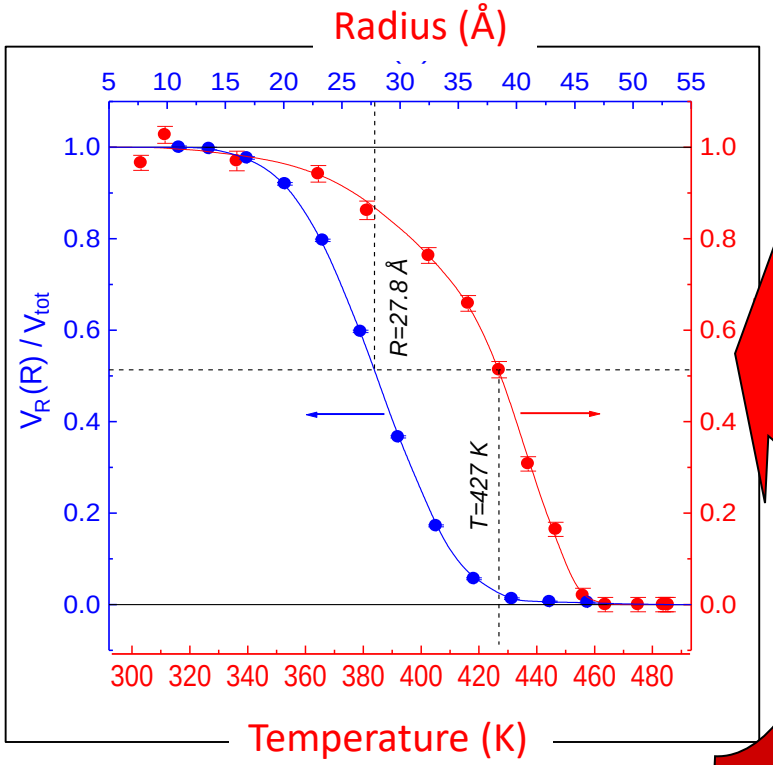

Volume fraction as a function of temperature

Melting temperature x Radius

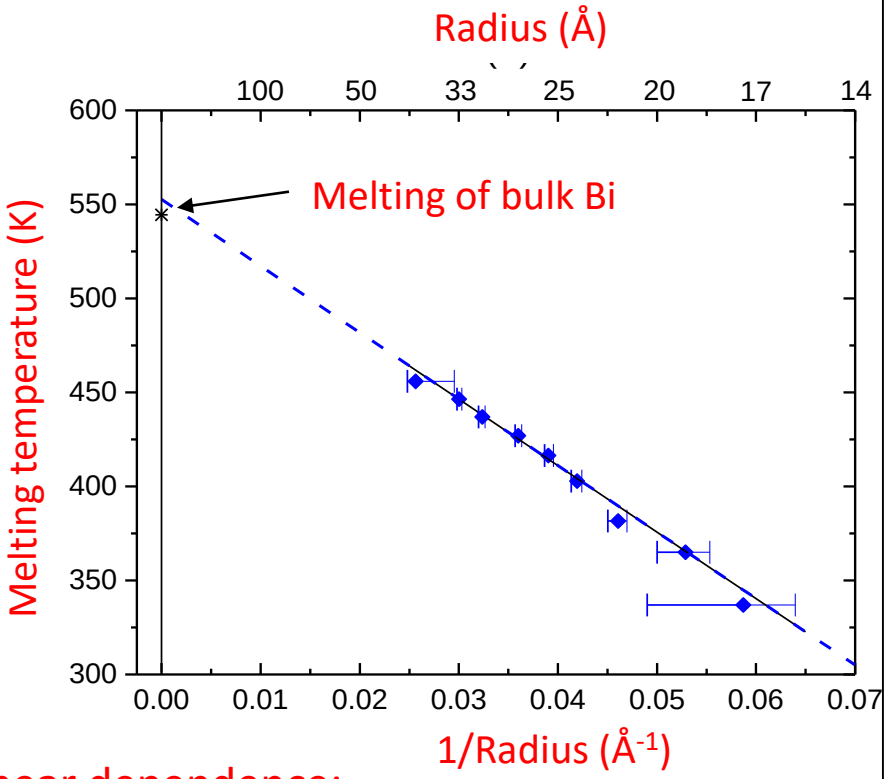

Linear dependence:

$$T_m - T_b = a + b/Raio$$

Couchman - Jesser (1977) e Allen *et al.*, (1980)

Comparison with previous results

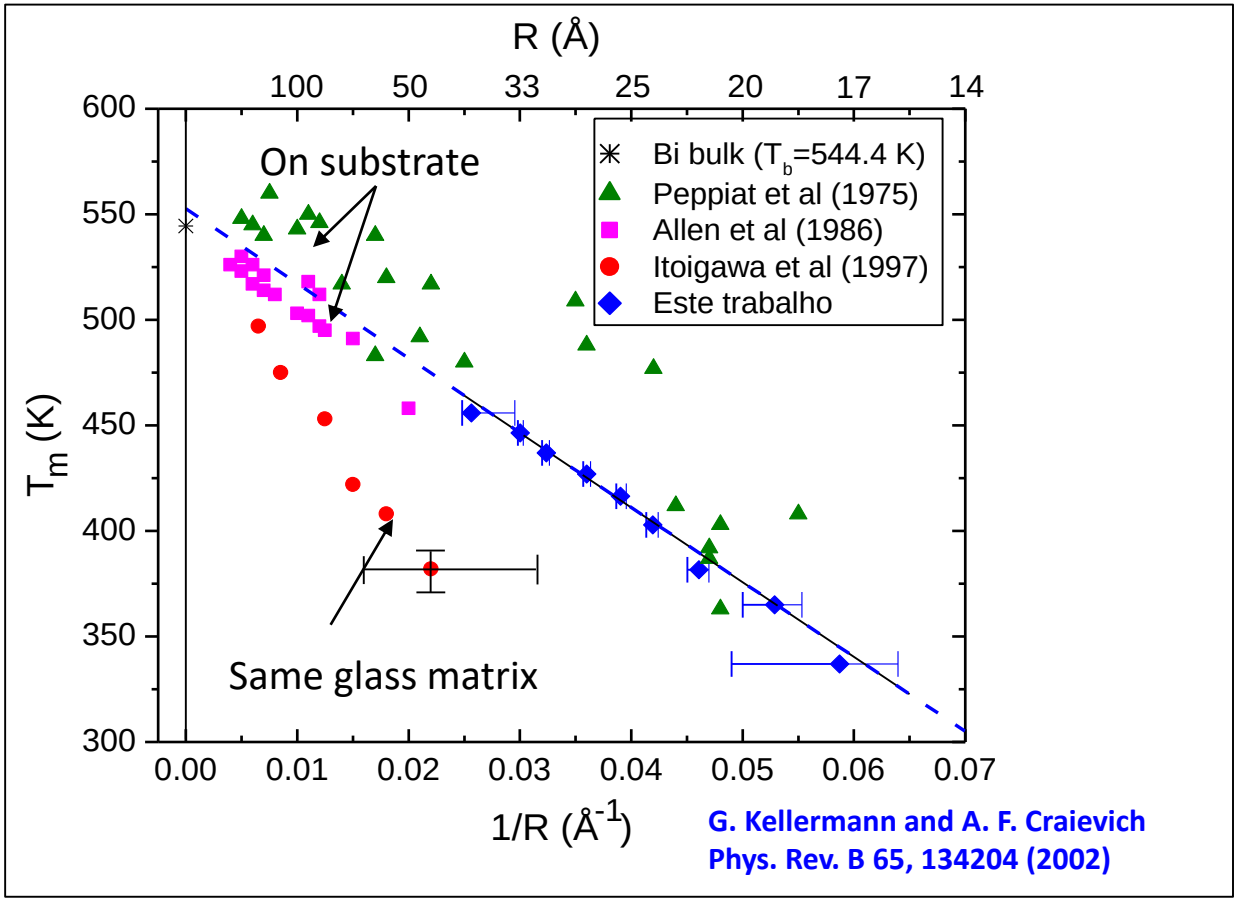

G. Kellermann and A. F. Craievich
Phys. Rev. B 65, 134204 (2002)

$\sigma_{vl} - \sigma_{vc} = 175 \times 10^{-3}$ J m^{-2}
C. J. Smithells, ed., Metal Reference Book, 4th Ed., Vols. 1-3 (Butterworth, London, 1967)

$\sigma_{vl} - \sigma_{vc} = 122 \times 10^{-3}$ J m^{-2}
G. L. Allen et al., Thin Solid Films 144 (1986) 297.

In this work:

$\sigma_{vl} - \sigma_{vc} = 115 \times 10^{-3}$ J m^{-2}

freezing of spherical Bi nanoparticles confined in a homogeneous sodium borate glass

G. Kellermann and A. F. Craievich

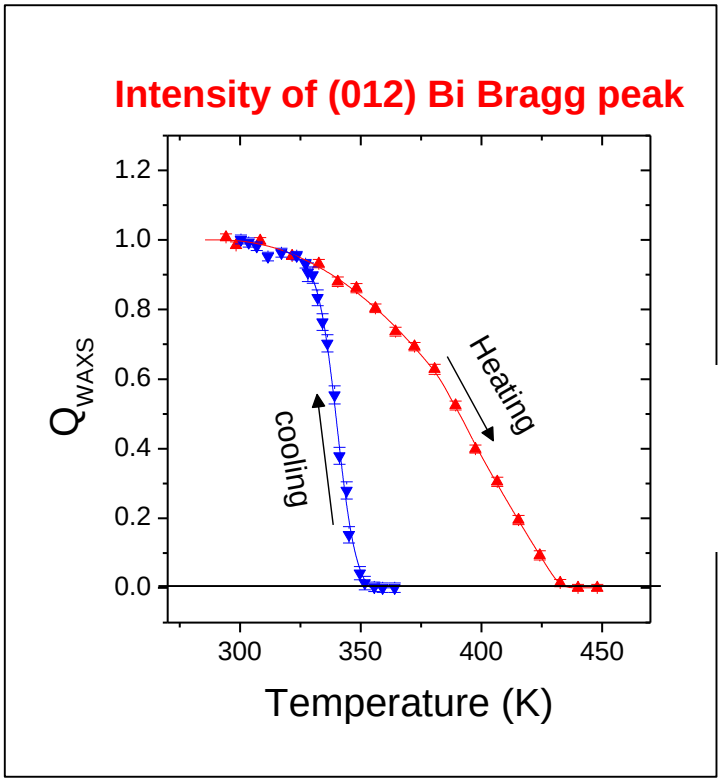

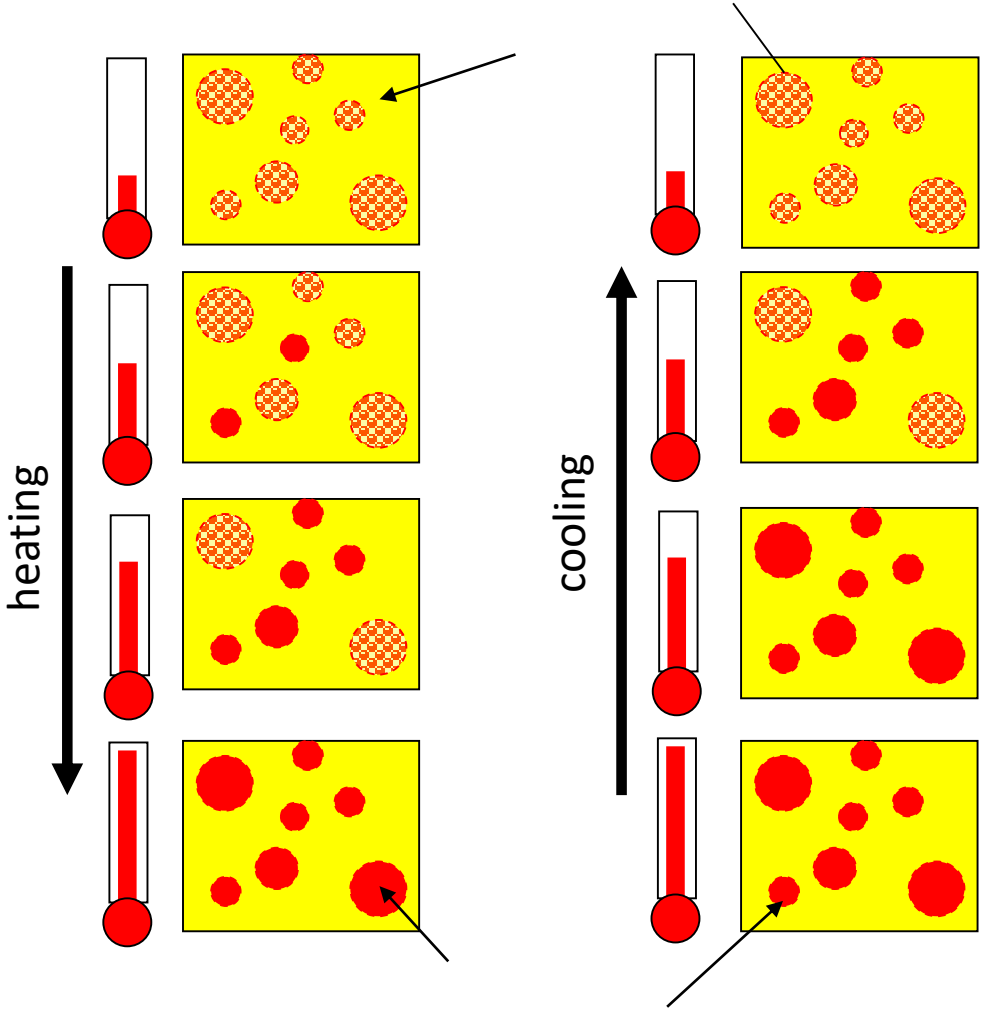

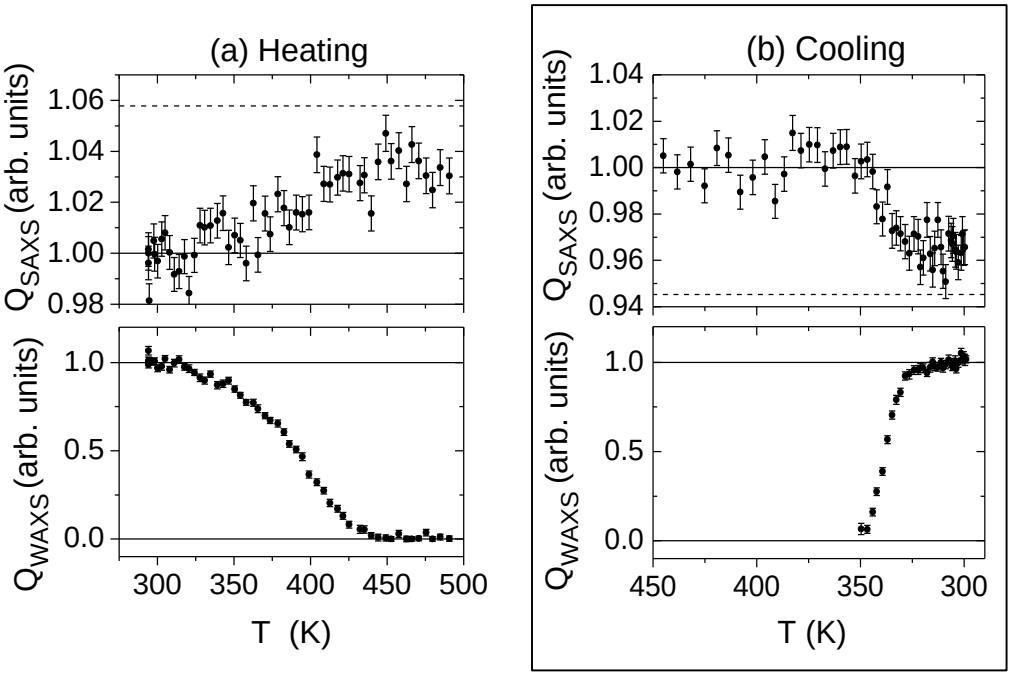
(a) Heating
(b) Cooling
Q_{SAXS} (arb. units)
Q_{WAXS} (arb. units)
T (K)

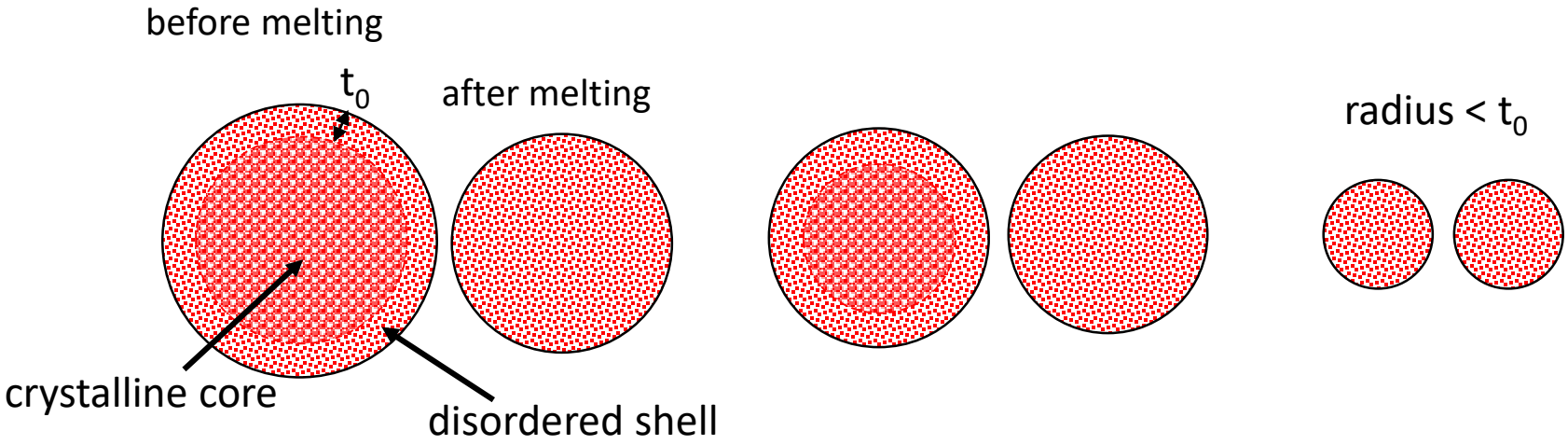
before melting
t_0
after melting
radius < t_0
crystalline core
disordered shell

RADIUS DEPENDENCE ON MELTING AND FREZEENG TEMPERATURES OF Bi NANOPARTICLE

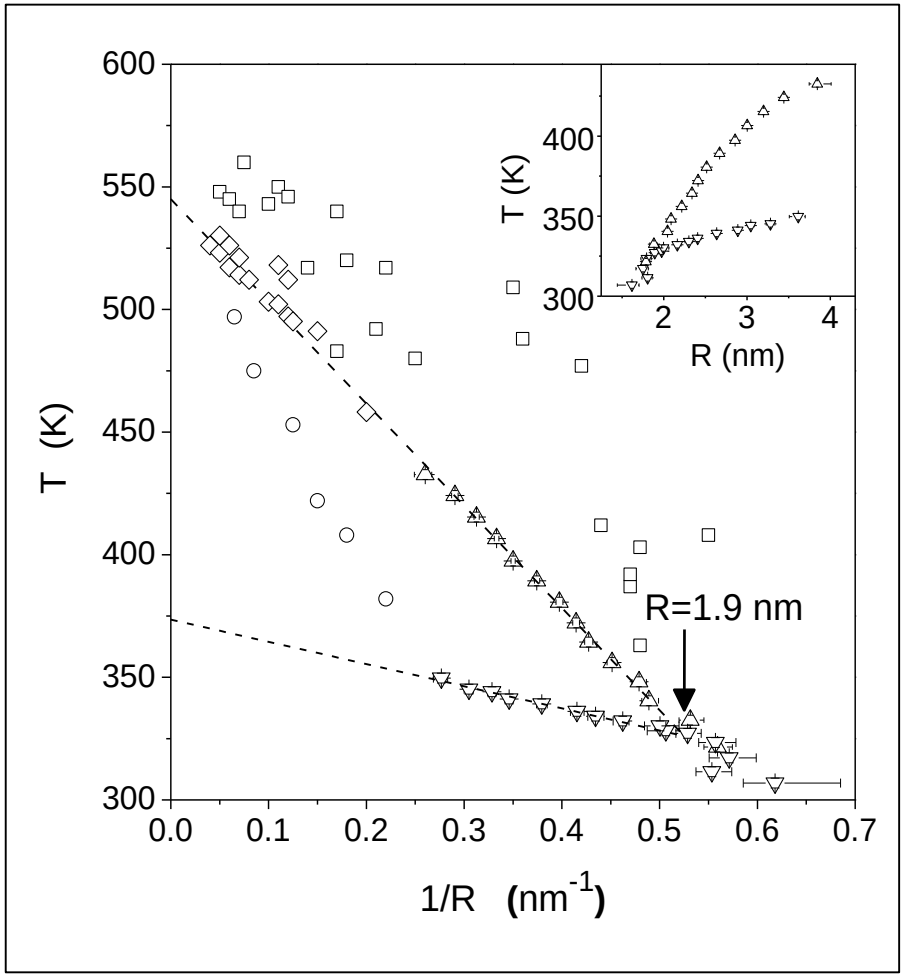

CORE-SHELL MODEL
Bi NANOPARTICLES

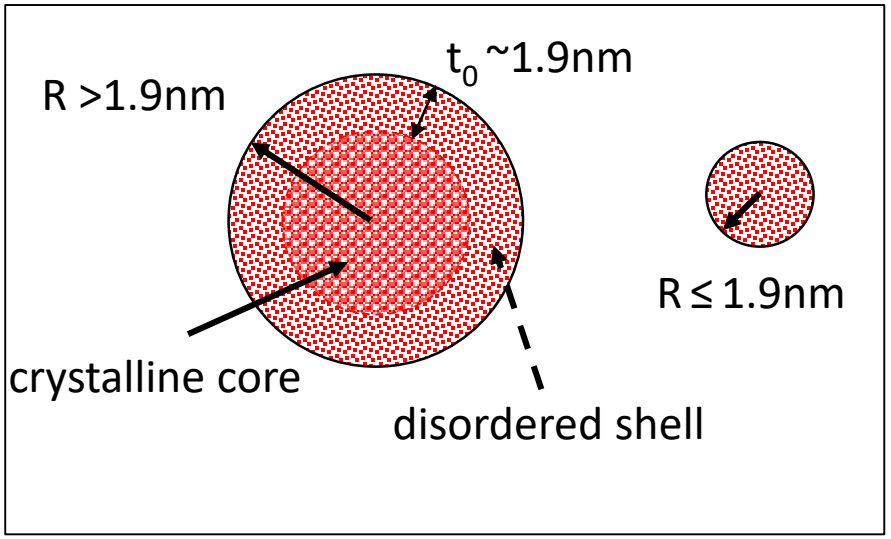

Anomalous small-angle x-ray scattering (ASAXS)

•Small-Angle X-ray Scattering (SAXS) is a technique of registering the intensity of X-rays scattered at angles typically below 5°. It is applied for investigating structures with spatial dimensions in the nanometre range, typically 0.5-100 nm. SAXS proves the nano-structure of a variety of different materials which can be solid (also very porous or powdered) or liquid.

•Anomalous Small-Angle X-ray Scattering (ASAXS) uses tuneable X-ray energy near X-ray absorption edges of the elements comprising in the investigated sample. Thus element specific information, composition and density fluctuation can be obtained.

The underlying physics of ASAXS

Atomic scattering factor (amplitude) far from the absorption edges:

$$f_{atm}(\vec{q}) = f_0(\vec{q}) \qquad f_0(\vec{q}) = \int_0^{\infty} \rho(\vec{r}) \frac{\sin(\vec{q}\cdot\vec{r})}{\vec{q}\cdot\vec{r}} d\vec{r} \qquad q = \frac{4\pi}{\lambda}\cdot\sin(\theta)$$

$\rho(\vec{r})$: electron density at $\vec{r}$ in the atom

f_0: Fourier transform of electron density over the atomic volume

for q=0 f_0=Z (atomic number)

q= ∞ $f_0 \rightarrow 0$

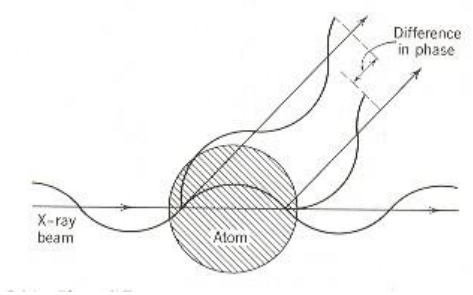

Scattering by a single atom. X-ray wavelength is of the order of the size of distribution of electrons around the atom

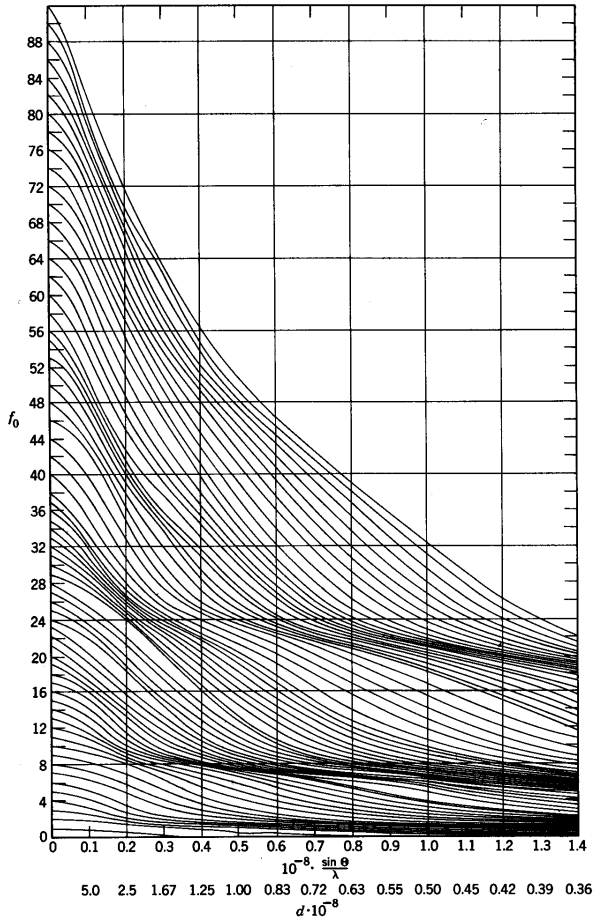

L. Pauling and J. Sherman, Z. Keystallogr.,81. 1(1932)

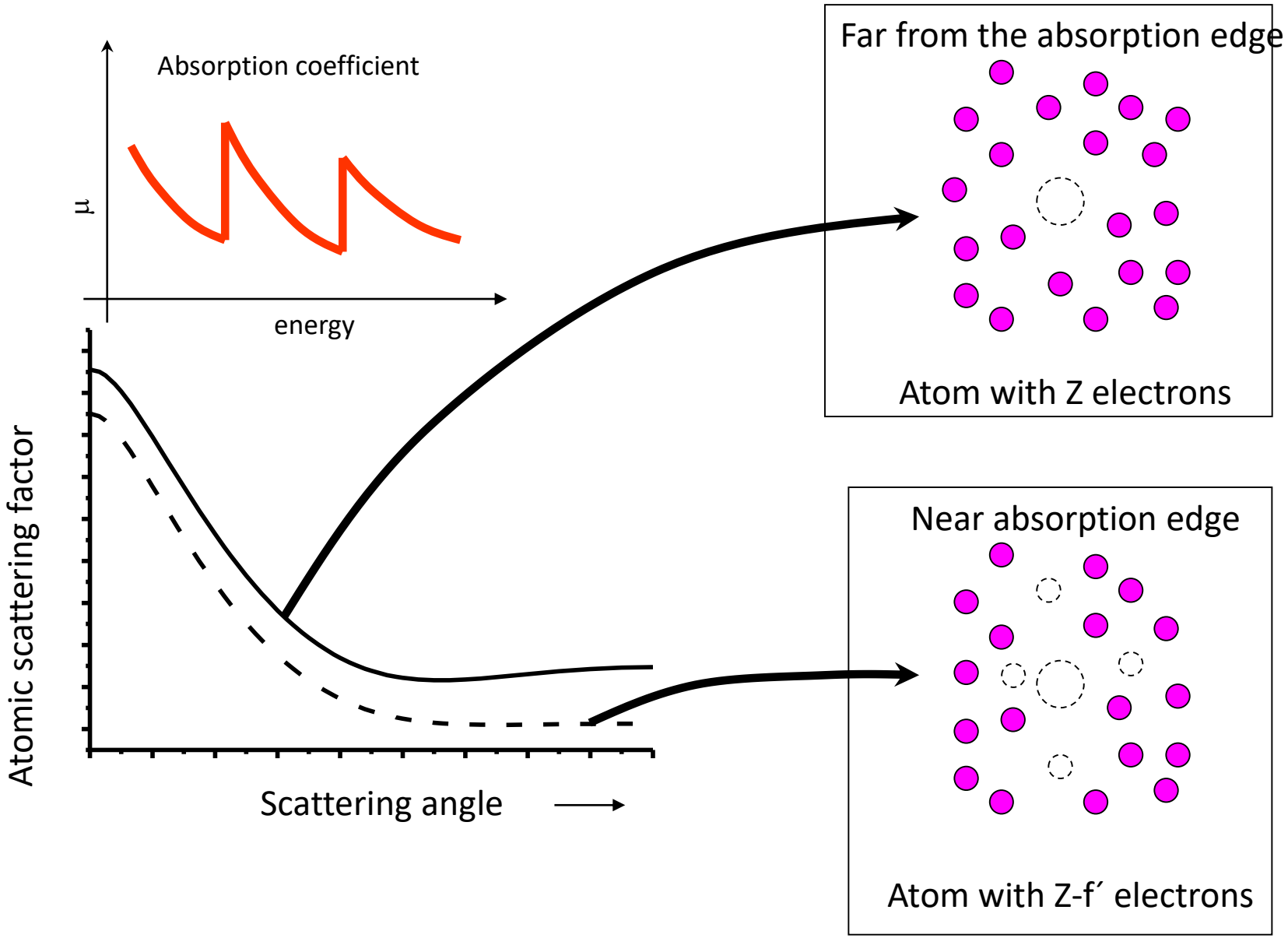
Absorption coefficient
μ
energy
Atomic scattering factor
Scattering angle
Far from the absorption edge
Atom with Z electrons
Near absorption edge
Atom with Z-f´ electrons

General expression for the atomic scattering factor

The atomic scattering factor shows a sharp fluctuation in the vicinity of absorption edges

Two correction terms, f´ and f´´, must be added to account for this "anomalous" behavior

$$f_{atm}(\vec{q},E) = f_0(\vec{q}) + f'(\vec{q},E) + i\ f''(\vec{q},E)$$

(complex number)

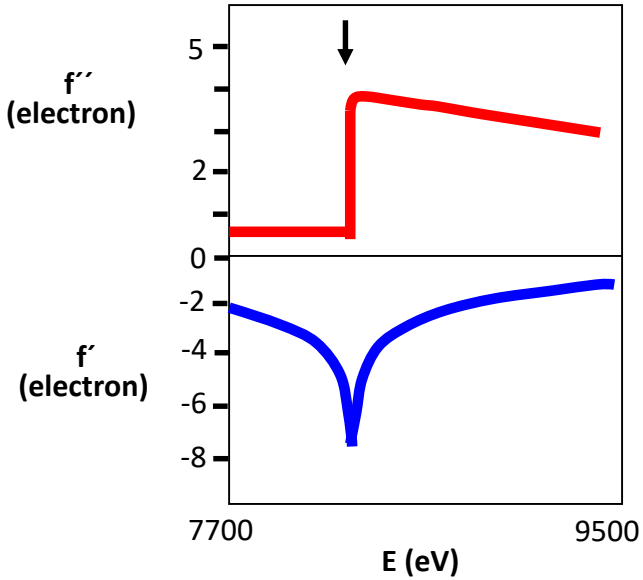

f´ and f´´ at Ni absorption edge (Z=28)

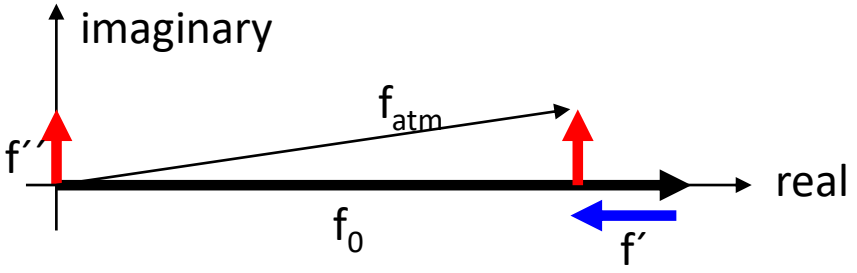

f_0 is the scattering factor far from the edge (= Z, atomic number)

f´(q,E) and f´´(q,E) are the real and imaginary part of dispersion correction. They are associated with scattering via absorption and reemission of photons, resulting in a phase shift

f´´(q,E) is weak and nearly constant below the absorption edge. It becomes more important above the edge where a strong background of fluorescence takes place

Finally, how can we take advantage from the anomalous behavior of the atomic scattering factor in SAXS experiments?

Example: Multicomponet systems

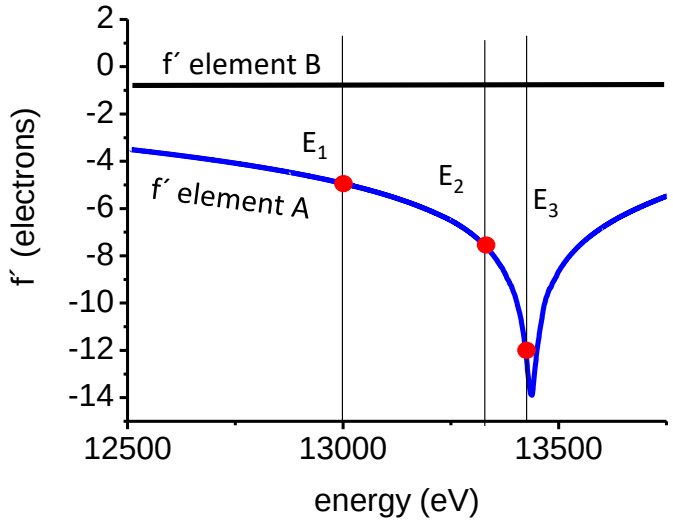

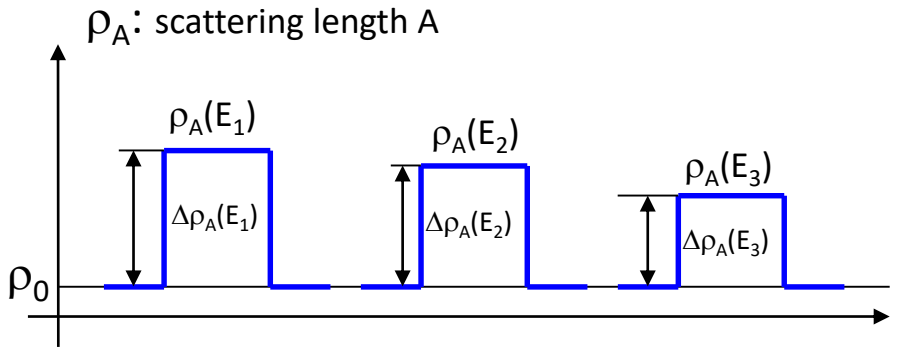

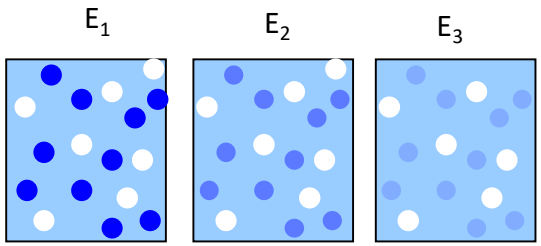

element A

element B

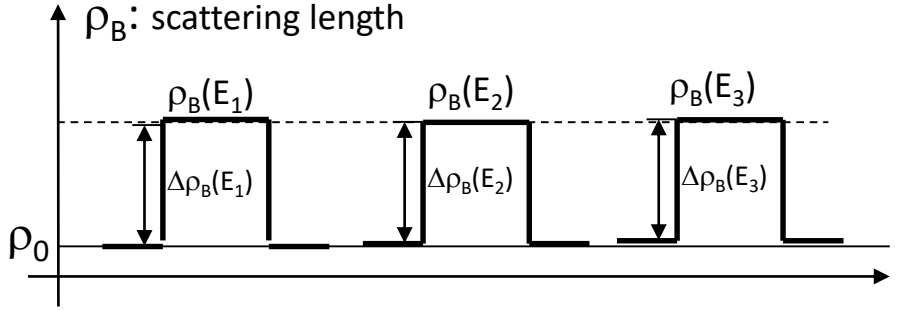

Only the scattering length of element A is affected

Mixture of spheres with different composition

Consider a diluted mixture of spherical objects composed by pure elements A or B embedded in a matrix composed by a element C. The spheres of element A have the same radius R_A and the spheres of element B have the same radius R_B. N_A and N_B, and ρ_A and ρ_B are the number density and effective electron density (scattering length) of elements A and B, respectively

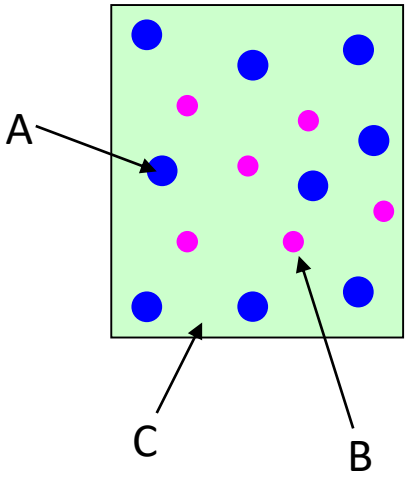

Total intensity: $$\frac{d\Sigma}{d\Omega}(q,E) = \sum_{i=A,B} \left(\rho_i - \langle\rho\rangle\right)^2 \left|F_i(q,R)\right|^2$$

$$\left|F(q,R)\right|^2 = \left|3\frac{\sin(qR) - qR\cos(qR)}{(qR)^3}\right|^2$$ (form factor of a sphere with radius R)

$$\frac{d\Sigma}{d\Omega}(q,E) = \underbrace{\left[\rho_A(E) - \rho_0\right]^2 \left|F(q,R_A)\right|^2 N_A}_{\text{Contribution of element A}} + \underbrace{\left[\rho_B - \rho_0\right]^2 \left|F(q,R_B)\right|^2 N_B}_{\text{Contribution of element B}}$$

$$\left(\langle\rho\rangle \approx \rho_0\right)$$

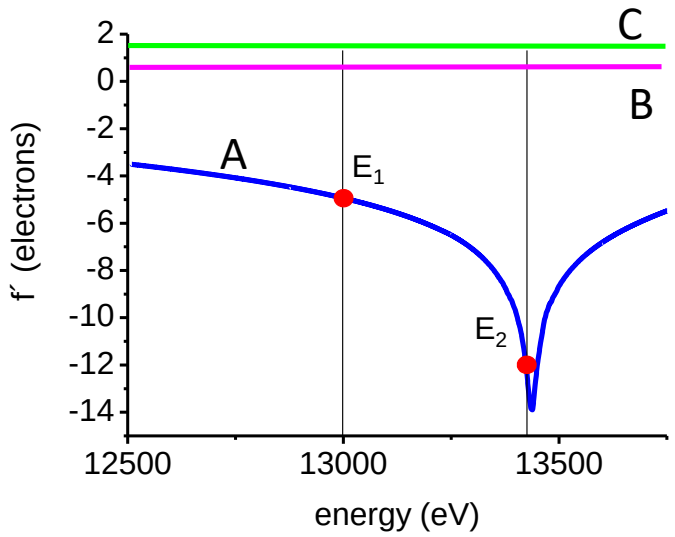

We assume also that only the form factor of element A is affected by the energy

The difference in the scattering intensity measured at energies E1 and E2 is given by:

$$\frac{d\Sigma}{d\Omega}(q,E_1)-\frac{d\Sigma}{d\Omega}(q,E_2)=\left[\frac{d\Sigma}{d\Omega_A}(q,E_1)+\frac{d\Sigma}{d\Omega_B}(q)\right]-\left[\frac{d\Sigma}{d\Omega_A}(q,E_2)+\frac{d\Sigma}{d\Omega_B}(q)\right]$$

$\frac{d\Sigma}{d\Omega_B}(q)$: =0

$$\frac{d\Sigma}{d\Omega}(q,E_1)-\frac{d\Sigma}{d\Omega}(q,E_2)=\frac{d\Sigma}{d\Omega_A}(q,E_1)-\frac{d\Sigma}{d\Omega_A}(q,E_2)$$

From the difference only the contribution of element A is obtained:

$$\frac{d\Sigma}{d\Omega}(q,E_1)-\frac{d\Sigma}{d\Omega}(q,E_2)=N_A\left|F(q,R_A)\right|^2\left\{\left[\rho_A(E_1)-\rho_0\right]^2-\left[\rho_A(E_2)-\rho_0\right]^2\right\}$$

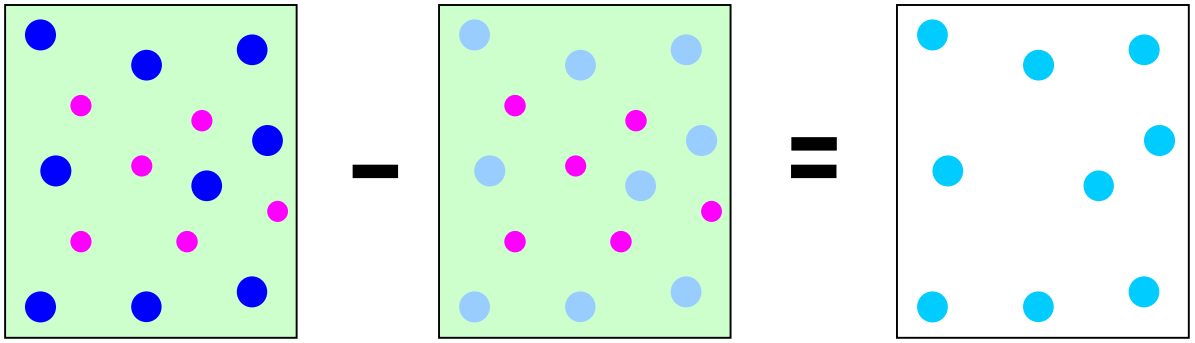

ASAXS from Bi nanocrystals embedded in sodium borate glass

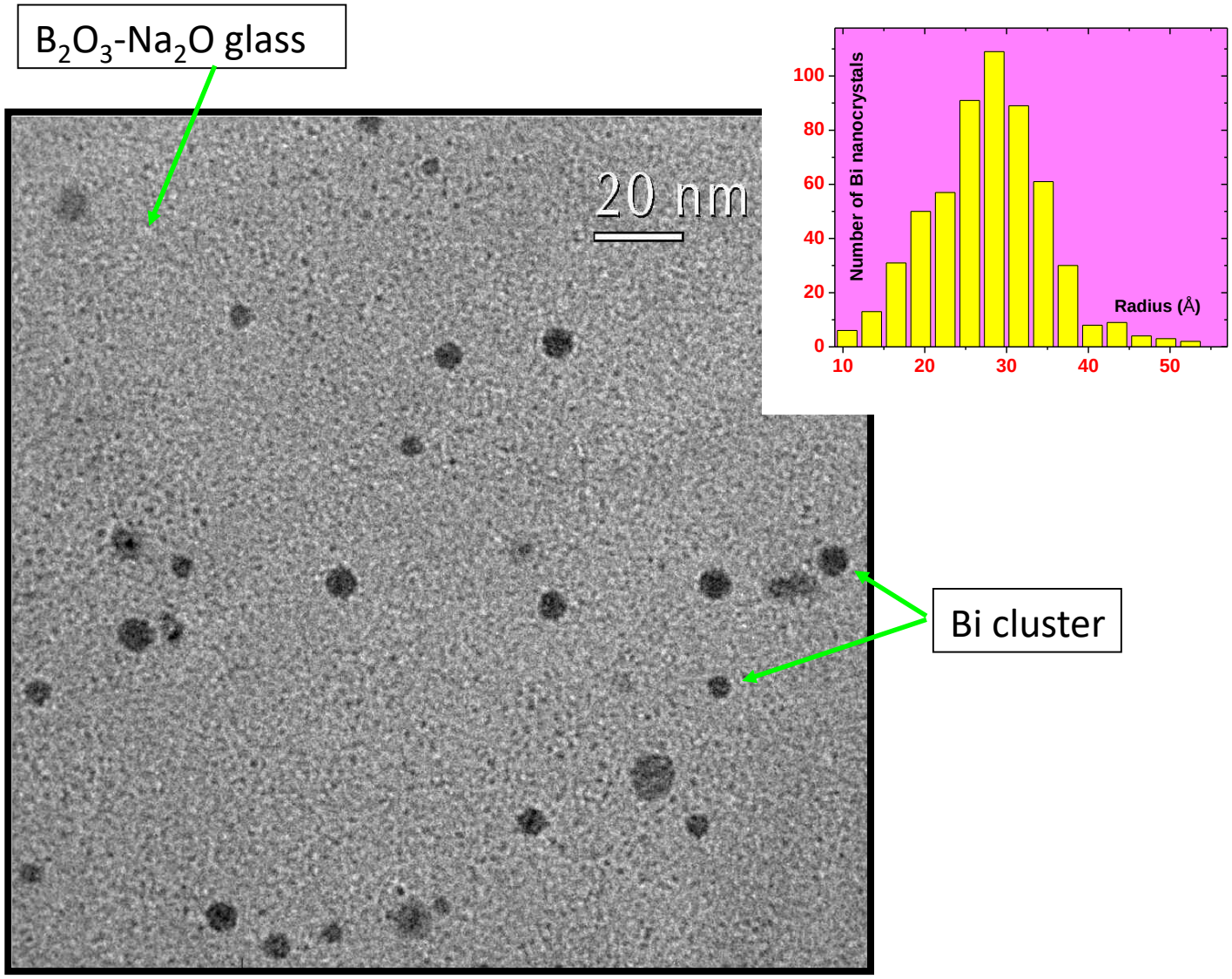

Structural investigation of Bi nanocrystals embedded in sodium borate glass

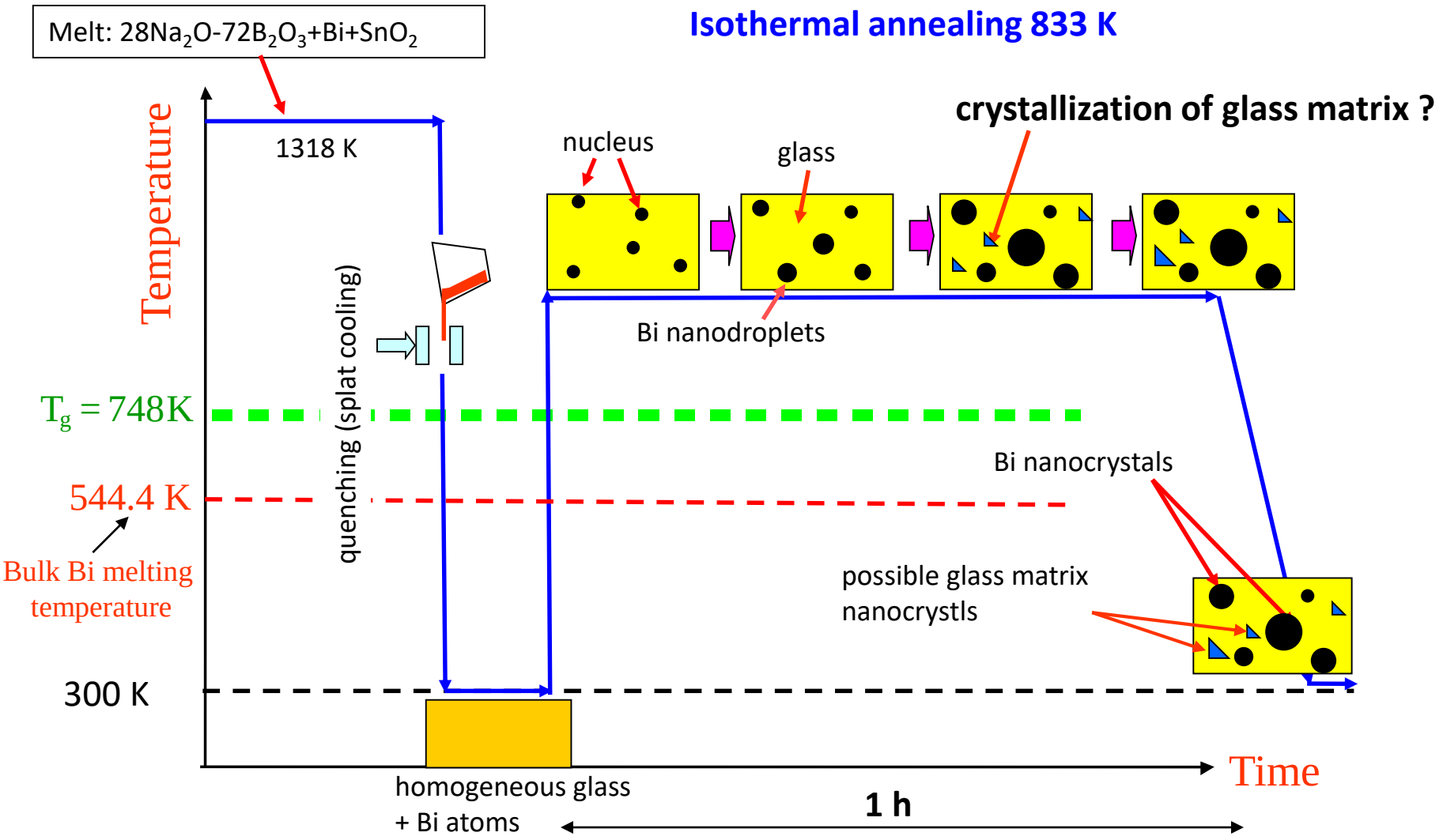

Mixture of spherical Bi nanocrystals + glass nanocrystals

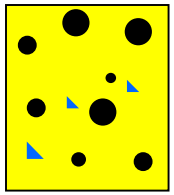

$$\frac{d\Sigma}{d\Omega_{total}}(q,E) = \sum_i \left[\rho_{Bi}(E)-\rho_0\right]^2 \left|F_{Bi}(q,R_i)\right|^2 + \sum_i \left[\rho_{gc}-\rho_0\right]^2 \left|F_{gc}(q,R_i)\right|^2$$

Contribution of Bi nanocrystals

Contribution of element glass crystallites

The difference in the scattering intensity measured at energies E_1 and E_2, close to Bi absorption edge, is given by:

$$\frac{d\Sigma}{d\Omega_{total}}(q,E_1) - \frac{d\Sigma}{d\Omega_{total}}(q,E_2) = \left[\frac{d\Sigma}{d\Omega_{Bi}}(q,E_1) + \cancel{\frac{d\Sigma}{d\Omega_{gc}}(q)}\right] - \left[\frac{d\Sigma}{d\Omega_{Bi}}(q,E_2) + \cancel{\frac{d\Sigma}{d\Omega_{gc}}(q)}\right] \quad (=0)$$

From the difference only the contribution of Bi element is obtained:

$$\frac{d\Sigma}{d\Omega_{total}}(q,E_1) - \frac{d\Sigma}{d\Omega_{total}}(q,E_2) = \frac{d\Sigma}{d\Omega_{Bi}}(q,E_1) - \frac{d\Sigma}{d\Omega_{Bi}}(q,E_2)$$

$$\frac{d\Sigma}{d\Omega}(q,E_1) - \frac{d\Sigma}{d\Omega}(q,E_2) = \left\{\left[\rho_A(E_1)-\rho_0\right]^2 - \left[\rho_A(E_2)-\rho_0\right]^2\right\} \sum_i \left|F(q,R_{Bi})\right|^2$$

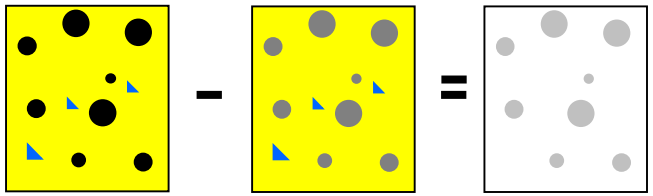

Real part of the Bi atomic scattering factor correction

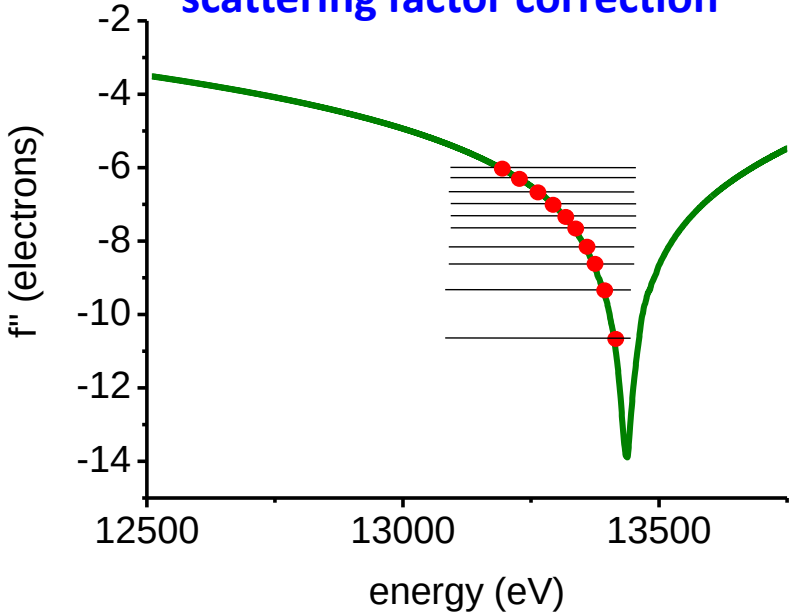

SAXS intensity as a function of photon energy

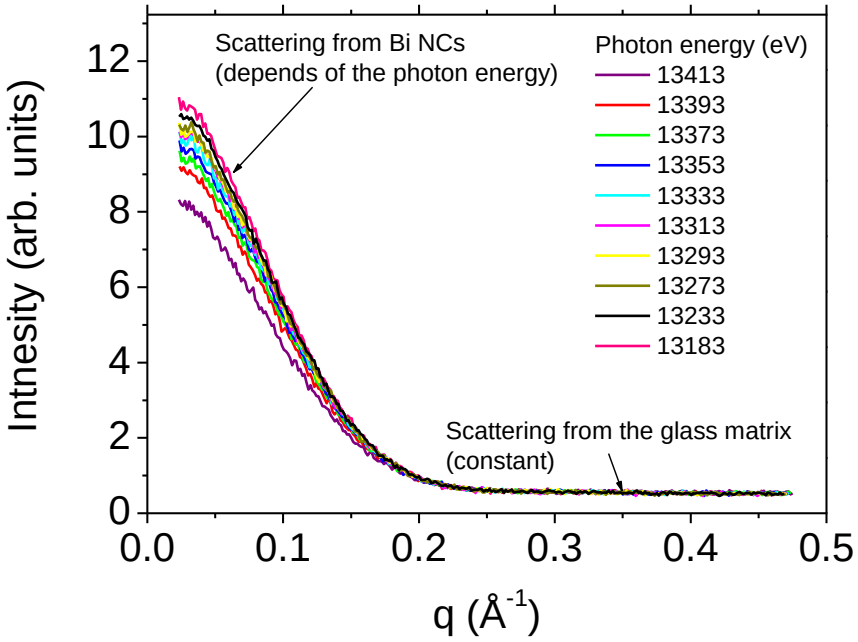

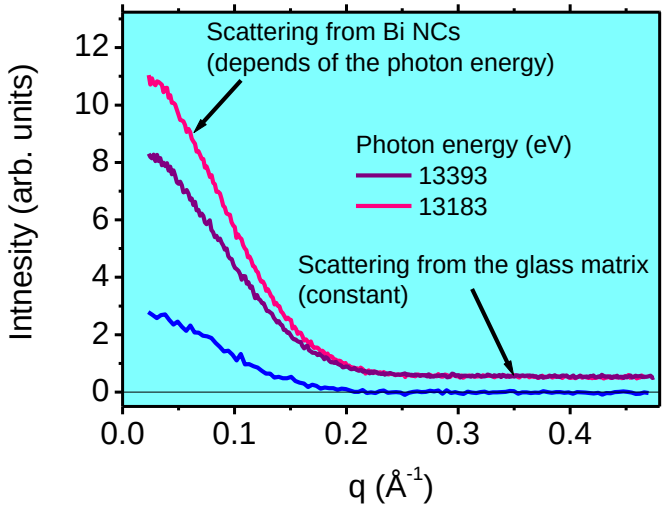

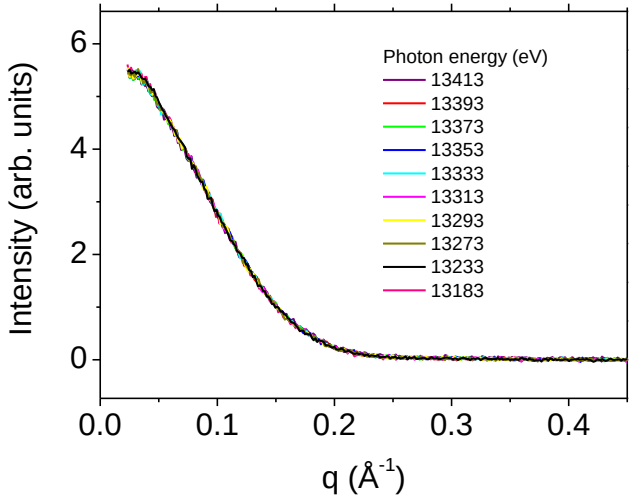

Determination of the size distribution function

SAXS intensity for diluted set of spheres in a homogeneous matrix:

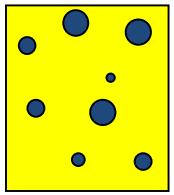

$$\frac{d\Sigma}{d\Omega}(q,E) = [\rho_{Bi}(E) - \rho_0]^2 \int_{Rmin}^{Rmax} |F(q,R)|^2 N(R) R^6 dR \qquad \text{where} \qquad |F(q,R)|^2 = \left| 3\frac{\sin(qR) - qR\cos(qR)}{(qR)^3} \right|^2$$

ASAXS intensity

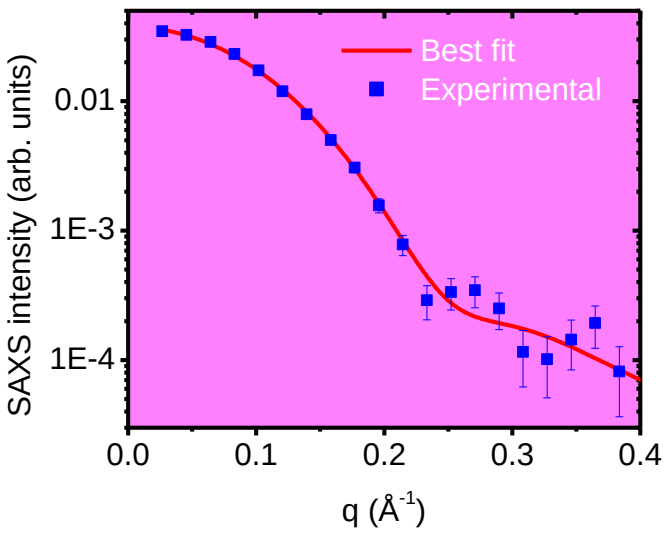

Diffrence of the SAXS intensity curves measured at 13183 eV and 13413 eV.

Radius distribution function

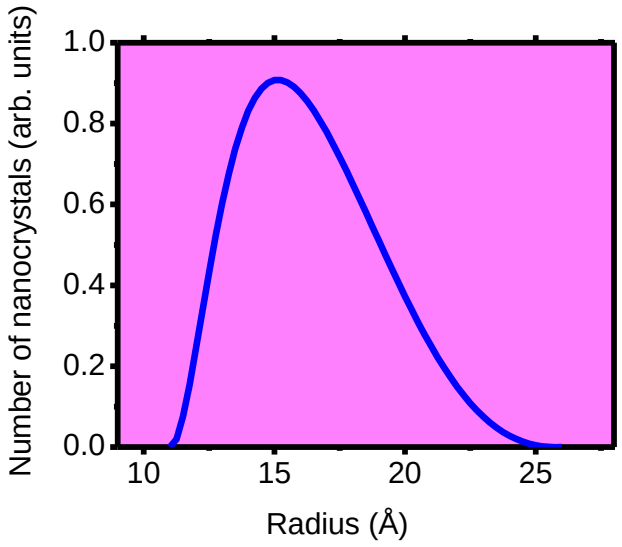

Average radius $\langle R \rangle$ = 16.4 Å

Relative size dispersion $\sigma / \langle R \rangle$ = 0.22

PHOTON ENERGY vs. SAXS INTENSITY CLOSE TO Bi ABSORPTION EDGE

$$I(q,E)=\frac{d\Sigma}{d\Omega}(q,E)=\left[\rho_{Bi}(E)-\rho_0\right]^2\int_{Rmin}^{Rmax}\left|F(q,R)\right|^2N(R)R^6dR$$

$$I(q,E)=\left[\rho_{Bi}(E)-\rho_0\right]^2k \quad \Rightarrow \quad \left[I(q,E)\right]^{1/2}=\pm\left[\rho_{Bi}(E)-\rho_0\right]k^{1/2}$$

$$k=\int_{Rmin}^{Rmax}\left|F(q,R)\right|^2N(R)R^6dR \text{ (is not a function of E)}$$

$$\left[I(q,E)\right]^{1/2}=\rho_{Bi}(E)k^{1/2}-\rho_0\,k^{1/2}$$

$$\uparrow_{y} \qquad \uparrow_{x}$$

ρ_{Bi}: scattering length of Bi

ρ_0:scattering length of glass matrix (electron density)

$$\rho_{Bi}(\vec{r},E)=c\,f_{Bi}(E)$$

c: Bi concentration [atoms/cm^3]

f_{Bi}: atomic scattering amplitude of Bi

$$f_{Bi}(E)=83+f'_{Bi}(E)\,[\text{electons}]$$

ρ_0: glass electron density [electons/cm^3]

$$y=bx+a$$

$$a=\rho_0k^{1/2}$$

$$b=k^{1/2}$$

$$\rho_0=a/b$$

Determination of the electrons density of the glass matrix ρ_0

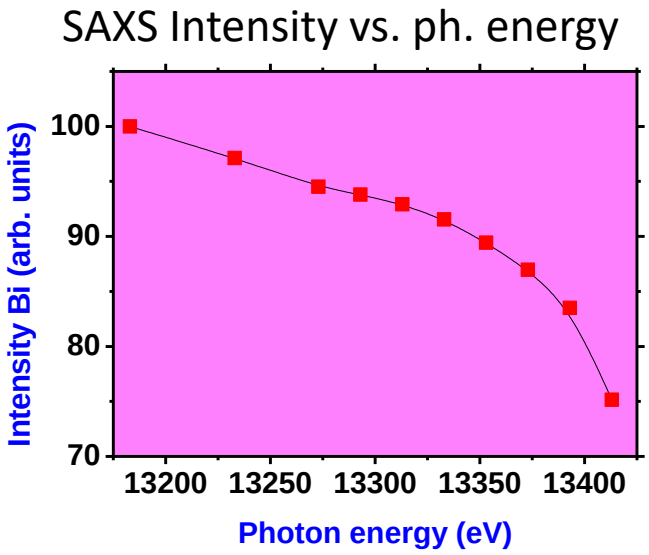

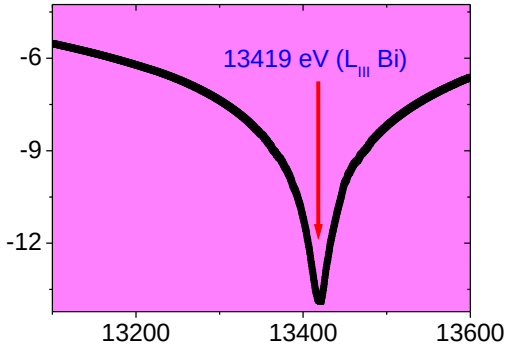

ρ_{Bi}: scattering length of Bi

ρ_0:scattering length of glass matrix

$$\rho_{Bi}(E) = c\, f_{Bi}(E)$$

c: Bi concentration [atoms/cm^3]

f_{Bi}: atomic scattering amplitude of Bi

$$f_{Bi}(E) = 83 + f'_{Bi}(E)\ [\text{electons}]$$

$$[I(q,E)]^{1/2} = \rho_{Bi}(E) k^{1/2} - \rho_0\, k^{1/2}$$

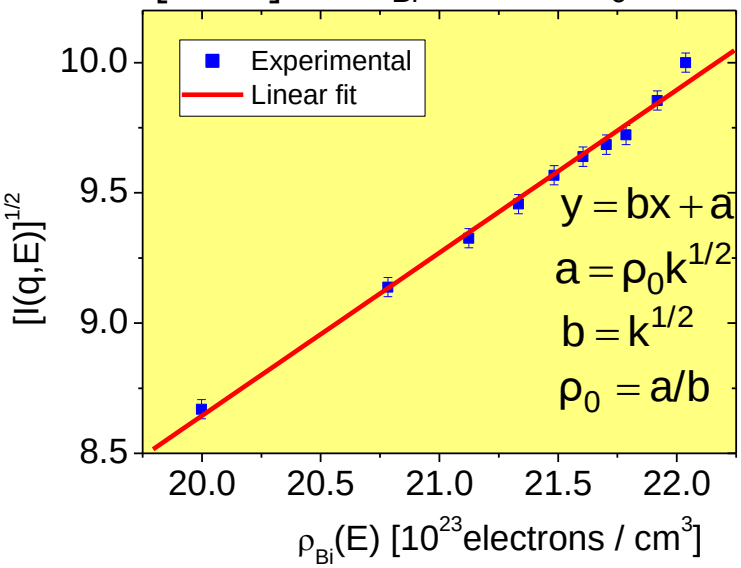

$$\rho_0 = (6.2 \pm 0.6) \times 10^{23}\ \text{electrons / cm}^3$$

From composition and mass density:

$$\rho_0 = (6.9 \pm 0.2) \times 10^{23}\ \text{electrons / cm}^3$$